INFORMATION TO USERS

This manuscript has been reproduced from the microfilm master. UMI films the text directly from the original or copy submitted. Thus, some thesis and dissertation copies are in typewriter face, while others may be from any type of computer printer.

The quality of this reproduction is dependent upon the quality of the copy submitted. Broken or indistinct print, colored or poor quality illustrations and photographs, print bleedthrough, substandard margins, and improper alignment can adversely affect reproduction.

In the unlikely event that the author did not send UMI a complete manuscript and there are missing pages, these will be noted. Also, if unauthorized copyright material had to be removed, a note will indicate the deletion.

Oversize materials (e.g., maps, drawings, charts) are reproduced by sectioning the original, beginning at the upper left-hand corner and continuing from left to right in equal sections with small overlaps. Each original is also photographed in one exposure and is included in reduced form at the back of the book.

Photographs included in the original manuscript have been reproduced xerographically in this copy. Higher quality 6" x 9" black and white photographic prints are available for any photographs or illustrations appearing in this copy for an additional charge. Contact UMI directly to order.

UMI

A Bell & Howell Information Company
300 North Zeeb Road, Ann Arbor MI 48106-1346 USA
313/761-4700 800/521-0600

TESTS AND ANALYSIS OF GEOGRIDS AS BASE REINFORCING MATERIALS

A

THESIS

Presented to the Faculty of the University of Alaska Fairbanks
in Partial Fulfillment of the Requirements
for the Degree of

DOCTOR OF PHILOSOPHY

Xuemin Fu, M.S.

Fairbanks, Alaska

May 1998

TESTS AND ANALYSIS OF GEOGRIDS AS BASE REINFORCING MATERIALS

By

Xuemin Fu

RECOMMENDED:

Sukumar Bandopadhyay

Lutfi Raad by J. Hilsey

J. Hilsey

Thos C Kinney

Chairman, Advisory Committee

J. Hilsey

Head, Civil Engineering Department

APPROVED:

Dean, College of Science, Engineering, and Mathematics

Dean of the Graduate School

5-5-95

Date

Abstract

A quantitative assessment of geogrids as base reinforcing material in paved roads is clearly necessary when a design is needed and decisions are to be made as a consequence. Two full scale single wheel load tests were conducted to determine the performance of geogrids as base reinforcing materials in paved roads. These two full scale tests were set up with different base thicknesses, material properties, loading conditions and geogrids. Load, speed, and direction of a test cart were controlled with a computer. Although many types of instruments were installed, measurements of vertical deformation of the pavement surface proved to be the most useful. The Traffic Benefit Ratio (TBR), defined as the ratio of the life of a reinforced section to the life of a similar unreinforced section, was used as a primary design parameter. Comparisons between reinforced and unreinforced bases are presented. The parameters used for comparison were permanent vertical deformation, number of repetitions to failure, tire load, and thickness of base course. Test results showed that the maximum TBR for a Tensar BR2 geogrid was 10. This TBR was obtained at a design deformation of 1.0 inch with 2 inches of asphalt over 10 inches of base over a CBR 3 clay subgrade. TBR's for other conditions ranged between 1 and 10. A design reference chart is presented for using Tensar BR1 and BR2 Geogrids.

Table of Contents

List of Figures

List of Tables

Acknowledgments

I would like to express my most sincere gratitude to Dr. Thomas Kinney for his encouragement, understanding, cordial help, continuous support and patient guidance; Dr. Lutfi Raad, Dr. Leroy Hulsey, Dr. Sukumar Bandopadhyay, and Dr. Brenton Watkins for their constructive discussions.

Special thanks are given to Mr. Sandy Tolme, Mr. Bub Mueller and Mr. Peter Dolan for their help in setting up the test facilities and electrical control systems.

I also would like to express my appreciation to Tensar Earth Technologies, Inc. for supplying the test materials, giving financial aid and sharing their experience and data. Dr. Jim Collin and Mr. Andy Anderson were particularly helpful with their special insight into the uses of geogrids in paved roads and the mechanisms involved in geogrid reinforcement of soils.

Thanks go to my beloved parents who live far away in China for their understanding and endless supporting during my pursuit of a Ph.D. at the University of Alaska Fairbanks. It is to them that I dedicate this dissertation.

Finally, I would like to express my appreciation to my dear wife, Jierong, and lovely daughter, Minye, for their encouragement, support and understanding.

Chapter 1. Introduction

The field of pavement system design is dynamic, in that, its concepts continually change as new data and techniques become available. There are many methods of design; the suitability of each design method varies from locale to locale. Materials available for construction of pavement systems in a given area greatly influence the design in that area. The design of highway pavement systems involves the behavior of soils, paving materials, and reinforcing materials under load.

There is a constant struggle today to balance the construction cost and maintenance costs to find the most economical way to build roads with acceptable serviceability. Geosynthetics have been used in many parts of the pavement system to help reduce cost and increase serviceability. The use of geogrids to reinforce the base material is one of the methods that has attracted a lot of attention lately. There are several design schemes available but data to verify the designs are lacking. This study presents full scale tests to define the benefit that can be gained from a manufacturer's geogrids under a variety of conditions.

1.1 Overview of Geogrids

ASTM D-35 defines a geogrid as a reinforcing geosynthetic formed by a regular network of tensile elements with apertures of sufficient size to allow strike-through of surrounding soil, rock or other geotechnical materials.

Geogrids using polyester fibers as the reinforcing component were developed in the United Kingdom around 1980 (Koerner, 1994). The original geogrids were made in the United Kingdom by Netlon, Ltd., and were brought to the United States in 1982 through Canada by Tensar Corp. The relatively recent discovery of the ability to make high-modulus polymer materials has raised the possibility that such materials could be used in the reinforcement of a number of construction materials including soil (G. Capaccio, 1974). The development of geogrids for soil reinforcement has been very rapid, with several different configurations, materials, connections, etc., entering today's market.

There are three basic methods of constructing geogrids: extruding (Tensar geogrid), stitching (Miragrid) and sheathing (Paragrid). Extruded geogrids are made from a single polyethylene sheet. Holes are punched in the sheet. The punched sheet is then sent over and under a number of rollers, each going faster than the one before it, thus inducing longitudinal stress in the remaining sheet. This stress causes the ribs to deform and elongate in the direction of movement, so that the sheet is drawn forming a single matrix of ribs and apertures. Stitched geogrids are formed by an open weaving process using high-tenacity polyester fibers that are subsequently knit stitched together at the junctions. The product is then latex coated in its final processing step. Sheathed geogrids consist of high tenacity polyester fibers held together by an encompassing polypropylene sheath. At the junctions where the longitudinal and transverse ribs cross, the contacting polypropylene sheaths are melt bonded to one another forming the connection.

Openings (apertures) between the longitudinal and transverse ribs large enough to allow soil strike-through from one side of the geogrid to the other are a key feature of geogrids. The ribs of geogrids are often quite stiff compared to the fibers of geotextiles. Rib stiffness and junction strength are also important for base reinforcement. The soil strike-through within the apertures bears against ribs which transmit their loads to other ribs through the junctions (Abd, 1983), and the system is more stable when the apertures themselves are more stable (Kinney and Yuan, 1993).

1.2 General Uses of Geogrids

Geogrids are generally relatively high-strength, high-modulus, low-creep-sensitive polymer grids with apertures varying from 0.5 to 4 inches across. Geogrids are used in reinforcement applications. The following uses have been reported in the literature (R. Koerner, 1994):

a. Beneath aggregate in paved roads

b. Beneath aggregate in unpaved roads

c. Beneath surcharge fills on temporary construction sites

d. Within embankment fills and earthen dams

e. Within repaired slope failures and landslides

f. As gabions for wall construction, erosion control structures and bridge abutments

g. Within construction of mattresses over peat, tundra, muskeg and other soft soils

h. As sheet anchors for retaining-wall facing panels

i. As sheet anchors and facing panels to form an entire retaining wall

j. Within concrete reinforcement in a wide variety of applications

k. As reinforcement of disjointed rock sections

l. As reinforcement of disjointed concrete sections

m. Within landfills to allow for vertical and/or lateral expansion

n. Within veneer reinforcement to stabilize leachate collection stone

o. Within veneer reinforcement to stabilize landfill cover soil

1.3 Significant Geogrid Properties

Properties of geogrids are usually divided into three categories: physical, mechanical, and endurance.

1.3.1 Physical Properties of Geogrids

The physical properties of geogrids include the dimensions of the ribs and apertures and can be measured directly. Sometimes a description of the polymer and construction technique are included in the physical description.

1.3.2 Mechanical Properties of Geogrids

Mechanical properties of geogrids include such things as: strength, modulus of elasticity, bending stiffness and rigidity of the grid matrix. The mechanical properties of geogrids covered here all relate directly to their use in basic reinforcement applications.

1.3.2.1 Single Rib Strength

The single rib tension strength test currently under consideration by ASTM uses a constant rate-of-extension testing machine to pull a single rib to failure. For uniaxial

geogrids (grids with one dominant direction), the longitudinal rib is usually tested. For biaxial geogrids (grids with similar properties in two directions), both longitudinal and transverse ribs are usually evaluated. ASTM is close to establishing a test method for the single rib strength.

1.3.2.2 Junction Strength

The junction strength test is meant to be used on geogrids which are constructed by welding or gluing strands together. The rib in one direction is held on both sides of the node while the other rib is pulled to break the bond at the node. Currently there is a lot of controversy surrounding the value of knowing the joint strength and exactly how the joint strength should be measured. ASTM is currently attempting to develop a standard test method for junction strength.

1.3.2.3 Geogrid Tensile Strength

Since geogrids are made up of many ribs at a significant spacing, the strength of a geogrid may well be less than the sum of its single rib strengths. In the field, the geogrid is not necessarily stressed uniformly; one rib might be stressed more than another and would therefore break first. This break would shift the load to other ribs, perhaps damaging them and causing them to fail non-uniformly. This non-uniform failure model, frequently termed progressive failure or cascading, causes a reduction in total strength.

When a test like ASTM D4595 (1996) is used, the degree of progressive failure is determined largely by the efficiency of the clamps and may or may not represent field conditions. Currently (Spring 1998) there is considerable work being done to develop a meaningful way to measure geogrid strength. ASTM is years away from developing a consensus standard. In the meantime, a modified wide width for geotextile test (D 4595) is frequently requested.

The same arguments hold for the modulus. Although a modified ASTM D4595 probably yields a good estimate of the modulus at low strain levels, 2 to 5%, creep or relaxation must be considered in developing a modulus for long term applications.

1.3.3 Endurance Properties of Geogrids

Numerous things may happen to a geogrid in the ground which may change the mechanical properties. These changes are typically referred to as endurance properties. With the use of geogrids in critical reinforcement applications, some of which require long service lifetimes, it is generally necessary to evaluate selected endurance properties.

1.3.3.1 Installation Damage

As with any geosynthetic, the placement of geogrids in the field requires a considerable degree of care and consideration to avoid nicking or knocking the ribs or breaking the joints. Loss in strength has often occurred due to inadequate installation. Investigations (Koerner, G. and Koerner, R., 1994) show reductions in geogrid strength of up to 30% as a result of improper installation.

1.3.3.2 Creep and Relaxation Behavior

Plastics tend to creep under constant load or relax under constant strain if the load is above the creep limit. Apart from the molecular structure of the geogrid, creep is predominantly a function of stress level, time, temperature, and other environmental factors.

Fig. 1.3.1 presents the creep test results on Tensar Geogrid SR2 (UX1200) by McGown, Andrews and Kavir (1982).

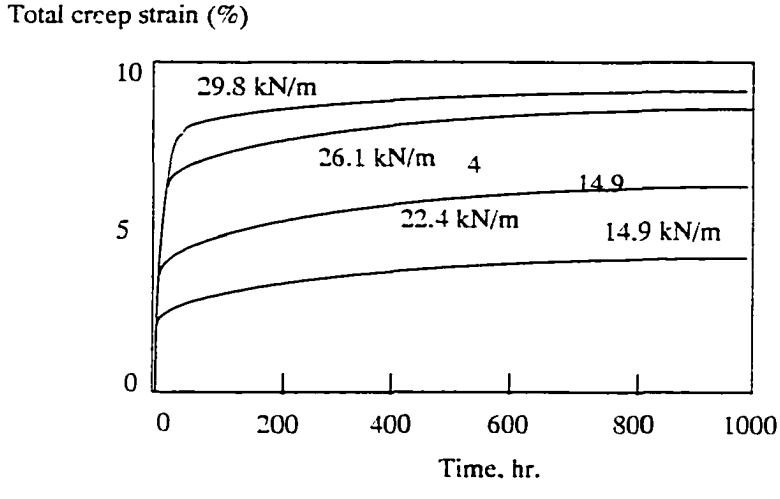

Fig. 1.3.1 Creep test results of SR2 geogrid

Greenwood (1991) has evaluated stress relaxation in geogrids. His experimental data was plotted, and from these data isochronous stress-strain curves were obtained. Greenwood concludes that in the absence of actual data, one can estimate geogrid stress relaxation response by using his plots in this manner.

1.3.3.3 Temperature Degradation

Within the temperature ranges of typical outdoor environments, temperature extremes (hot or cold) should have no serious adverse effects on geogrids. Extremely high temperatures increase creep and/or stress relaxation and extremely low temperatures are expected to make grids more brittle.

1.3.3.4 Hydrolysis Degradation

The phenomenon of hydrolysis causes both internal and external degradation. Extremely high pH values can affect some polyesters, while extremely low pH values can be harsh on plyamides (Hsuan, et al., 1993). Within the normal ranges found in roads no hydrolysis degradation is expected with any geogrid material currently used in highway applications.

1.3.3.5 Biological Degradation

Latex, bitumen, or plasticizers in PVC may be sensitive to microorganisms, but no such studies on geogrids are available. Even if such attacks on the coatings were possible, the high crystallinity polyester fibers would probably remain unaffected.

1.3.4 Geogrid Soil Interface

1.3.4.1 Shear Strength

One type of performance test that has been used on geogrids is an adapted form of the conventional geotechnical engineering direct shear test.

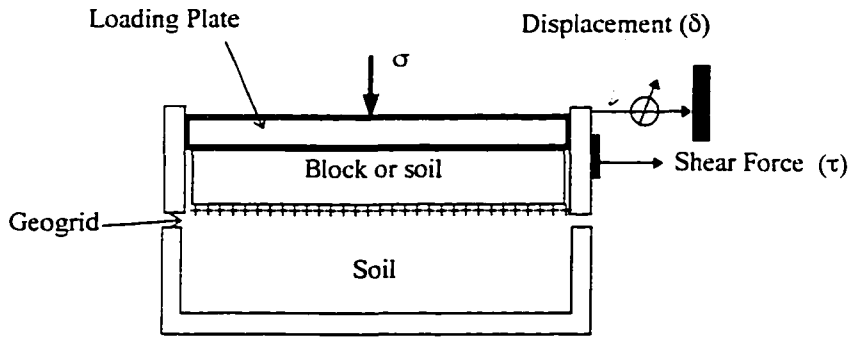

(a) Schematic of test setup

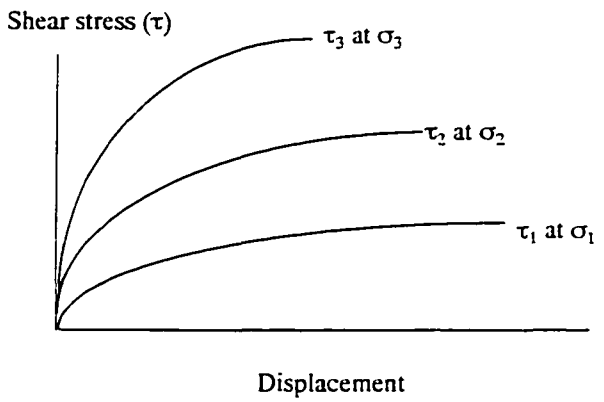

(b) Typical test results

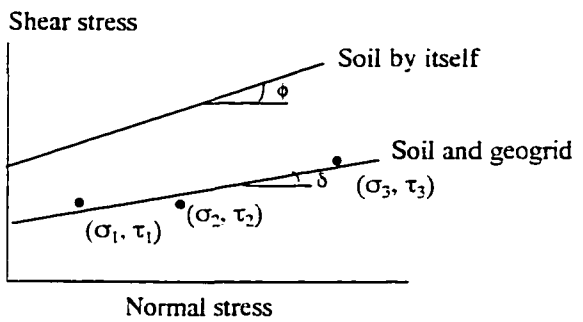

(c) Mohr-Coulomb Stress space for shear strength parameters

Fig. 1.3.2 Direct shear testing of geogrids.

In this test, the geogrid is fixed to a block and is forced to slide over stationary soil in a shear box while being subjected to normal stress (see Fig. 1.3.2a). The maximum shear stress is obtained (see Fig. 1.3.2b), and then a new test at a different normal stress is conducted. This process is repeated to develop a locus of points called a failure envelope, as shown in Fig. 1.3.2c. This last figure plots normal stress vs. maximum shear stress and is known as the Mohr-Coulomb stress failure envelope.

A large shear box must be used for geogrid testing to minimize scale effects. ASTM requires a 12-by-12- in. box or larger for geogrid shear testing.

Sarby (1985) investigated the influence of aperture size versus soil particle size on the frictional efficiency of a number of geogrids. He found that the optimum transfer of shear stress, that is, the highest efficiency, occurs when

$$B_{GG} \geq 3.5 d_{50} \qquad (1.1)$$

where B_{GG} = the minimum width of geogrid aperture, and

d_{50} = the average particle size of the soil.

This is an important consideration when selecting the type of backfill to be used around geogrids.

1.3.4.2 Geogrid Pullout from Soil Mass Above and Below

Pullout strength is a result of three separate mechanisms (Wilson-Fahmy and Koerner, 1993), see Fig. 1.3.3.

One is the shear strength along the top and bottom of the longitudinal ribs of the geogrid. The second is the shear strength along the top and bottom of the transverse ribs.

The third mechanism is that of passive resistance against the front of the transverse ribs. The soil goes into a passive state and resists pullout by means of bearing capacity. It has been analytically shown that this bearing capacity can be a major contributor to the overall pullout strength of geogrids (Koerner, Wayne and Carroll, 1989).

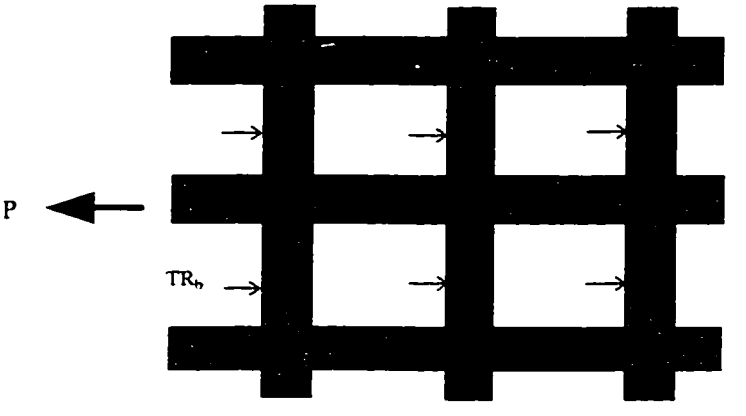

P = Total pullout strength
LR_s = Longitudinal rib shear strength
TR_s = Transverse rib shear strength
TR_b = Transverse rib bearing strength

Fig. 1.3.3 Mechanisms involved in geogrid pullout strength.

1.4 Geogrid Improvement Mechanisms

There are numerous mechanisms whereby the inclusion of geogrids in a pavement system improves performance. These mechanisms are logical and can be described, but virtually no data is available which isolates and quantifies any mechanism to date.

1.4.1 Interlock

Geogrids placed between the base and subgrade can provide interlocking of the aggregate at the subgrade interface and prevent the lateral movement of aggregate, as shown in Fig. 1.4.1.

Fig. 1.4.1 Interlock Mechanism

1.4.2 Reinforcement

The primary function of geogrids is reinforcement. Geogrids, with a high modulus in the tension zone, provide tensile reinforcement in the aggregate base course. This property is discussed in Section 1.3.

Geogrids can act to reinforce a pavement system in much the same way that steel reinforces concrete. If the geogrid is in an area where the system would go into extension strain, the geogrid will go into tension. This will help resist the outward migration of the soil particles, help reduce the load on the subgrade on the concave

upward portion of the rut and resist the upward movement of the subgrade on the concave downward portion of the rut. The resistance to the outward movement of the soil on that interface acts in the same way as applying an inward lateral stress (confining stress) on the layer. This confining stress increases the strength and stiffness of the granular material causing it to behave more like a beam than a granular fill.

1.4.3 Separation

There are three mechanisms by which the aggregate base and subgrade soils intermix. The first is pumping, where repeated load cycles cause the fines to migrate up into the voids in the base. This mechanism requires high loads and a large difference in grainsize between the base and subgrade. In general this mechanism does not take place for more than a few millimeters in a well designed pavement system. The second mechanism is the large stones in the base being pushed down into the subgrade. This may be a problem in marginally designed roads, and a geogrid should completely eliminate it. The third mechanism is soft subgrade squeezing up into cracks formed in the base as it spreads laterally during rutting. In a properly designed system, the grid will keep these cracks from forming and completely eliminate the problem. See Fig. 1.4.2.

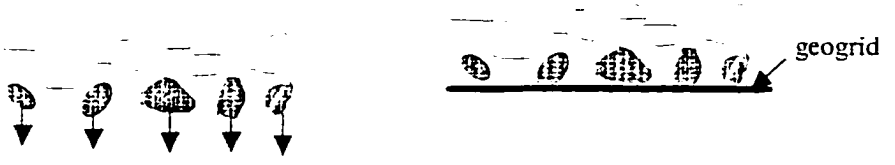

Without geogrid With geogrid

Fig. 1.4.2 Separation mechanism of geogrids

Geogrids can act as both reinforcement and a separator in base reinforcement and subgrade improvement applications. The US Army Corps of Engineers (Webster, 1992), found that with geogrid reinforcement "no significant amount of aggregate sinking into the subgrade occurred in the items tested."

1.5 Application of Geogrid Reinforcement in Paved Roads

The use of geogrids in paved road base courses is an area in which the large aperture size of geogrids provides an excellent advantage. The geogrids are placed under or within the granular base course (e.g., crushed stone) with the intention of providing an increased modulus of the base course and a lateral confinement to the system. The lateral confinement is intended to resist the tendency for base courses to "walk out" from beneath the repetitive traffic loads imposed on the concrete or bitumen wearing surface. A number of laboratory tests have been conducted to assess the potential benefits and mechanisms involved.

1.5.1 Tests by Haas and Halim

The works of Haas (1984) and Abd El Halim, et. al. (1983) are significant. Five test series (called loops) were performed in a large test track measuring 4.0 m long by 2.4 m wide by 2.0 m deep, using 10 kN loads applied sinusoidally at a frequency of 10 Hz on a 300 mm (12 in.) diameter circular plate. See schematic of testing in Fig 1.5.1.

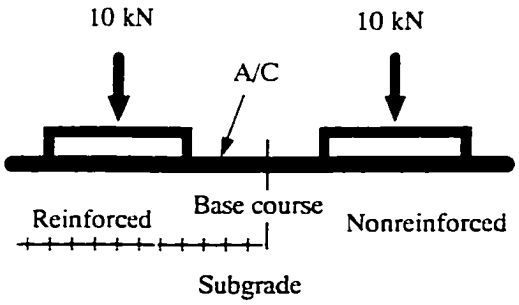

Fig. 1.5.1 Schematic of Plate Tests after Haas (1984).

Loop 1 compared the response of nonreinforced and reinforced sections using both dry (strong) and saturated (weak) subgrade conditions. Failure appeared in the nonreinforced sections earlier than the reinforced sections under both conditions. Loop 1 showed little difference in elastic deflection between the reinforced and nonreinforced sections. More significant is the radius of curvature and the vertical strain at the bottom of the asphalt. The tests in loop 2 indicated a 50% reduction in both the radius and strain in the reinforced sections, thereby indicating a significant load-spreading phenomenon.

The permanent surface deformation of the reinforced section was substantially reduced compared to the nonreinforced section. At 20 mm of deformation. the nonreinforced section carried 110,000 load repetitions, compared to 320,000 for the reinforced case, giving a Geogrid Effectiveness Factor (GEF) of 2.9. Loop 3 investigated the equivalent thickness that can be attributed to reinforcement. The results indicate that the reinforced section for 150-mm thickness A/C carried about 80,000 load cycles compared to only 34,000 load cycles for the "200-mm nonreinforced section" and 92,000 load cycles for the "250-mm nonreinforced section." In other words, 150 mm of reinforced paved road nearly equaled the performance of 250 mm of nonreinforced paved road. Loop 4 confirmed these results: reinforced sections result in a saving of 50 to 100 mm of nonreinforced asphalt. Loop 5 involved pressure cells in the soil subgrade and confirmed the load-spreading capability of the reinforcement.

1.5.2 Tests by Austin and Coleman

Austin and Coleman (1993) presented the results of a full-scale field study conducted to evaluate the effectiveness of various geosynthetics as the primary reinforcement at the bottom of aggregate layers placed over very soft subgrades. Although, these tests were performed using an unpaved section., they are significant to the work presented herein.

A test road containing several test sections (total length is 54.9 m) was constructed on soft, expansive clays. There were four sections dedicated to the tests on geogrids. The tensile strengths of the geogrids were: geogrid 1 - 15.5 kN/m, geogrid 2 -

17.6 kN/m, geogrid 3 - 14.2 kN/m, and geogrid 4 - 26.5 kN/m. The data in Table 1.5.1 clearly demonstrates that sections containing geogrid reinforcement carried between 1.3 and 3.2 times the number of passes as the unreinforced sections for a 50 mm rut depth.

Table 1.5.1 Summary of Austin and Coleman's test results on Geogrids

	Geogrid 1		Geogrid 2		Geogrid 3		Geogrid 4	
	subgrade	subbase	subgrade	subbase	subgrade	subbase	subgrade	subbase
Thickness mm		265		225		260		175
CBR, %	0.8	14	0.9	15	1.0	15	0.6	20
D_γ (kg/m^3)	1270	2120	1220	2020	1250	2050	1240	2080
water content,%	41.9	4.1	43.2	4.0	40.1	2.8	39.2	2.8
passes to failure		53		31		21		X
PF at 50 mm		3.2		2.2		2.2		1.3 at 40 mm

Note: PF = Performance Factor
= passes over reinforced section / passes over control section

1.5.3 Tests by Carroll

Carroll, et. al. (1987) have further refined the technique using the same experimental database to back-calculate a structural number as per the AASHTO Guide for Design of Pavement Structures.

$$SN = \sum a_i d$$

where SN = structural number,

a_i = layer coefficients (= 0.4 for asphalt and 0.14 for granular stone base),

d_i = thickness (in inches) of each layer.

A load correction factor was then calculated for the geogrid reinforced sections within each experimental test loop. An estimate of the reinforced pavement structural number was derived, and a ratio for reinforced-to-nonreinforced sections was generated. When plotted against the actual reinforced base course thickness, this ratio was seen to be linear. Different values, with the same trend, were seen for geogrids placed in the middle and at the bottom of the base course.

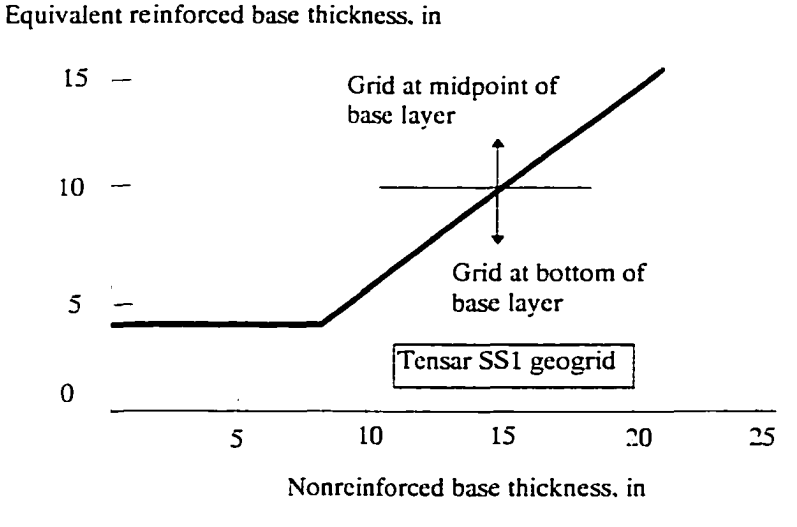

Fig. 1.5.2 Geogrid reinforced base course for paved highway section using Tensar BX1100 geogrids.

A design chart that enables a conventional nonreinforced base course thickness to be converted to a geogrid reinforced section is given in Fig. 1.5.2. Note that this curve is based on experimental data for the Tensar BX 1100 geogrid only and is not applicable to other geogrids. A transition occurs at 10 inches. For a thickness of less than 10 in., the geogrid is placed below the base. For a thickness greater than 10 in., the geogrid is placed at midheight in the base.

1.5.4 Tests by Webster

The US Army Corps of Engineers Waterways Experiment Station (WES) performed a set of full scale tests on model runways in 1991 (Webster,1993). Four lanes were tested. Each had 2 inches of A/C, and different base and subgrade materials. Six different geogrids were used in the test. Their final report suggests that some geogrids have significant beneficial effects to the pavement system while others do virtually nothing. Their conclusions state that if Tensar SS-2 is used, the life of the pavement will be increased by a maximum Traffic Improvement Factor (TIF) of about 5 with a 14 inch-base (CBR= 93%) and 3% CBR clay subgrade, and a maximum TIF of about 22 with a 6 inch-base (CBR=104%) and 8% CBR subgrade. Fig. 1.5.3 shows the design criteria for reinforced thickness vs. equivalent reinforced thickness provided by WES.

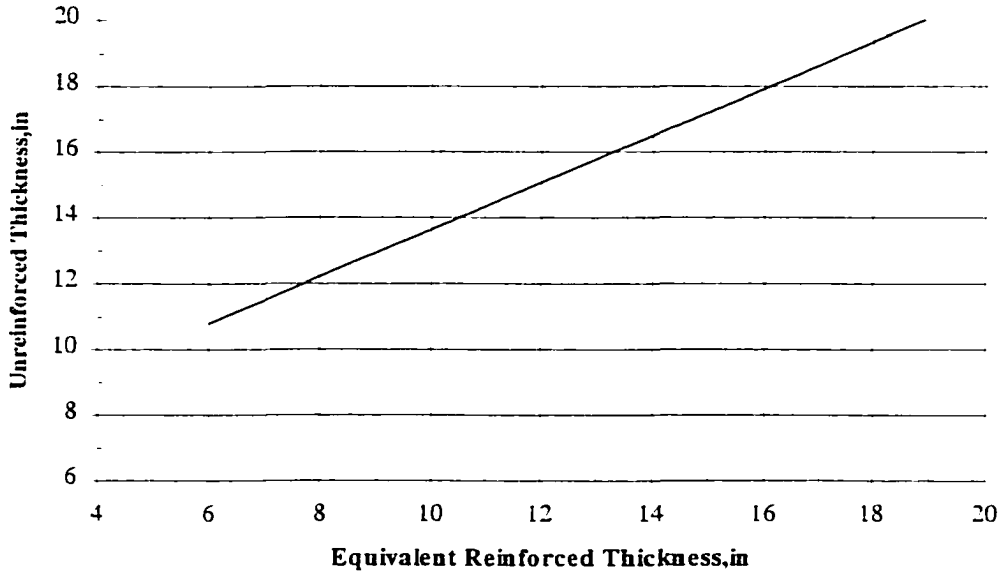

Fig. 1.5.3 Design criteria for Tensar SS-2 Geogrid from Webster (1993)

1.5.5 Tests by Kinney

Kinney (1993) conducted several field and laboratory tests to verify the validity of using geogrids to reinforce laterally spreading roads. The results of his study demonstrate that geogrids can be used to reduce maintenance costs in areas where longitudinal cracking is a serious problem. His design methodology was used on roads in Interior Alaska.

1.6 Outline of the Research

The concept of using geogrids to reinforce roads has existed for about 15 years. Some laboratory model testing and some field testing, and several design guides on geogrids have been developed. Many researchers have speculated on how the geogrid might affect the performance of pavement systems, and some of the reinforcement mechanisms have been explored theoretically.

Table 1.6.1 shows the tests conducted by different people who used geogrids as base reinforcement in paved or unpaved roads or runways and used wheel loading to test the response.

Table 1.6.1 Summary of tests used for geogrids as base reinforcement

Name	Application	Test	Load	Date
Kinney	flexible pavement light traffic	full scale	4,500 lbs	1993
Webster	flexible pavement light aircraft	full scale	30,000 lbs	1991
Banksdale	flexible pavement light traffic	full scale	1850 lbs	1982
Austin	unpaved road	full scale	9000 lbs	1993

To date there has not been a rigorous experimental and theoretical analysis made of the effects of geogrids on base course materials, even though these effects are among the most frequent practical concerns of pavement researchers and designers. It is, therefore, important to provide data on the effects of geogrids as road reinforcing materials based on full size paved road tests.

The objective of this research is to develop data for use in a design guide for the use of geogrids to reinforce the base course materials in paved road. In order to develop

this data, five different full scale tests on paved roads were performed. These tests included various configurations of base and subbase materials, reinforcing materials, numbers of load repetitions and road profiles. The tests were designed to evaluate the factors influencing pavement behavior and performance, to compare the results of reinforced sections with nonreinforced sections, and to develop the relationships between rutting and depth of base course with different loads. Tests No. 1 and No. 2 were run as shakedown tests to evaluate the test procedures and performance of instrumentation, such as Bison gauges, markers on geogrids and markers buried in soils. while Tests No. 3 (hereafter referred to as Test A) and No. 5 (hereafter referred to as Test B) were run to evaluate the geogrids in base reinforcement tests which included two different geogrids and a wide variety of base thicknesses. The loading on test No. 4 was varied throughout the test, making it very difficult to compare the results to the other two tests, hence only the results of Test No. 3 (Test A) and No. 5 (Test B) are discussed herein.

This research includes the following:

1. Design and construction of the test cart.
2. Design and construction of the control systems.
3. Design and installation of the instrumentation.
4. Design and construction of the road sections.
5. Measurement of the test material properties.
6. Measurement and analysis of the test results.

Chapter 2. Design of the Test Facilities

The purpose of this study is to compare the performance of paved road sections with Tensar geogrid reinforcement to those without reinforcement under the influence of a single truck tire loaded to 4500 pounds. Its intent is to determine the relative benefit of using Tensar geogrids in a base reinforcement application over a soft subgrade.

The general purpose of designing the test facility was to design a test cart which could be controlled by a computer to provide precise loads and repetitions.

The testing facility was constructed in Building 16 of the US Army Cold Regions Research and Engineering Laboratory (CRREL)'s field test site on the east end of Farmers Loop Road in Fairbanks, Alaska.

2.1 Design of Loading Cart

2.1.1 Loading Cart

The loading cart consisted of two frames, one over the other. The bottom frame supported the loading wheel and the top frame supported four reaction wheels which pushed up on overhead reaction beams. The two frames were hinged at one end and were separated by a pneumatic jack on the other end. The load on the wheel was twice the load on the jack plus the total weight of the cart minus the force required to lift the upper frame up to the reaction beams. See Fig. 2.1.1.

TEST CART

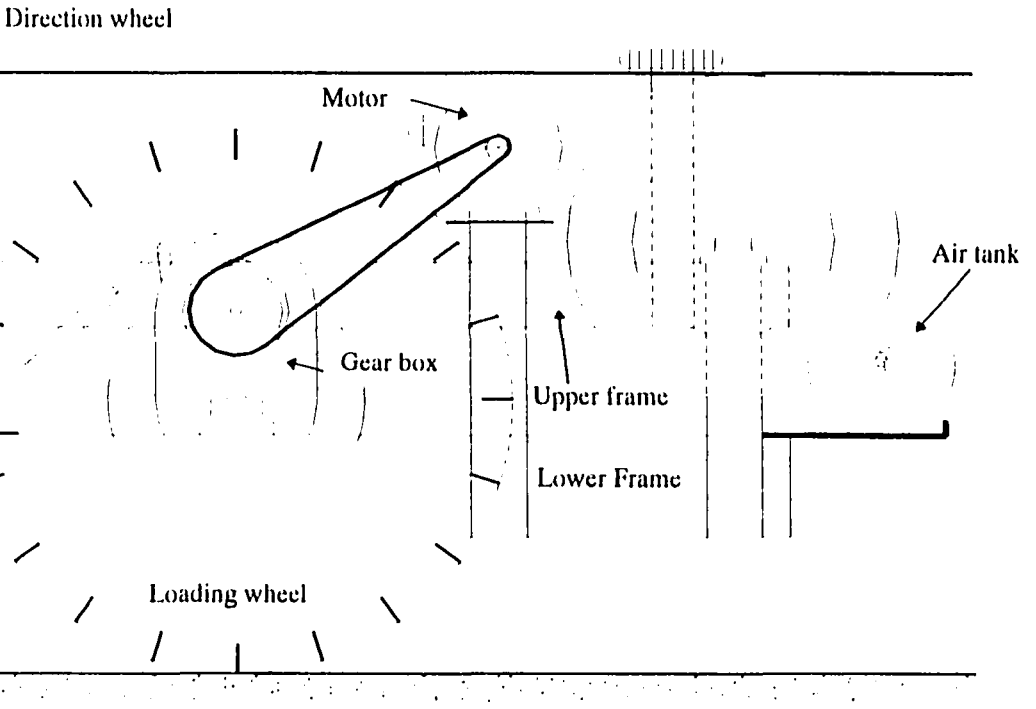

Fig. 2.1.1 Loading cart

The loading wheel was 9 inches in width and rigidly attached to an axle which runs through bearings bolted to the top of the lower frame.

The reaction wheels were attached to axles which ran through bearings on the upper frame. The electrical motor drove the gear box through a belt and forced the cart to run forward and backward. The gear box and motor controlled the speed of the test cart up to 6 ft/sec. The pneumatic jack forced the upper wheel against the reaction beam and provided a vertical force on the pavement through the loading wheel. The details of the control system will be presented later in this chapter.

2.1.2 Reaction Beams

The reaction beams were attached to I-beams, which were, in turn, attached to pipe columns. The pipe column were bolted to timbers which ran under the box. The reaction beams were designed to provide a maximum of 10,000 pounds on the loading wheel.

2.2 Control System

The control system consisted of load control, direction control, speed control, and safety control. Fig. 2.2.1 shows the general control system.

A light beam sensor was placed at each end of the test box. When the cart passed the sensor, the sensors sent a signal to the inverter which slowed the cart to a stop, reversed its direction and sped it up again, all at carefully controlled rates. The

light beam sensor also sent a signal to the computer which loaded or unloaded the pneumatic jack depending upon which direction the cart was moving.

Another sensor was placed at the middle of the test box which was used to count the number of repetitions. When the cart triggered the sensor two times (one cycle), it sent the number to the computer to be recorded.

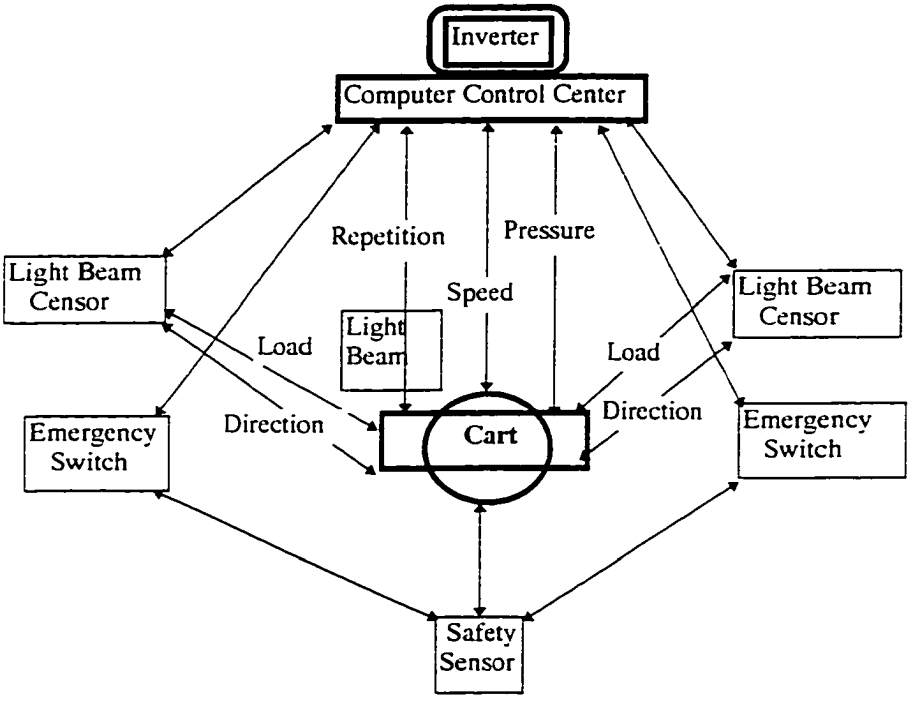

Fig. 2.2.1 The control system

In addition, the pressure in the jack and the time of day was recorded each time the cart passed a sensor. A series of switches were strategically placed around the test box so that, if the cart was somewhere it should not be, the entire system would shut down.

2.2.1 Load Control

The air pressure came from the air pump. The load was controlled by the pressure in the pneumatic jack, see Fig. 2.2.2. There were solenoid valves on both the input and output sides of the jack. The two solenoids were set so that when one opens, the other closes, and vice versa. Each side of the jack had a surge tank in which the pressure was controlled. As the cart moved down the track it traversed various rut depths which caused the pneumatic jack to extend and compress. The surge tanks dampened out the pressure variations so that the total load on the test tire(s) remained within about 100 pounds of the desired load.

In general, the cart ran one way under full load and was unloaded on the return. The load was controlled by the computer based on signals from the light beam sensors at each end of the test track. In the unloaded configuration, the weight of the cart plus the force needed to keep the reaction wheels tight against the reaction beams was actually on the loading wheel. This load depended upon the configuration but was on the order of 2,000 pounds.

The pressure in the jack was measured with a pressure transducer and was recorded by the computer several times during each cycle.

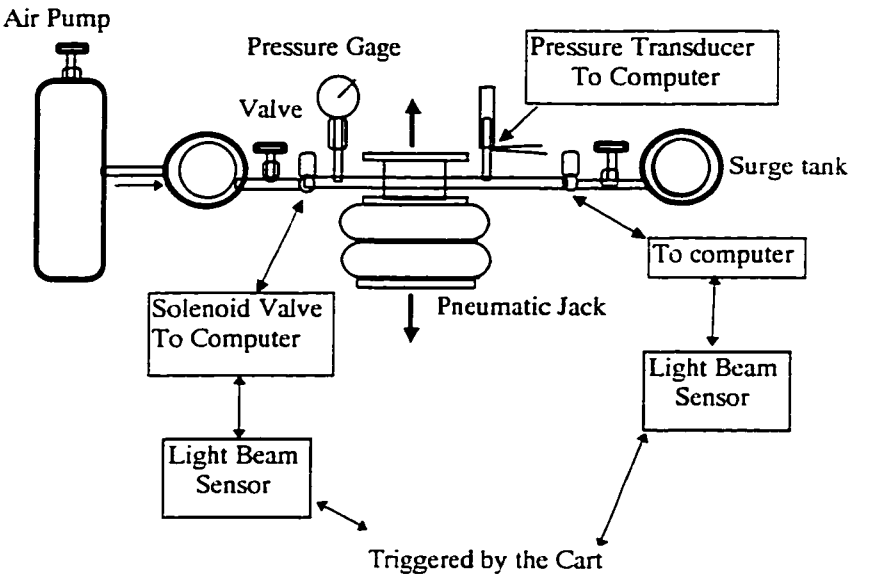

Fig. 2.2.2 The schematic of load control system

2.2.2 Speed Control

The cart was propelled by a 3-phase 3-HP motor which drove the axle. There was a 15:1 gear reduction box on the axle. A polychain and two shivers connected the motor to the gear box and added an additional 3:1 gear reduction. The electric motor was controlled by an inverter which took single phase 220 V electricity, converted it to direct current and then sent it out as 3 phase 220 V at a chosen frequency. The inverter was programmable with several options. Of most interest to this project are the ability to change direction, frequency (speed), and the rate of acceleration.

The system was designed for a maximum speed of 6 ft./sec., although that could be increased with minimal changes. A speed of 4 ft./sec. was usually used for the tests described herein. The cart stopped for 1 second at each end, and reached its design speed in 1 second. The system appeared to bog down slightly at the higher loads with speeds in excess of 5 ft./sec.

The speed of the vehicle is an interesting and very complex issue. The first and most obvious consideration is creep. If the wheel moves slow enough to allow creep, there will be more rutting in the slow test. The problem exists in both the clay subgrade and the asphalt. Although no definitive data was found, it seems unlikely that the difference between a 500 millisecond and a 20 millisecond rise time is significant. The second issue is one of dynamic loading caused by the truck passing over a rough road. This cart was loaded pneumatically so the dynamic aspects of the problem would be minimal even if the test track cart had been operated at highway speeds. Therefore, changing the speed of the cart would not effect this aspect of the performance. The third aspect is one of the non-uniform loading caused by the tire when it rotates at high speeds. It is likely that the outer edge of the tire carries more of the load at high speeds. No definitive data was found with regard to the tire used, but it is likely that there would be more difference between types of tires than there would be between low speeds and high speeds in this test apparatus.

2.2.3 Direction Control and Repetition Counting

A light beam sensor was set up at each end of the model road to control the loads and the direction of the test cart. The sensors were connected to the computer. When the cart triggered the sensor, the computer commanded the cart to load or unload, to stop, and to start again in the reverse direction as required.

Another sensor in the middle of the model road was used to count the repetitions of the cart as it traveled the road. After the cart passed by the sensor twice (loaded and unloaded), the computer counted one cycle.

2.2.4 Safety Control

Safety was controlled in two ways: emergency switches were set up at each end of the road, and a 50 ft. range light beam sensor was set up parallel to the cart movement. The emergency switches were connected to strings fastened across the road, so that if the car hit a string, the power was turned off and the cart stopped, see Fig. 2.2.3. The light beam sensor was set up on the north end of the road and aligned with a reflector fixed on the cart. The sensor was normally in the open state. If the cart deviated by more than 0.5 inch for any reason, the light from the sensor was not reflected back to the sensor, creating a closed state and immediately turning off the power to the cart.

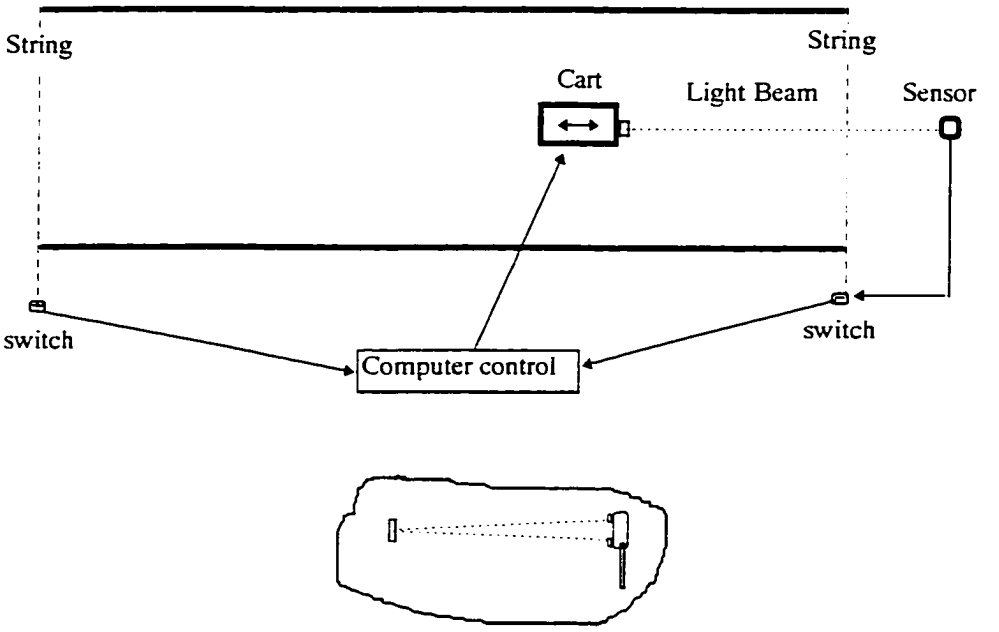

Fig. 2.2.3 Safety control system

2.3 Instrumentation

2.3.1 Surface Displacement

The primary method of measuring surface displacement of the road is to place an aluminum bar across the road and measure down to the surface. Secondary measurements are made by measuring down from the reaction beams and by a surveyor's level and rod. These secondary measurements are to the nearest 0.25 inches and are used only to catch blunders in the primary system.

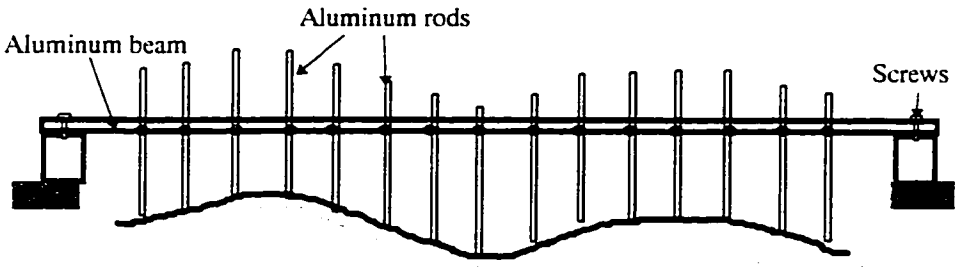

Fig. 2.3.1 Surface Displacement measurement

One quarter inch diameter aluminum rods ran vertically through the aluminum beam at 3 inch center intervals throughout the six feet of the beam. The aluminum beam rested on screws in the plywood at the end of the box. The screws were installed so that the rod was replaced at the same location every time. The rods were dropped through the beam to the surface and then locked into place with set screws. See Fig. 2.3.1. The length of the rod sticking out through the beam was measured with a micrometer caliper to the nearest 0.001 inch.

2.3.2 Bison Gauges

Bison gage sensors (coils) were usually buried in the road cross section in order to measure the vertical displacement of the base and subgrade. Typically there were several stacked vertically in the center of the test section and occasionally one or more horizontally from one of those on the centerline. See Fig. 2.3.2.

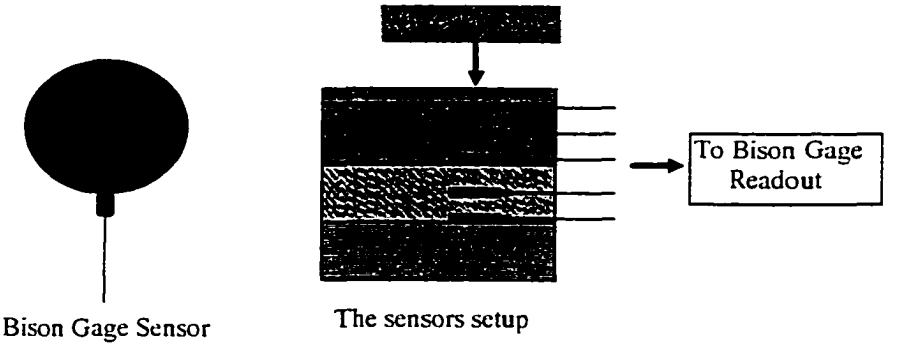

Fig. 2.3.2 Bison gage sensor and its setup

The Bison gages were read with the standard Bison readout. In addition, the signal was converted to digital information and fed directly into the computer for future processing of the dynamic response. The accuracy was normally within 0.005 inch. However, there was a radio station near the laboratory which created an interference that we were unable to filter out. Therefore, all Bison Gage data was suspect and was not used in the final analysis.

2.3.3 Markers Buried in the Soil

On several of the tests an attempt was made to bury markers of various sizes and shapes in order to measure soil movement. Virtually no useable information was gained from any of these attempts.

2.3.4 Lateral Displacement of Geogrid

Wires were tied on the geogrid to measure the lateral displacement of the geogrid, see Figure 2.3.3. The wires extended to the edge of the test box and were measured with dial gauges and/or micrometer calipers. Similarly, wires were attached to washers buried above and below the geogrid. This measurement technique proved not to be accurate enough to measure the small movements experienced, hence the data is not shown herein.

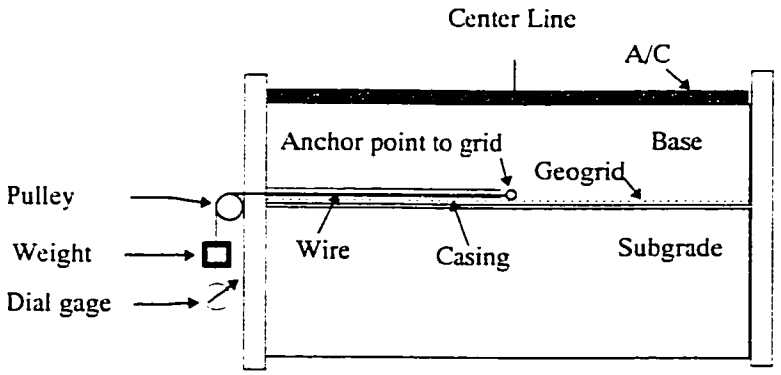

Fig. 2.3.3 Geogrid lateral displacement (cross section)

Chapter 3. Properties of the Test Materials

The base reinforcement study included five tests. Each test used a subgrade material, a base material, an asphalt, and geosynthetics. Many of these materials were common from test to test and as the testing progressed the properties of each material became better defined.

3.1 Base Materials

Two different base materials were used in this research. Test A used one base material, Test B another.

3.1.1 Crushed Rock Base for Test A

The crushed rock base course material for Test A was a processed material which conformed to the standard State of Alaska Specification D-1 for crushed rock base course materials. The allowable grainsize distribution is shown in Fig. 3.1.1 along with the results of a grainsize test on the material used. The standard specification calls for 70% by weight of the particles retained on the #4 sieve to have at least one fracture face. The sample tested was within the gradation specification and had about 75% percent fracture.

The Modified Proctor compaction moisture - density relationships are shown in Fig. 3.1.2 along with the immediate CBR values. The maximum density was 133 pcf at

a moisture content of 6.5%. The CBR varied dramatically with compaction conditions from below 25% to over 75%. The maximum CBR was 77% at moisture content of 6.5%.

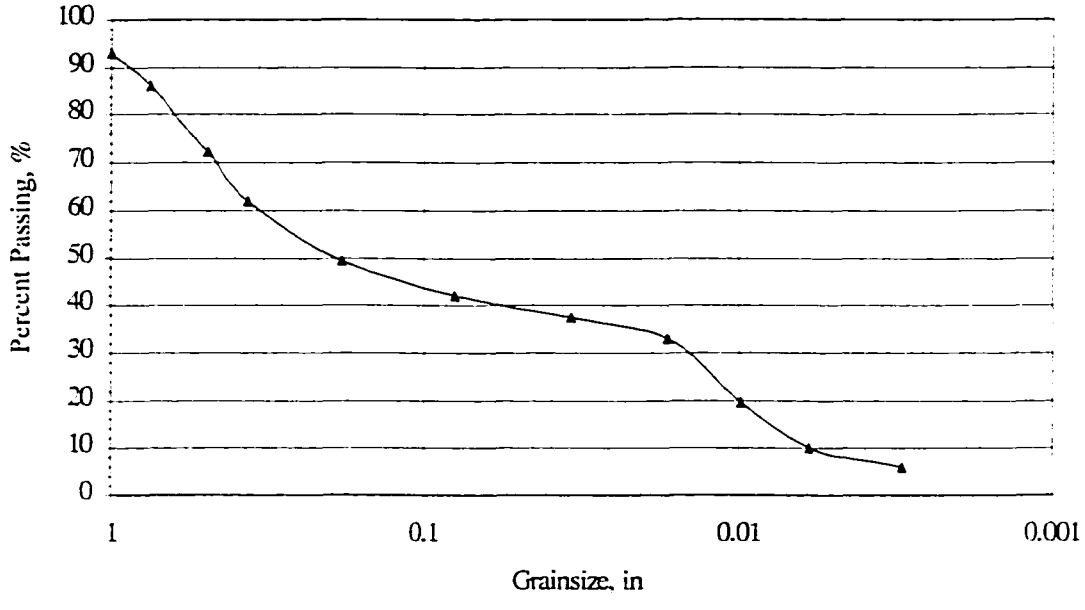

Fig. 3.1.1 Grainsize Distribution of Base

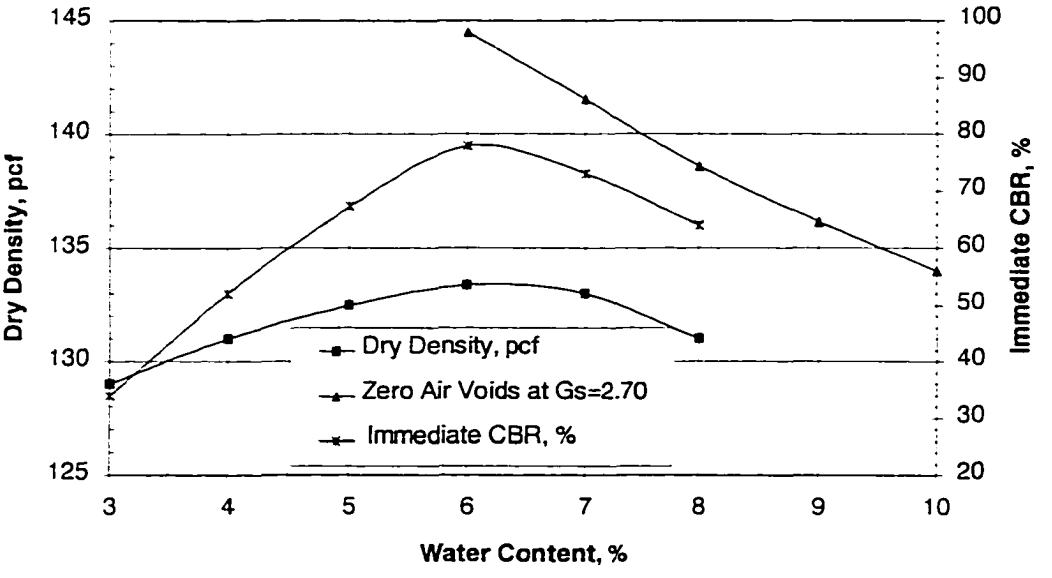

Fig. 3.1.2 Moisture Content with Dry Density and CBR of Base

3.1.2 Crushed Rock Base for Test B

The base course material for Test B was manufactured to resemble that used in a previous set of tests (Test No. 2). The ratios of the different feed materials and the degree of crushing were varied. The grainsize distribution is shown on Fig. 3.1.3.

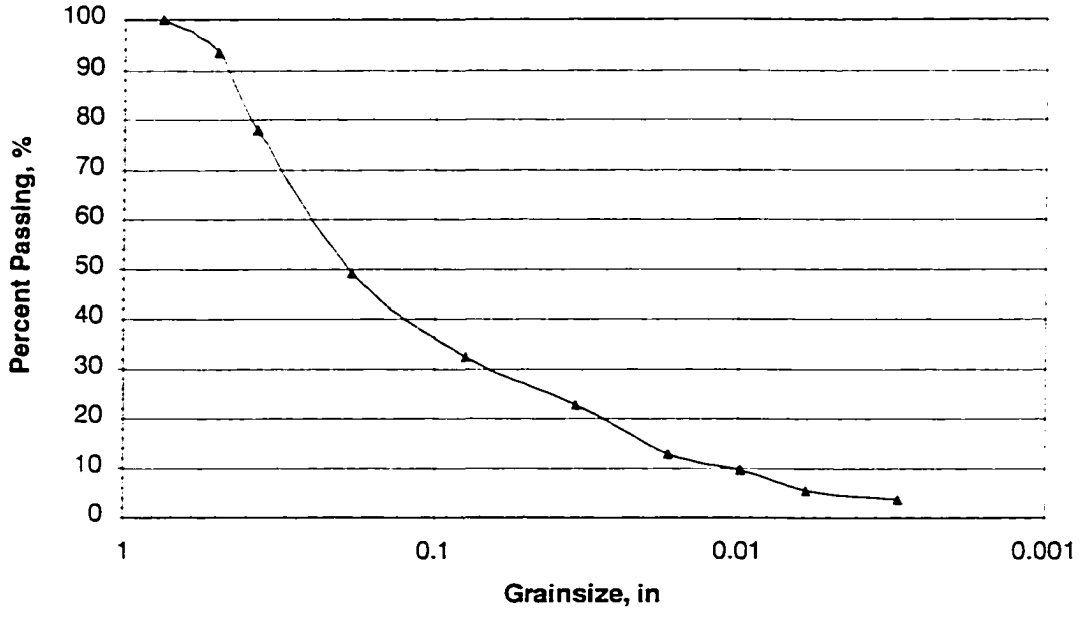

Fig. 3.1.3 Grainsize Distribution of Base Course

The Modified Proctor compaction Moisture - Density relationships are shown on Fig. 3.1.4 along with the immediate CBR values. The maximum density was 142 pcf at a moisture content of 5.5%. The immediate CBR varied dramatically from about 25% to nearly 90%. The maximum CBR was 89.7% at a moisture content of 4.8%.

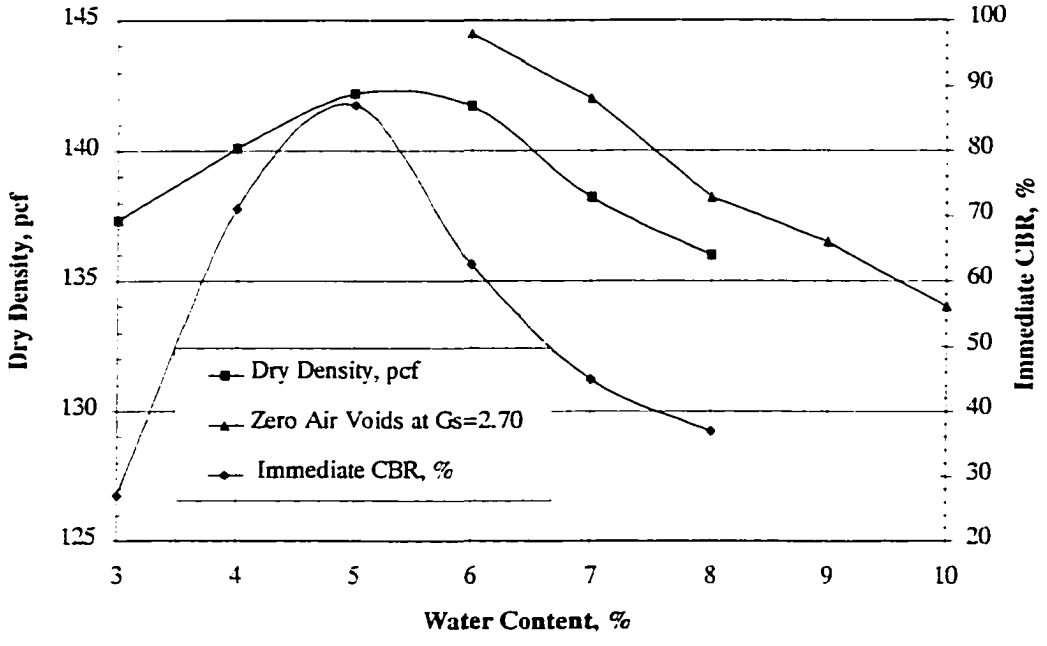

Fig. 3.1.4 Moisture vs. Density and CBR

3.2 Subgrade Materials

Healy clay was used for the subgrade on both Tests A and B. Thirty cubic yards of Healy clay were brought from the Usibelli Coal Mine near Healy, Alaska. Upon delivery it was dry and very hard. The material was initially prepared in a building with a concrete floor. Prior to use on Test No. 2 the Healy clay was broken down by grinding it under the tracks of a D-4 Caterpillar, running a large steel wheeled vibratory drum roller over it and pounding it with a jackhammer. It was passed over a 3/8 inch sieve and the part retained was returned to the grinding operation.

Once the material had all been broken down to a 3/8-inch maximum size, it was wetted and mixed with a Mustang front-end loader. The material was scooped up in 1/4 yard globs and dropped on the floor. These globs were kneaded with the bucket, then lifted and dropped again.

The mixing continued until the desired strength was reached. The desired strength was determined by mixing two cubic-foot samples at various water contents, compacting the samples with the techniques to be used in the test and running an immediate CBR on the compacted sample. At the same time a Proctor Needle was pushed into the clay. In this way a correlation between the Proctor Needle value and the immediate CBR was developed. At a CBR of 3 the Proctor Needle value was about 27. The Proctor Needle was used frequently on the kneaded soil to determine if it had achieved the proper consistency. The material was either wetted or mixed with dryer material until the Proctor Needle value was between 24 and 30.

The material was then transported to the test box and compacted into place. The compaction consisted of a combination of kneading with the Mustang bucket, using a vibrating plate compactor and working the soil with shovels and by foot. The objective of the compactive effort in the box was to remove all of the air pockets and to form a homogeneous mixture with a CBR of 3.0.

For each test after the first one, the gravel was removed from the surface of the clay and the surface was reworked, wetted slightly and compacted by foot, and compacted with a compactor to attain a CBR of 3.0. A vibrating plate compactor was used to reconstruct Test A and a drum compactor was used to reconstruct Test B.

A grainsize curve is shown in Fig. 3.2.1. The Modified Proctor compaction and associated immediate CBR curves are shown on Fig. 3.2.2. The density and water content at a CBR of 3 were about 86 pcf and 27% respectively. There were a series of dry density and water content tests run during construction. The relationship between dry density and water content from these tests is shown on Fig. 3.2.3.

The liquid limit of the Healy Clay was 32% and the plastic limit was 25% giving a plasticity index of 7.

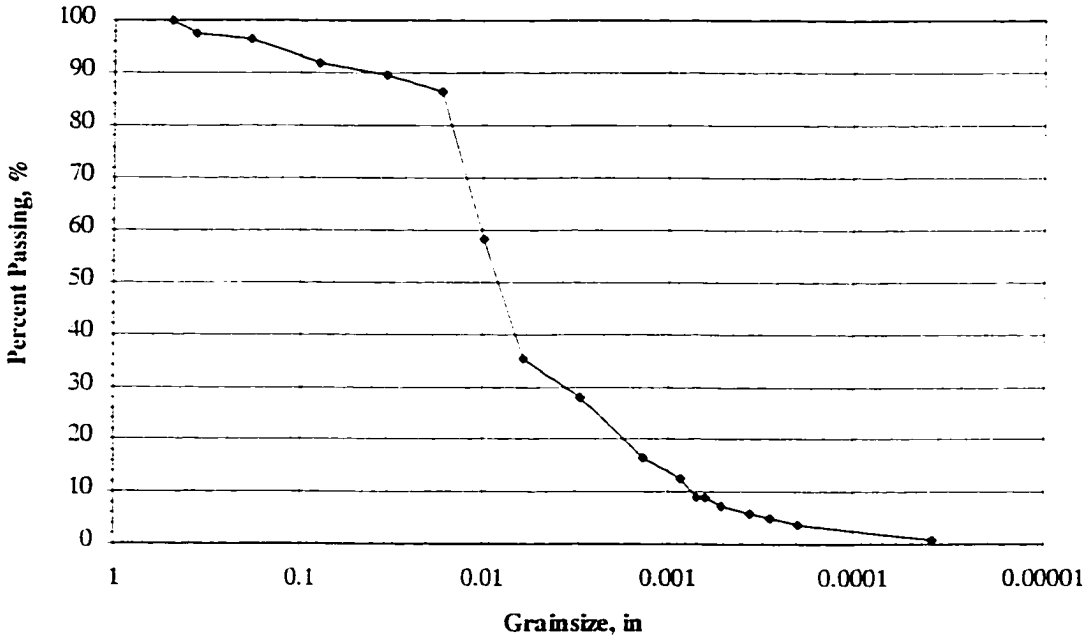

Fig. 3.2.1 Grainsize Distribution of Healy Clay subgrade

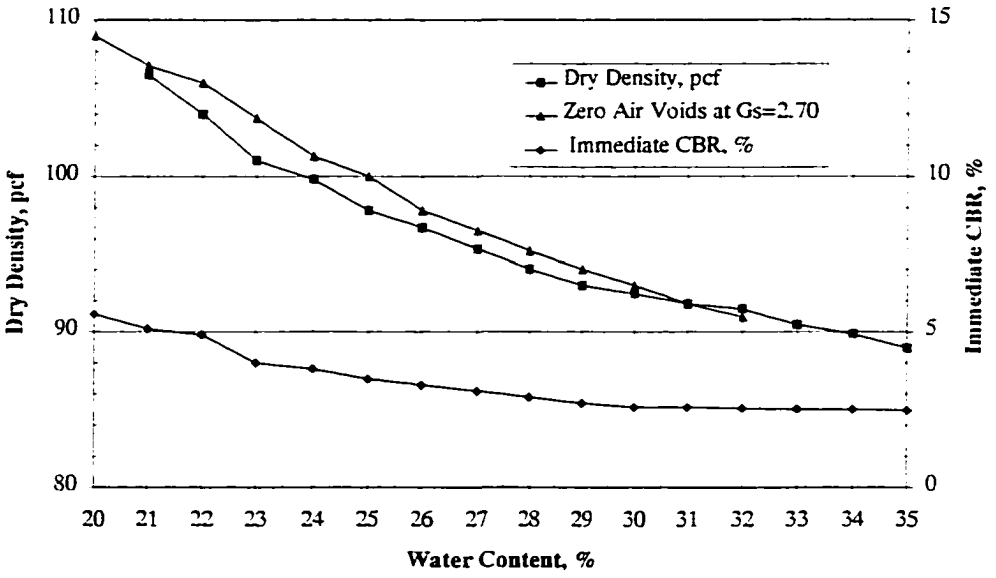

Fig. 3.2.2 Relationship between Water Content, Density and CBR from Modified Proctor Compaction Tests

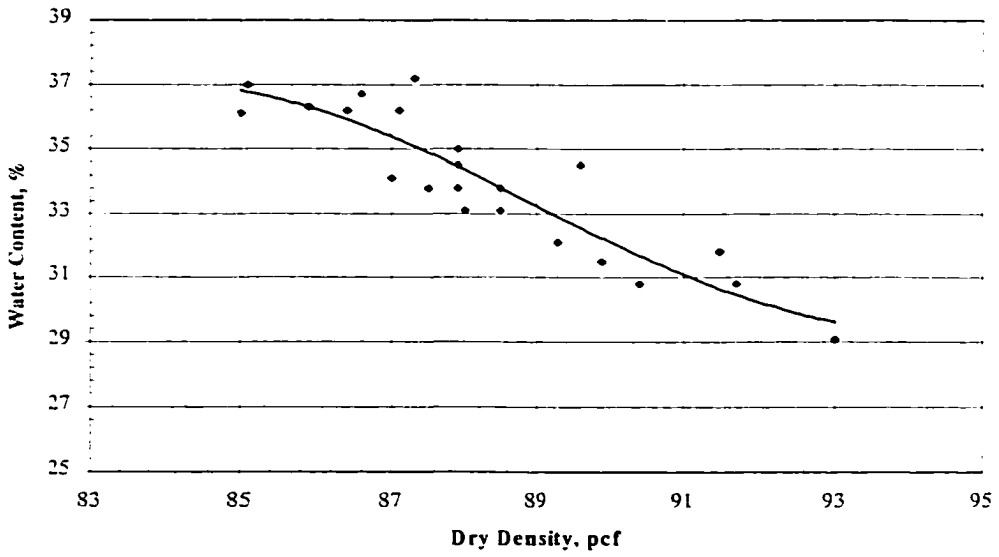

Fig. 3.2.3 Relationship between water content and dry density from Nuclear Tests in the field

3.3 Asphalt

The asphalting for Test A was done by a Fairbanks paving company, specializing in driveways and other small areas. They used a type II gradation for their aggregate and about 5.5% of a 2.5 penetration grade asphalt for the binder. The resulting mix was expected to be weak for highway paving purposes, but it is easy to work with in the test facility. Normally, asphalt is placed and compacted in less than two hours. It took about 3 hours to place and compact the asphalt in this test. This means that the asphalt was marginally cool by the time compaction was complete. Therefore the asphalt for this test was not up to highway specifications, however, since this is a comparative study, it should not effect the conclusions developed by the research. This statement is explored further below.

Due to an unusual fall storm which shut down all asphalting in Fairbanks on September 11, the asphalt for Test B was brought from Anchorage (about 350 miles away). In spite of the circumstances, the asphalt was hot and the placement and compaction went well. The asphalt was prepared for pothole patching in Anchorage and we do not have any data on its composition. Its density was slightly below that usually required in highway construction. The asphalt density does have some effect on the vertical deformation. Since the test was for comparison of a reinforced section with an unreinforced section, if the two sections have the same conditions, the significance is diminished. This statement is further examined below.

A pavement design software, ELSYM5, was used to compare the effects of variable asphalt modulus on the vertical deformation. Asphalt elastic modulus values

of 70,000 psi, 25,000 psi, 8,000 psi, and 1,000 psi were used. The other moduli are shown below.

	Asphalt	Base	Subgrade	Geogrid
Thickness, in	2	8	24	0.05
Elastic Modulus, psi	varies	25,000	16,000	85,000

Fig. 3.3.1 shows the effects of variable asphalt modules on the vertical deformation of the road surface. Select values are show below.

Reinforcing	A/C Modulus	Calculated deflection
Reinforced	70,000	0.01868
Reinforced	1,000	0.02221
Calculated variance		15.9%
Unreinforced	70,000	0.01882
Unreinforced	1,000	0.02262
Calculated variance		16.8%

However, if we consider the ratio, R=dc/dr, (deformation in reinforced section with unreinforced section), the results are very close as shown below.

Reinforcing	A/C Modulus	Calculated deflection
Reinforced	70,000	0.01868
Unreinforced	70,000	0.01882
Calculated variance		0.7%
Reinforced	1,000	0.02221
Unreinforced	1,000	0.02262
Calculated variance		1.8%

A variance of less than two percent is certainly within the range of acceptability for highway design.

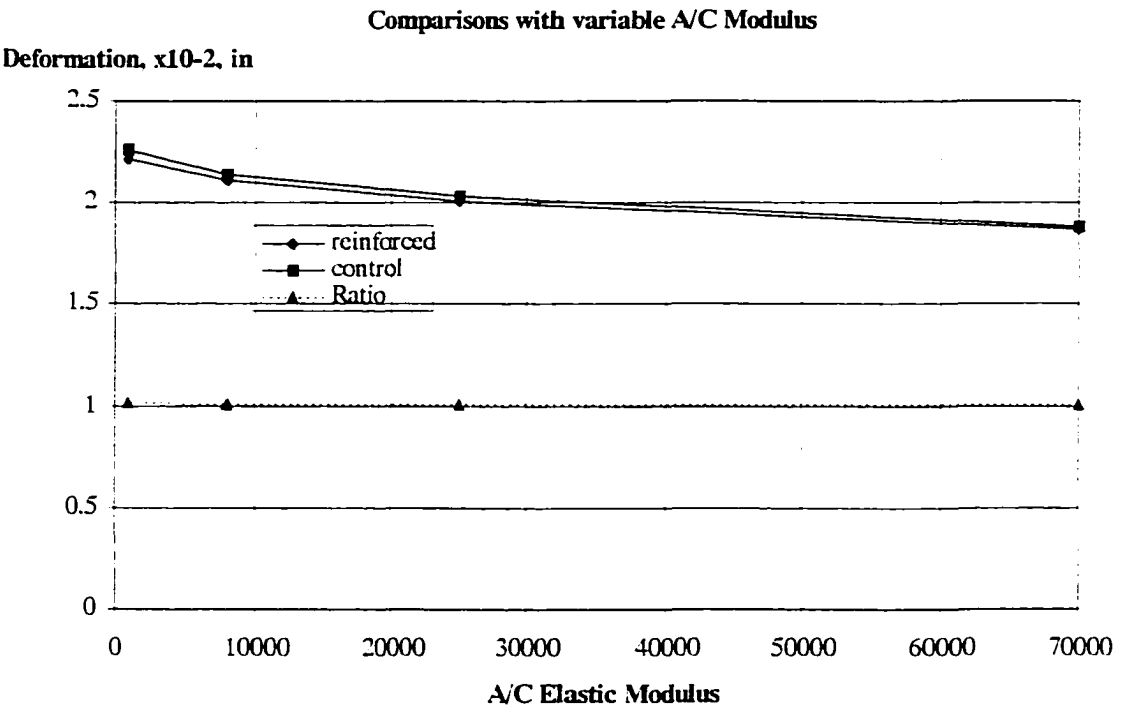

Fig. 3.3.1 The influence of Asphalt Modulus

3.4 Geosynthetics

Table 3.4.1 lists the geosynthetics used in Tests A and B.

Table 3.4.1 Geosynthetics used in the research

	BR-1	BR-2
Test No.	B	A, B

The properties of geogrid BR-1 and BR-2 are listed in Table 3.4.2. These tests were run in the Tensar Corporation Laboratories.

Table 3.4.2 The properties of geogrid BR-1 and BR-2 (Tensar)

PROPERTY	TEST METHOD	UNITS	BR-1	BR-2
Interlock				
Aperture Size	I.D. Calipered			
MD		in	1.0 (nom)	1.0 (nom)
CMD		in	1.3 (nom)	1.3 (nom)
Open Area	COE Method	%	70 (min)	70 (nom)
Thickness	ASTM D1777-64			
Ribs		in	0.03 (nom)	0.05 (nom)
Junctions		in	0.11 (nom)	0.16 (nom)
Secant Aperture Stability Modulus @ 20 cm-kg	Grid Aperture Test University of Alaska Fairbanks	cm-kg-deg	3.2	6.5
Reinforcement				
Flexural Rigidity MD	ASTM D1388-64	mg-cm	250,000 (min)	750.000 (min)
Tensile Modulus MD	GRI GG1-87	lb/ft	14,000(min) 1	
Junctions				
Strength	GRI GG2-87	lb/ft	765 (min)	18,500
Efficiency	GRI GG2-87	%	90 (min)	1080 (min)
Material				
Polypropylene	ASTM D4101 Group1/Class1/Grade2	%	98 (min)	98 (min)
Carbon Black	ASTM 4218	%	0.5 (min)	0.5 (min)

3.5 In Situ Material Properties

In order to check the consistency of the reinforced and non-reinforced sections, several field tests were conducted, such as CBR tests, dry densities, moisture content tests, and vane shear tests.

The field CBR test apparatus used is shown in Fig. 3. 5.1.

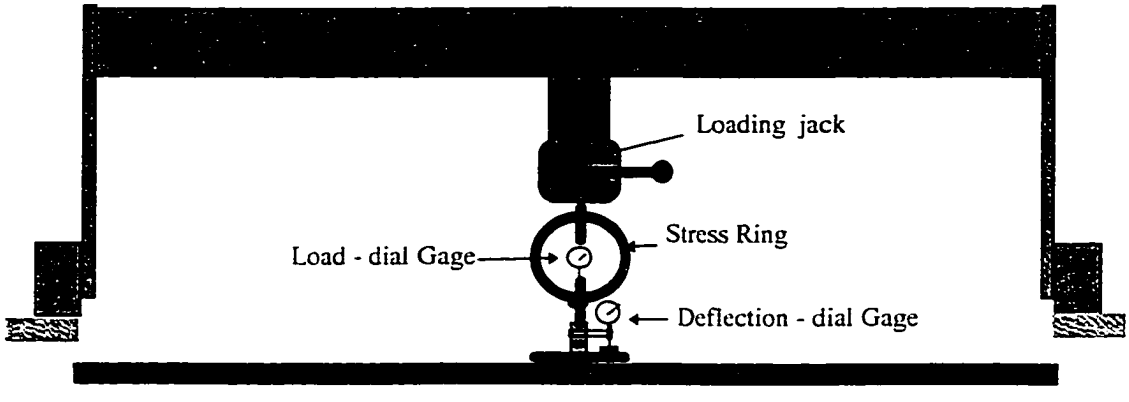

Fig. 3.5.1 Field CBR test setup.

Vane Shear is a type of test (ASTM D-2573) that can be used during the construction. The Vane Shear apparatus consists of four blades on the end of a rod, as shown in Fig. 3.5.2. The vanes of the apparatus are pushed into the soil, and torque is applied at the top of the rod to rotate the vanes. This induces failure in a soil of a cylindrical shape surrounding the vanes.

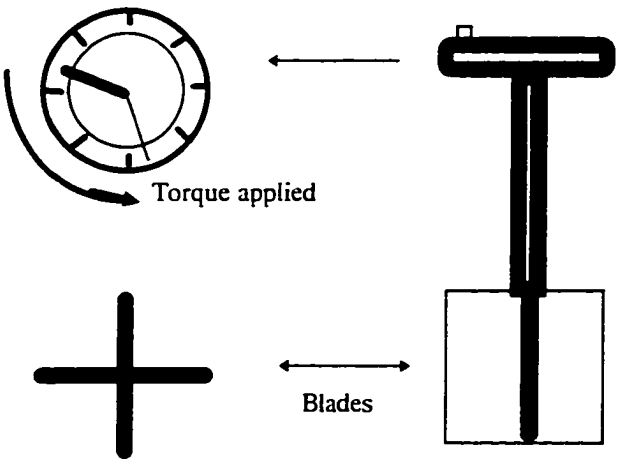

Fig. 3.5.2 Vane Shear Test

The field Dry Density and Moisture content were measured by Nuclear Method (ASTM D 2950). See Fig. 3.5.3.

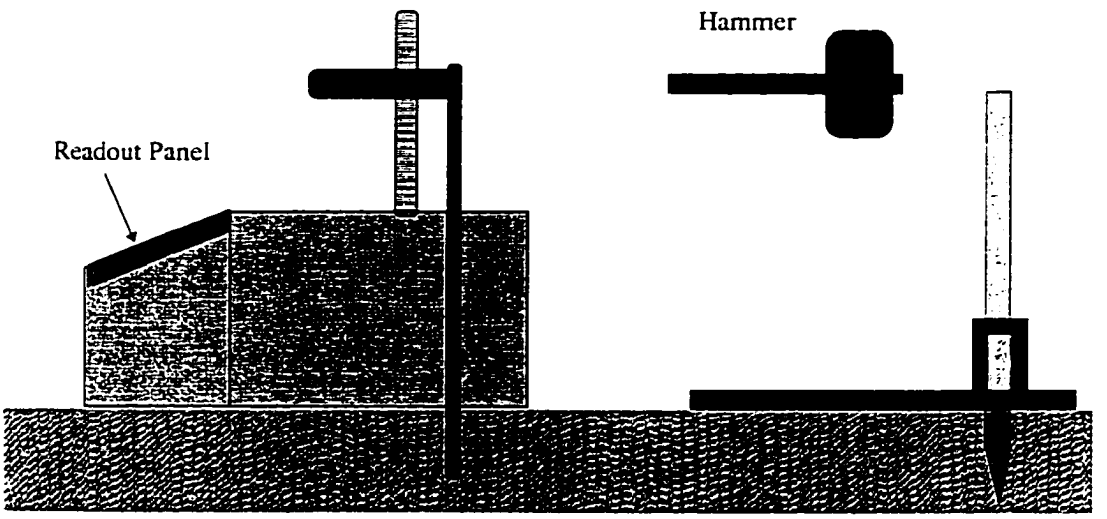

Fig. 3.5.3 Nuclear Test Equipment

3.5.1 Test A

Test A consisted of two sections, one with BR-2 at the bottom of the base and the other unreinforced (control). Two inches of A/C over 2 inches to 10 inches of crushed base and a clay subgrade were used over the entire area.

The field properties of the asphalt, base, and subgrade are shown in Table 3.5.1. The dry density of the base in section 1 is a little lower than that in section 2.

Table 3.5.1 The field properties of Test A

Section	Line #	Dry Density pcf			Water Content %	
		A/C	Base	Subgrade	Base	Subgrade
Section 1	4	119.7	127.2	90.5	3.0	30.0
BR-2	12	115.1	128.8	91.4	4.5	28.3
	20	119.4	128.4	93.6	8.6	19.7
Section 2	28	120.4	130.1	92.7	3.9	30.4
Control	36	116.4	133.2	93.3	4.3	29.1
Average		118.2	129.54	92.3	4.86	29.5
CV, %		0.18	1.58	1.31	39.92	0.67

* Note: CV = Coefficient of Variation = $\frac{s}{\bar{x}}$, where

$$s = \text{Standard Deviation} = \sqrt{\frac{n\sum \bar{x}^2 - (\sum x)^2}{n^2}}$$

$$\bar{x} = \text{Average value} = \frac{\sum_{1}^{n} x_i}{n}$$

3.5.2 Test B

Test B consisted of 4 sections. The 2 inches of A/C were over a crushed rock base of 6 inches to 12 inches in sections 1 and 2, and 6 inches to 18 inches in sections 3 and 4.

Fig. 3.5.4 shows the in situ dry density and water content of the Healy clay. It appears that all the sections have similar values.

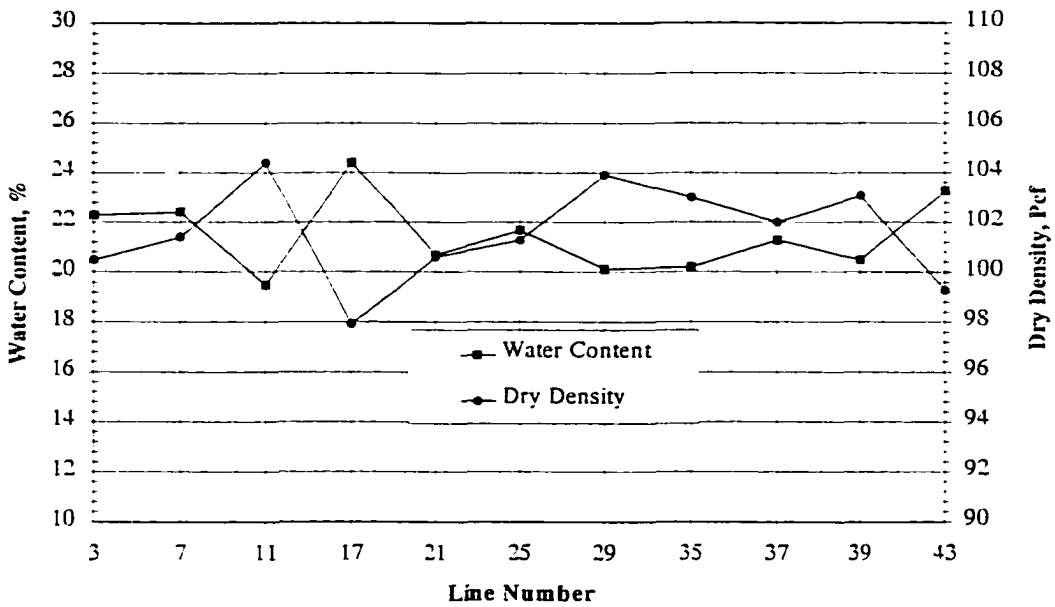

Fig. 3.5.4 Dry Density and Water Content of Healy Clay

Many vane shear strength tests were conducted on the Healy clay subgrade used in Test B. Fig. 3.5.5 shows the test results. The vane shear strength values appear to be consistent except for section 4 where they are slightly lower than for other sections.

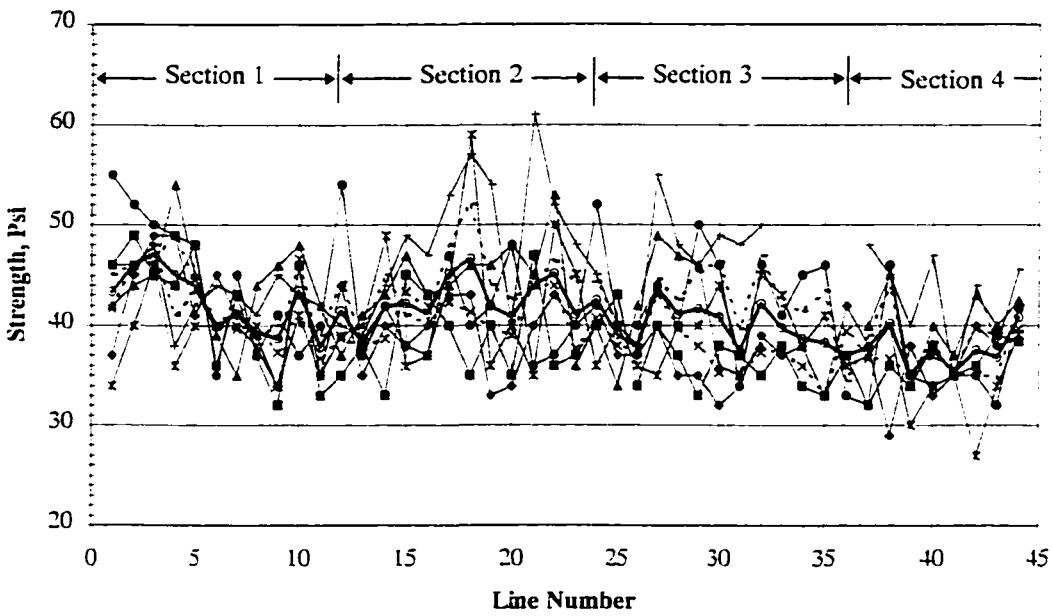

Fig. 3.5.5 Vane Shear Tests on Healy Clay

Table 3.5.2 is the summary of the field properties of materials used in Test B. It shows that the CBR values of clay subgrade on Section 2 are higher than for other sections; however, the other properties are reasonably consistent.

Table 3.5.2 In Situ Material Properties of Test B

		Section 1	Section 2	Section 3	Section 4	Average	CV, %
A/C	Density pcf	142.7	138	141.5	139.3	140.4	1.51
	Stability lbs	245	265	260	322	273	12.36
Base	CBR %	16.0	14.2	13.4	17.7	15.3	12.55
Subgrade	CBR %	1.8	2.8	1.6	1.6	1.9	27.89
	Vane Shear, psi	42	43	41	37	40.8	0.64
	Density pcf	102.1	99.3	102.7	101.5	101.6	1.94
	Water Content, %	21.4	22.6	20.7	21.7	21.5	6.93

Chapter 4. Test Road Design and Test Results

The test box was 48 feet long, 8 feet wide, and 4 feet high. The bottom 18 inches was filled with compacted pit run sand and gravel. The test road sections were constructed by compacting the soil in layers in the box. The layers of base and subgrade are varied from test to test. The surface was paved throughout the full area.

As mentioned before, Tests No. 1 and No. 2 were run as shakedown tests to evaluate the test procedures and instrumentation. Tests No. 3 (Test A), No. 4 and No. 5 (Test B) were run to evaluate the geogrids performance as base reinforcement. Test A was run with 2,500 pounds in the loaded direction and 2,000 pounds in the unloaded direction throughout the test. Test B was run with 4,500 pounds in the loaded direction and 2,000 pounds in the unloaded direction. The loading on Test No. 4 was varied throughout the test making it very difficult to compare the results to the other two tests, hence only the results of Tests No. 3 (Test A) and No. 5 (Test B) are presented herein.

4.1 Test A

Test A consisted of two sections, one with BR-2 at the bottom of the base and the other unreinforced (control). Each consisted of 2 inches of asphalt over a crushed rock base and a clay subgrade. The base was tapered from a thickness of 2 inches to 10 inches. This setup was used in order to define the benefit of the geogrid at a variety of base course depths.

4.1.1 Design of the Test Road

Fig. 4.1.1 shows a plan view and a cross section of the test apparatus.

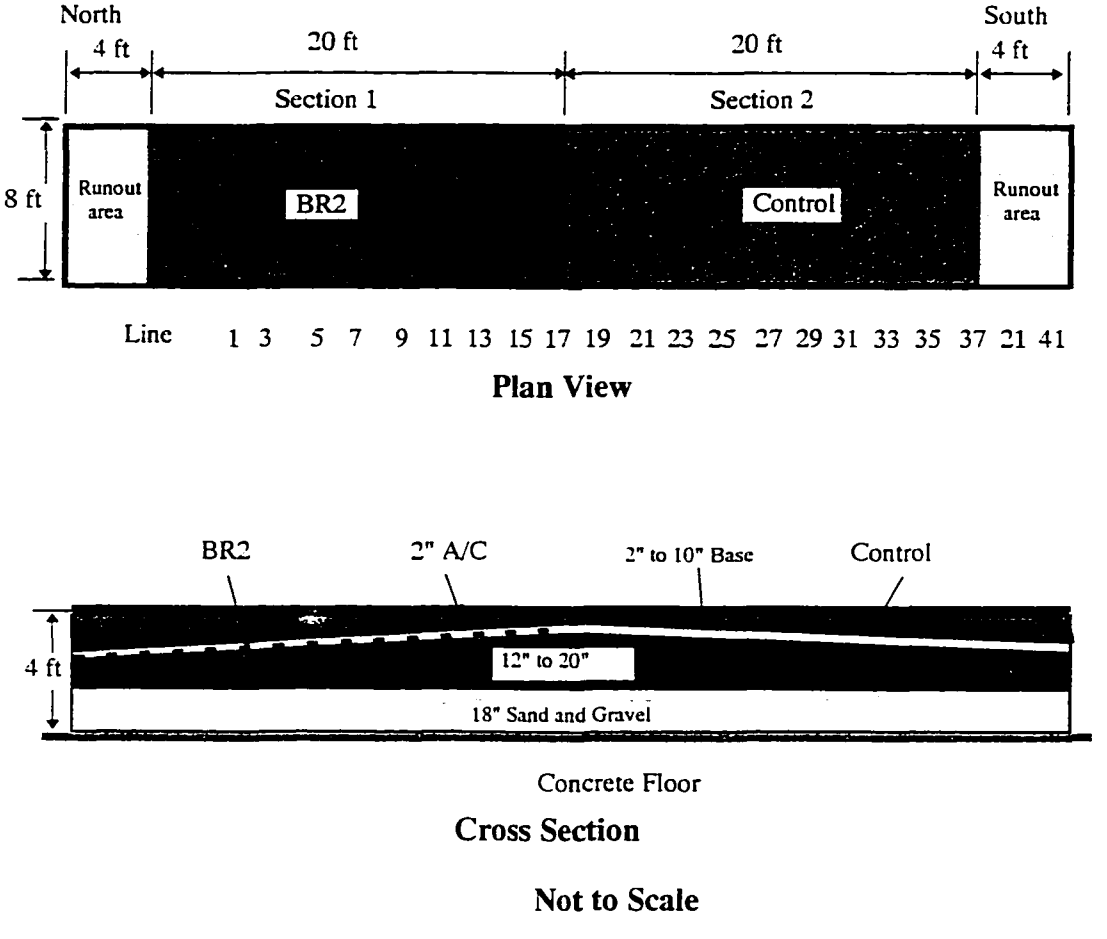

Fig. 4.1.1 Plan view and cross section of Test A.

The center 40 feet of the test box were divided into two test sections. The northern half of the test had BR-2 under the base and the southern half was a control section, otherwise they were mirror images of each other. The entire surface was covered with 2 inches of A/C. The base was sloped from 2 inches at the center to 10 inches at the end of the test section. The subgrade from Test No. 2 was left in place. The clay surface was regraded and the instrumentation was reconstructed, but otherwise the subgrade was left untouched.

4.1.2 Loading Sequence

The load was applied through a single 10.00 tire inflated to 80 psi. The tread was 9 inches wide and the tire diameter was approximately 42 inches. The cart was kept in a single track.

It was the intent to start with low loads and gradually work up to 4,500 pounds in the loaded direction. However, there was significant deformation at 2,500 pounds per cycle in the areas where there was less than 3 inches of crushed rock base and a maximum load of 2,500 lb. was used throughout. The test was continued until there was at least 1.5 inches of vertical deformation everywhere. The first time a pavement section reached 3 inches of deformation a strip was cut from the surface to measure the shape of the deformed subgrade and the thickness of the A/C and base. The rut was then filled with base course materials and the test was continued. The rutted areas were filled with base course materials every time the rut approached 3 inches to allow the cart to

continue, but no measurements were made after the first filling. The test was continued until the most stable portion of the test experienced at least 1.5 inches of deformation.

4.1.3 Deformation Measurements

Surface Deformation

The surface deformation was measured after a set number of cycles at intervals of every two feet along the test box as shown in Fig. 4.1.1. The number of cycles required to create 0.5, 0.75, 1.0, 1.25, and 1.5 inches of deformation was recorded.

4.1.4 Test Results

The asphalt surface deformation (rut depth) and number of cycles were recorded many times during the test. The number of cycles refers to the number of complete trips down and back.

4.1.4.1 Deformation in Longitudinal Cross Section

Since the deformation was recorded at intervals of every two feet, the deformation versus number of repetitions and base thickness in both reinforced and control sections were compared. Fig. 4.1.2 shows a longitudinal cross section through the test road at the center line of the wheel path. From the figure it is clear that:

- The thicker the base, the less the deformation;
- The deformation in the reinforced section is much less than in the control section for equal depths of base and equal number of cycles;

The maximum deformation occurred about 2 feet to the south of the intersection of the two sections.

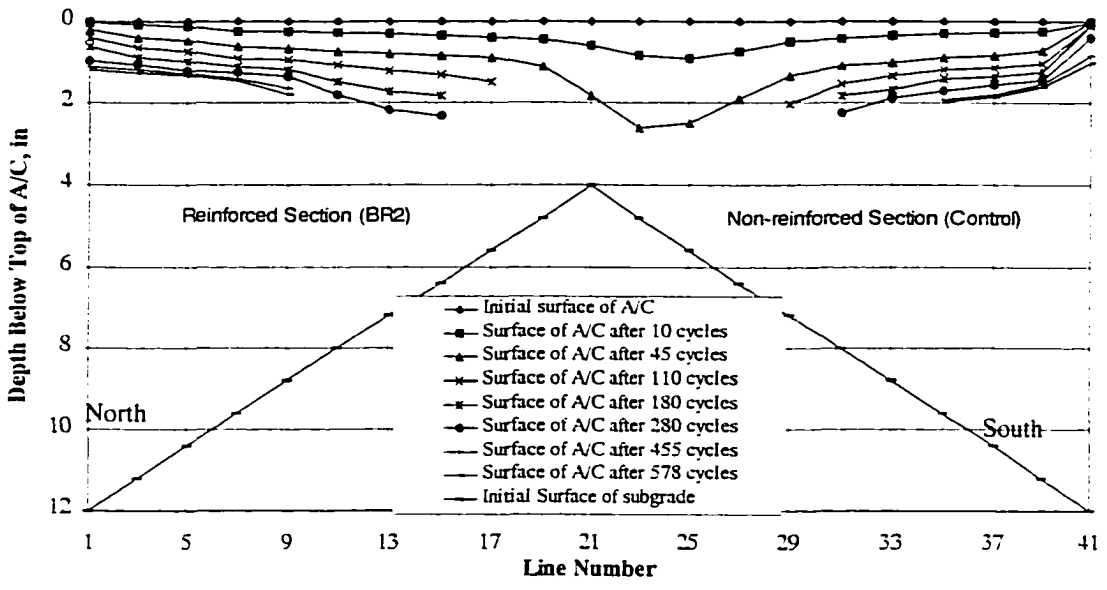

Fig. 4.1.2 Surface of A/C and subgrade at centerline of wheel during test

4.1.4.2 Number of Cycles vs. Average Maximum Deformation

The number of cycles versus deformation for the reinforced section and the control section are shown in Figures 4.1.3 and 4.1.4 respectively. The deformation shown is the average of the three maximum deformation readings under the tire.

It is obvious from these curves that the deformation is inversely proportional to the base thickness and that the reinforced section performed better than the control section.

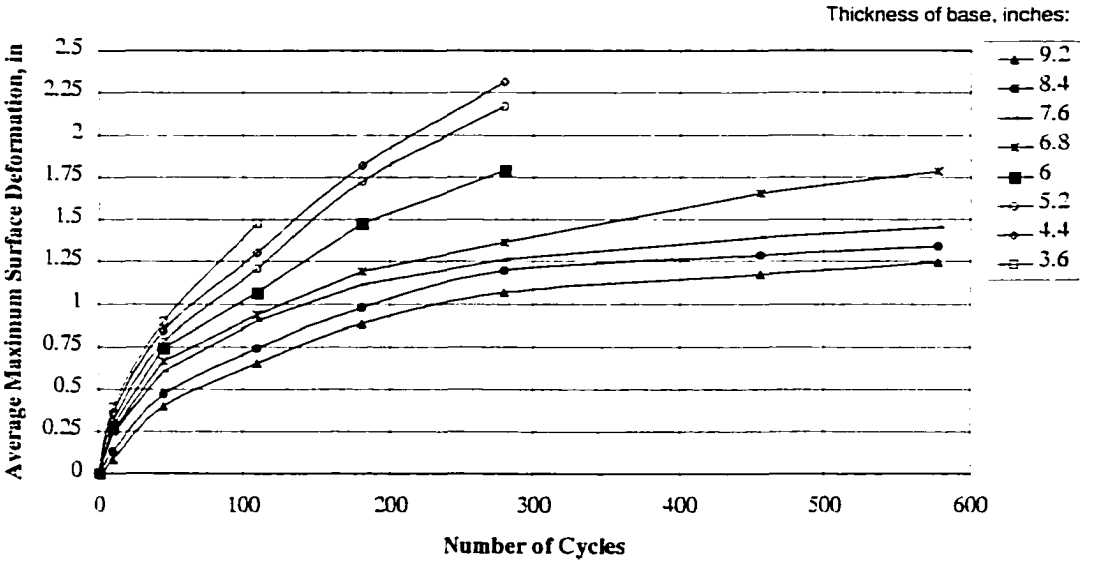

Fig. 4.1.3 Number of cycles vs. average deformation of reinforced section

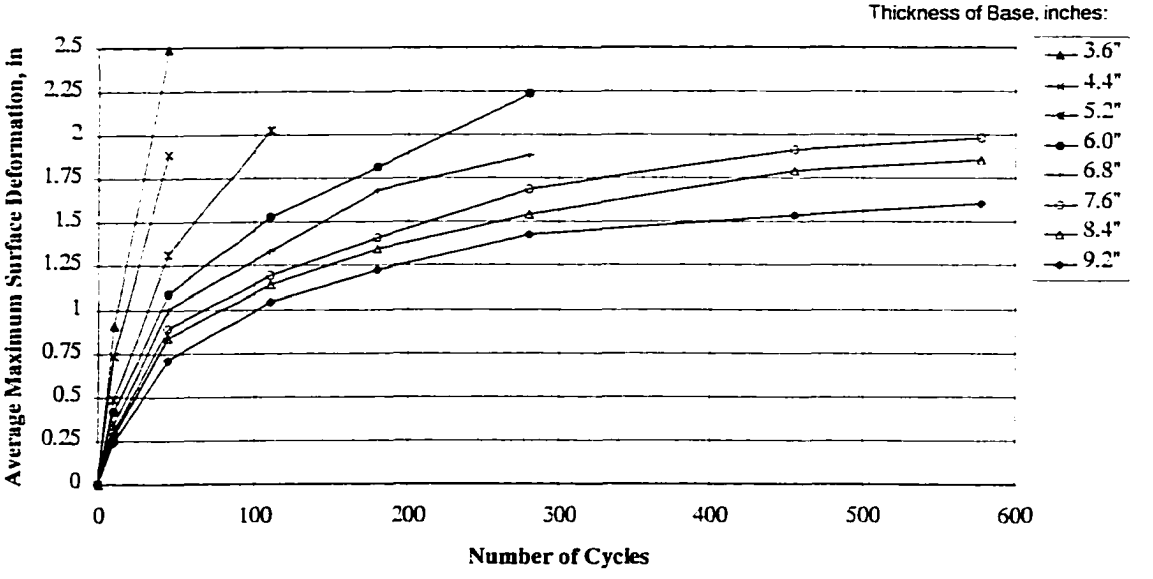

Fig. 4.1.4 Number of cycles vs. average deformation of unreinforced section

4.1.4.3 Shape of Rut

The rut shapes for various numbers of cycles at selected base thicknesses (5.2" and 8.4") are shown in Figures. 4.1.5 through 4.1.8.

The curves for the sections with 5.2 inches of base show that the maximum deformation in the reinforced section after 110 cycles is 1.4 inches and maximum upheaval is 1.1 inches, while the deformation in the control section at the same number of cycles is 2.5 inches and upheaval is 1.7 inches. For 8.4 inches of base, the maximum deformation in the reinforced section at 280 cycles is 1.4 inches, while the maximum deformation in the control section at the same number of cycles is 1.75 inches. The upheaval is about 0.4 inches in both sections.

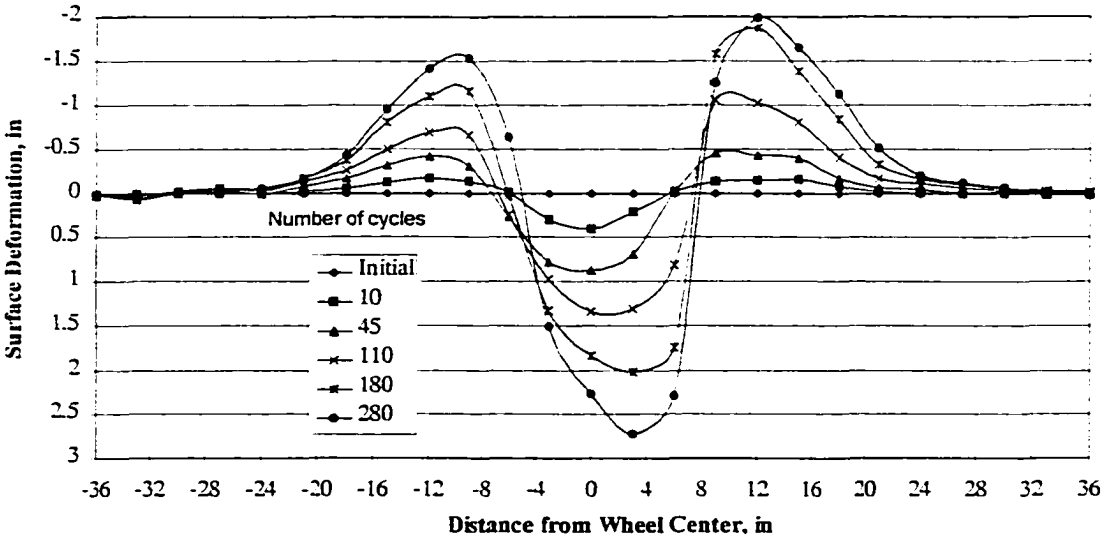

Fig. 4.1.5 Shape of rut in reinforced section (5.2" base)

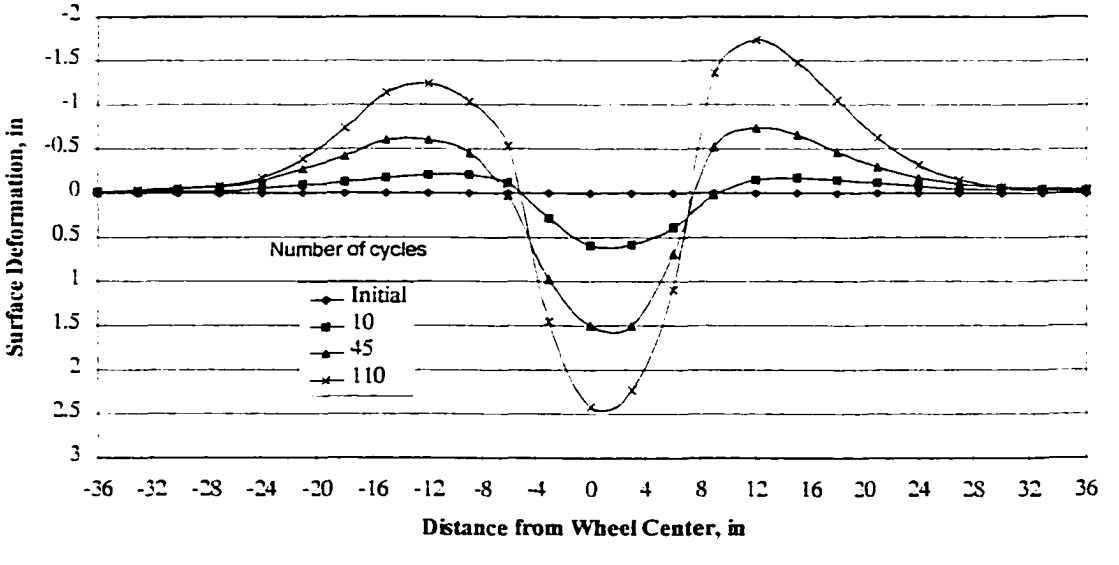

Fig. 4.1.6 Shape of rut in unreinforced section (5.2" base)

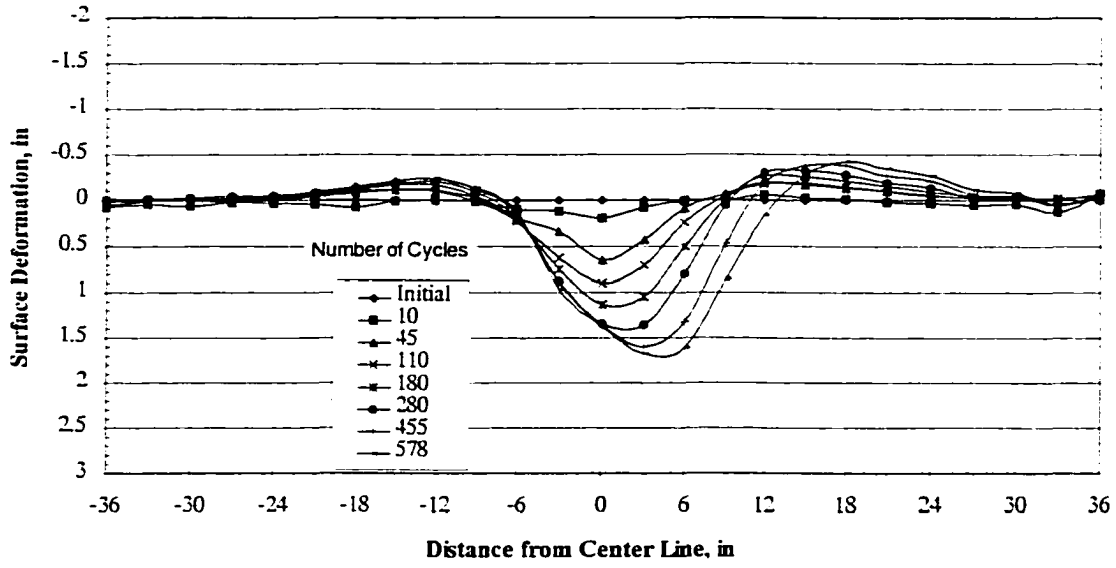

Fig. 4.1.7 Shape of rut in reinforced section (8.4" base)

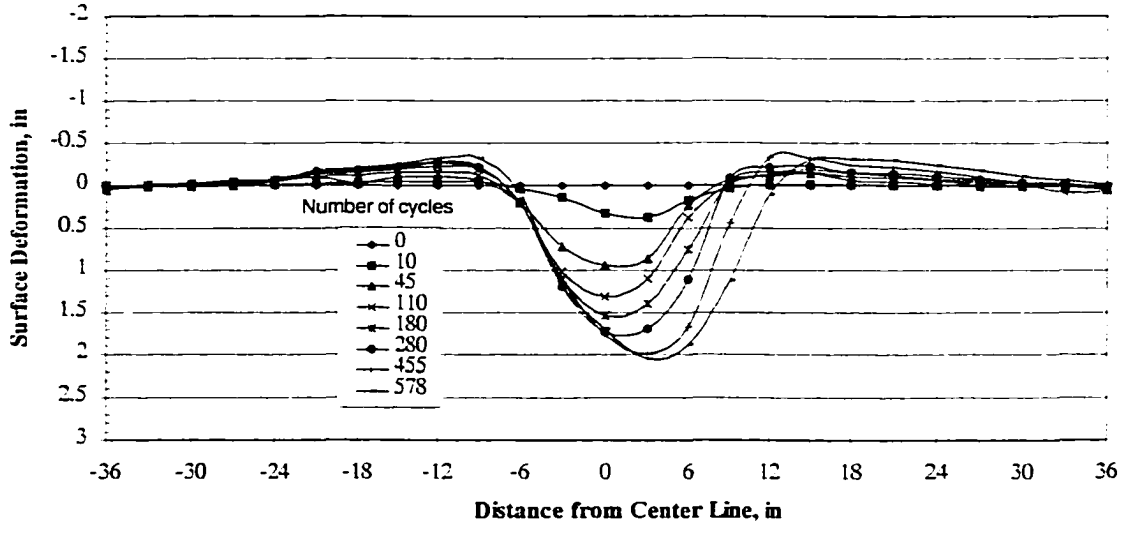

Fig. 4.1.8 Shape of rut in unreinforced section (8.4" base)

4.2 Test B

After the framework from Test No.4 was dismantled and the test bed was cleaned, the clay subgrade and base material were reconstructed for Test B. This test consisted of four sections. Each section had two inches of asphalt over crushed rock base over Healy clay subgrade.

4.2.1 Test Road Setup

Four test sections were constructed. Each section was 11 feet long. Two feet of each end were runout areas. The contact between the base and subgrade was tapered in each section to test a wide range of base thicknesses. See Fig. 4.2.1.

The four sections had these different combinations of geogrid reinforcement:

Section	1	2	3	4
Reinforcement	BR2	BR1	None	Double layers BR1

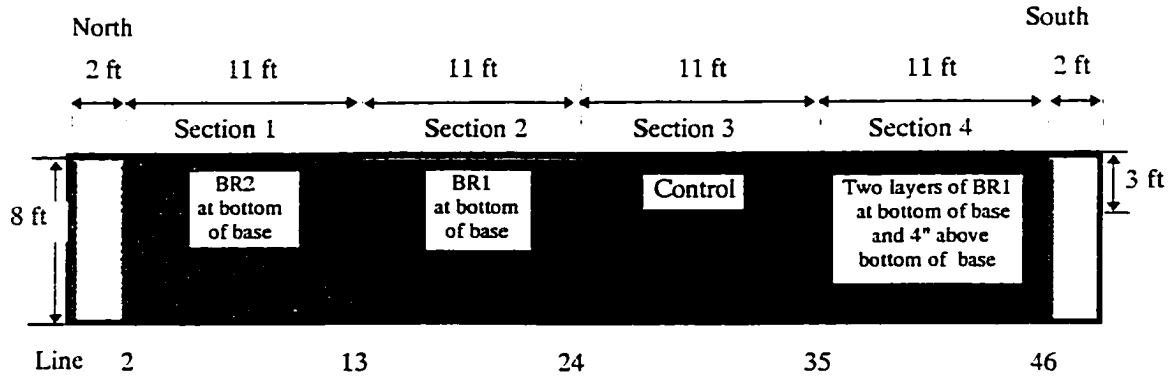

Plan View

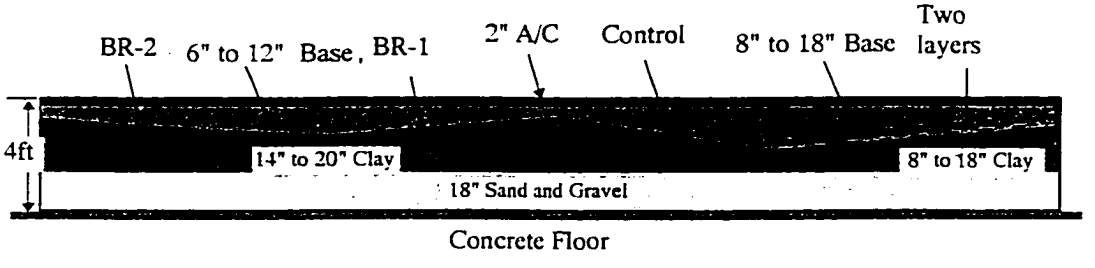

Cross Section

Not to Scale

Fig. 4.2.1 Setup of Test B

4.2.2 Loading Sequence

The load was applied through a single 10.00 bias ply tire inflated to 80 psi. The tread was 9 inches wide and the tire diameter was 42 inches. The cart was kept in a single track.

The load was kept at 2,000 pounds while moving in the return (unloaded) direction and 4,500 pounds in the forward (loaded) direction throughout the entire test. After the area between the control section and the BR-1 section reached 3 inches of deformation, the A/C pavement was cut and filled with wooden boards, and the test was continued until the most stable portion reached 1.5 inches of deformation.

On the highway, all the traffic moves in one direction. In the test, it was impossible to move the cart in only one direction. The weight of the cart is 2,000 lbs, therefore the return load was 2,000 lbs.

The following equation was used to evaluate the effect of the return load on the test results (E.J. Yoder, 1975):

$$F_j = (P_j/P_s)^4$$

where: F_j is the Equivalent Wheel Load Factor,

P_j is the actual wheel load,

P_s is the standard wheel load.

In this, P_j = 2000 lbs, P_s = 4500 lbs, therefore,

F_j = (2000/4500)^4 = 4%.

The effect of the return load is only 4% of the forward load.

This research was to compare the unreinforced section with geogrid reinforced sections. Thus, the effect of the return load on the benefit ratio is essentially zero.

4.2.3 Measurements

A/C Surface

The deformation of the asphalt surface was measured at every foot along the box several times during the test.

Deformation Within the Profile

Bison Gauges were installed in each section at several depths vertically below the center. The Bison gauge data is all suspect because it is impossible to get an electrical ground in permafrost that is good enough to mask the adjacent radio station signal. The data is not reported herein.

4.2.4 Test Results

After the test was set up, the asphalt surface deformation was measured at intervals until the deformation reached at least 1.5 inches. The test results shown here are the profile of the wheel track, the deformation vs. number of cycles, and the cross sections.

4.2.4.1 Longitudinal Profile of Wheel Track

Fig. 4.2.2 shows the longitudinal profile of the test road before and after the test. It shows that:

(1) the BR2 section takes more repetitions than the BR1 section and the control section to develop the same maximum permanent deformation;

(2) the number of repetitions required to reach the same deformation increases with increasing base thickness.

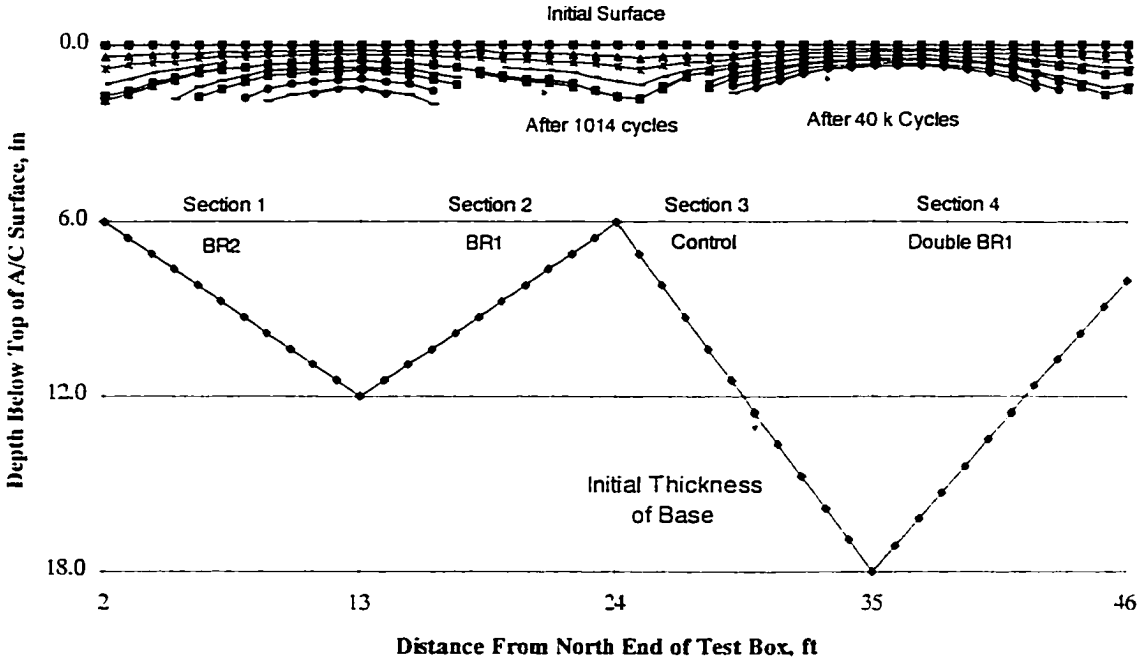

Fig. 4.2.2 Longitudinal profile of the road before and after tests.

4.2.4.2 Number of Cycles vs. Average Maximum Deformation

The number of cycles versus the average maximum deformation is shown in Figures 4.2.3 through 4.2.10. The average maximum deformation is the average of the three maximum deformation readings. These figures present the deformation within 45000 repetitions and 2000 repetitions, respectively, from section 1 to section 4.

At the lines where sections meet (13, 24, and 35), the deformations are a function of both sections; therefore the data from these lines are not considered in the later analyses.

After about 1,500 cycles the pavement between lines 18 and 26 was replaced and data no longer collected, because the deformation was so great that the cart could no longer ride over it. The test was continued until other lines reached about 1.5 inches deformation.

These figures show that the deformation of the pavement strongly depends on the thickness of base. Before about 5,000 cycles, the deformation versus number of cycles is a curved line. After 5,000 cycles, it is almost a straight line.

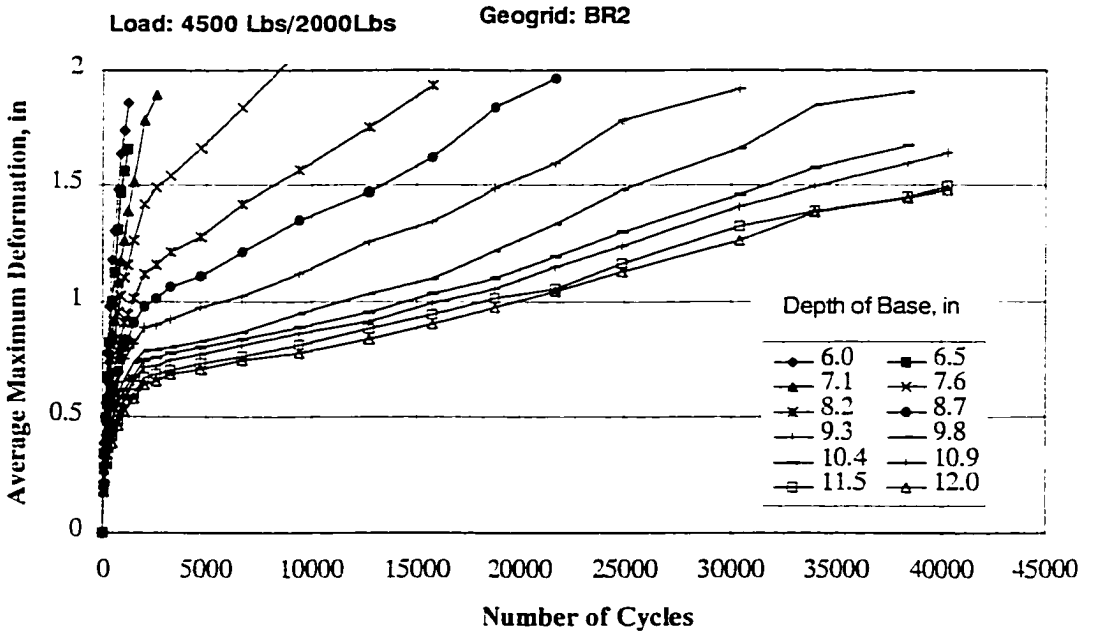

Fig. 4.2.3 Number of Cycles vs. Average Maximum Deformation in Section 1

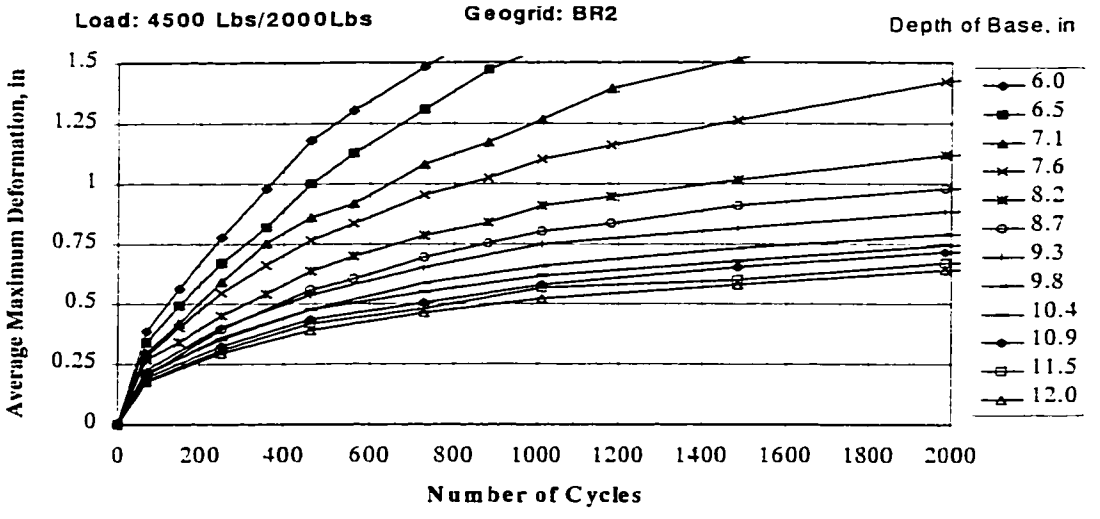

Fig. 4.2.4 Section 1 - N vs. D (0-2,000 cycles)

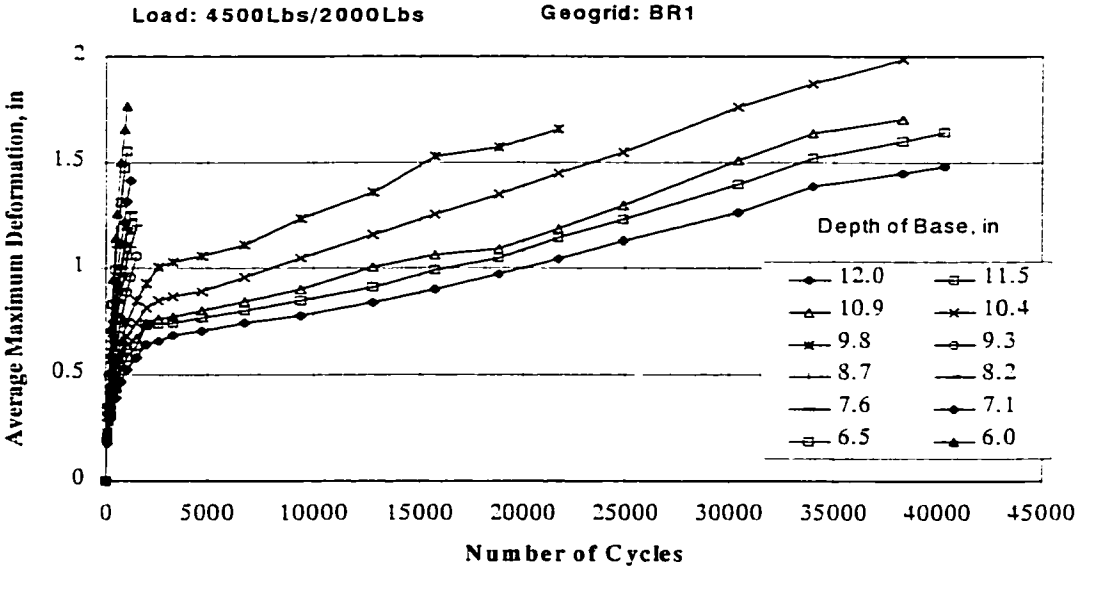

Fig. 4.2.5 Number of Cycles vs. Average Maximum Deformation in Section 2

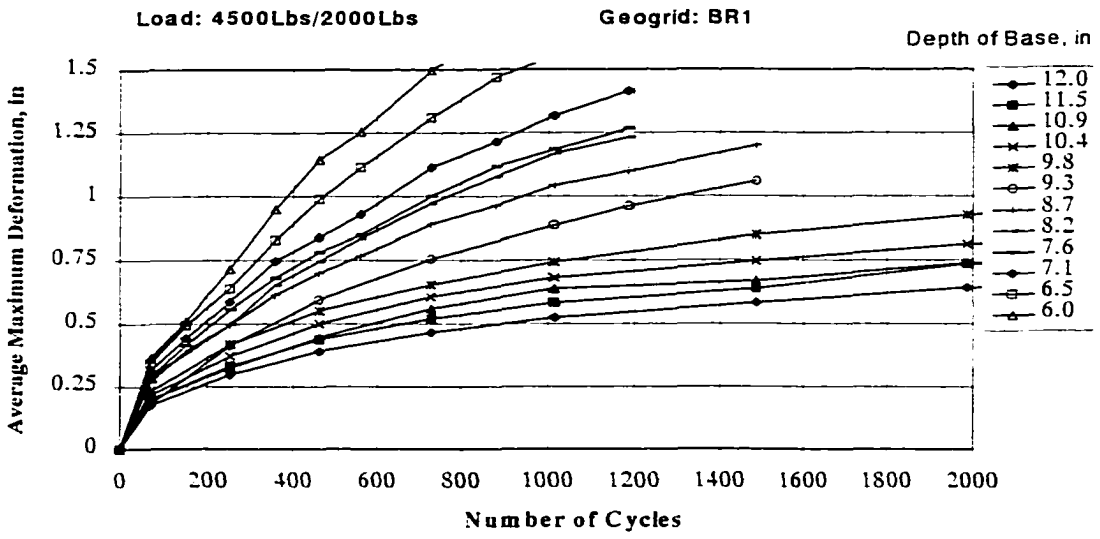

Fig. 4.2.6 Section 2 - N vs. D (0-2,000 cycles)

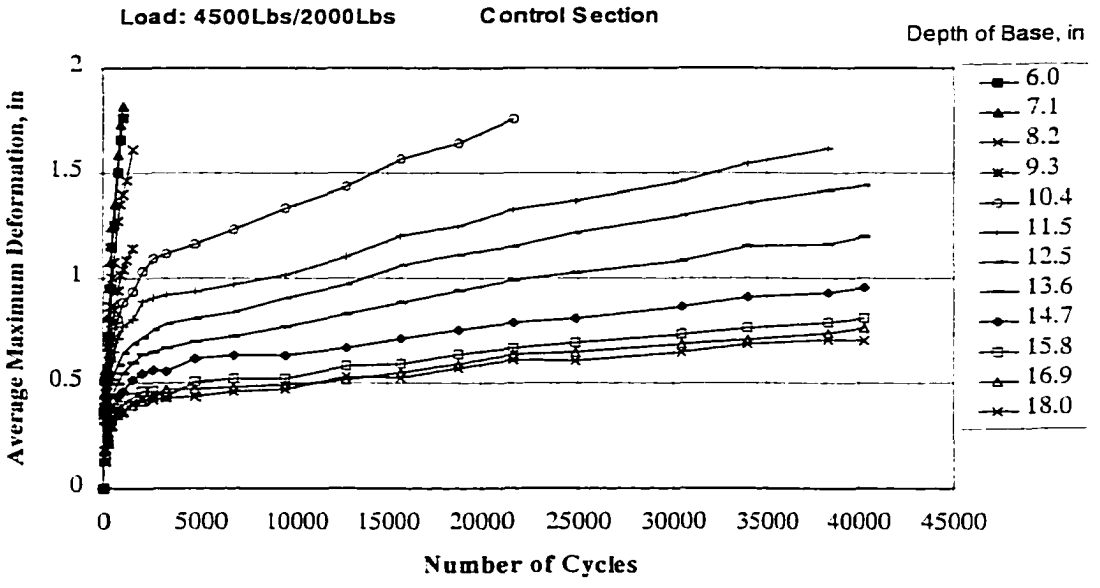

Fig. 4.2.7 Number of Cycles vs. Average Maximum Deformation in Section 3

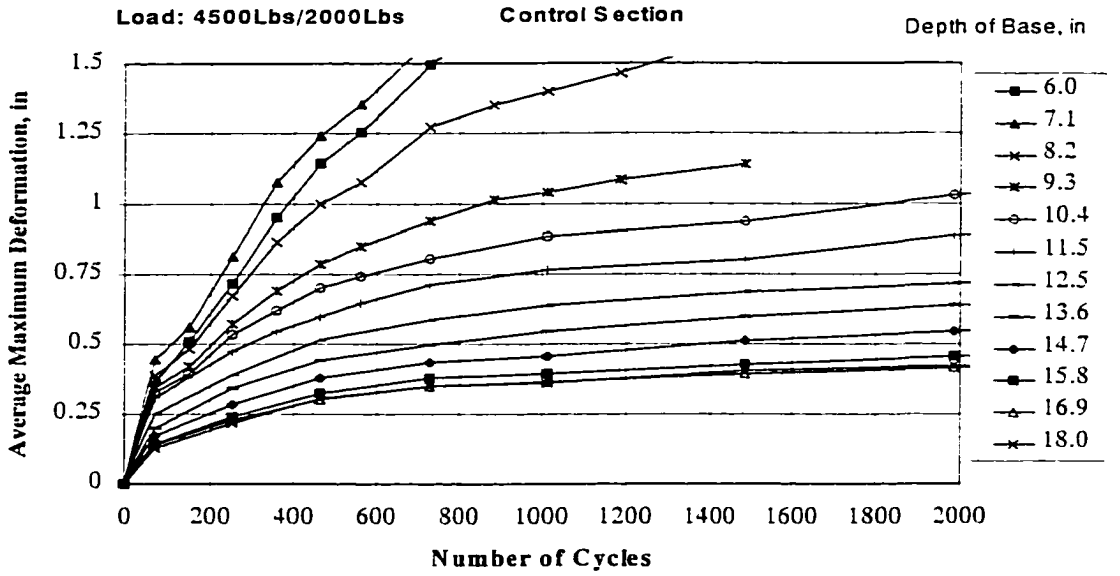

Fig. 4.2.8 Section 3 - N vs. D (0-2,000 cycles)

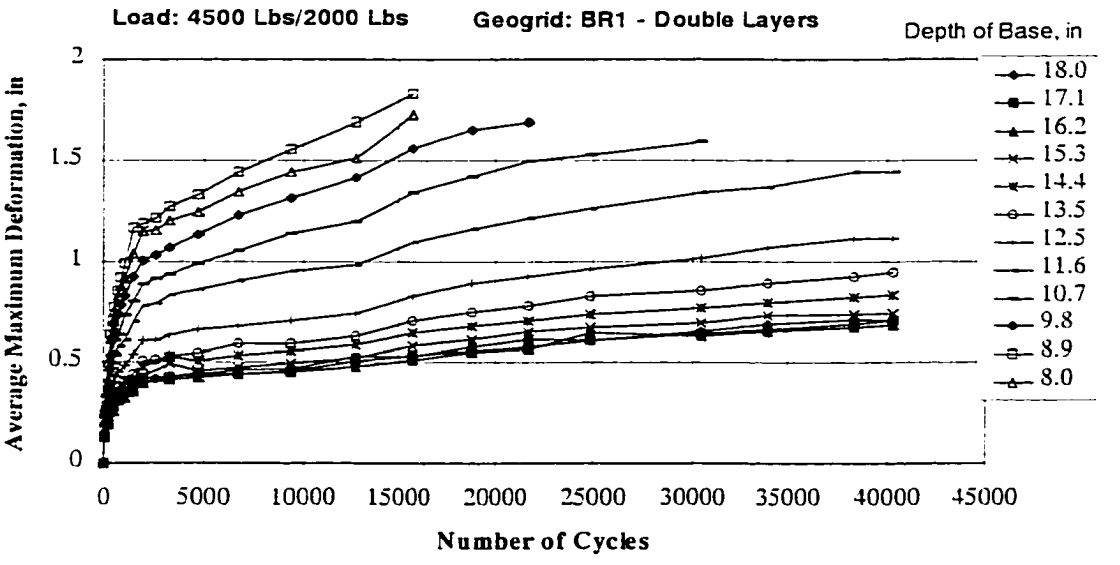

Fig. 4.2.9 Number of Cycles vs. Average Maximum Deformation in Section 4

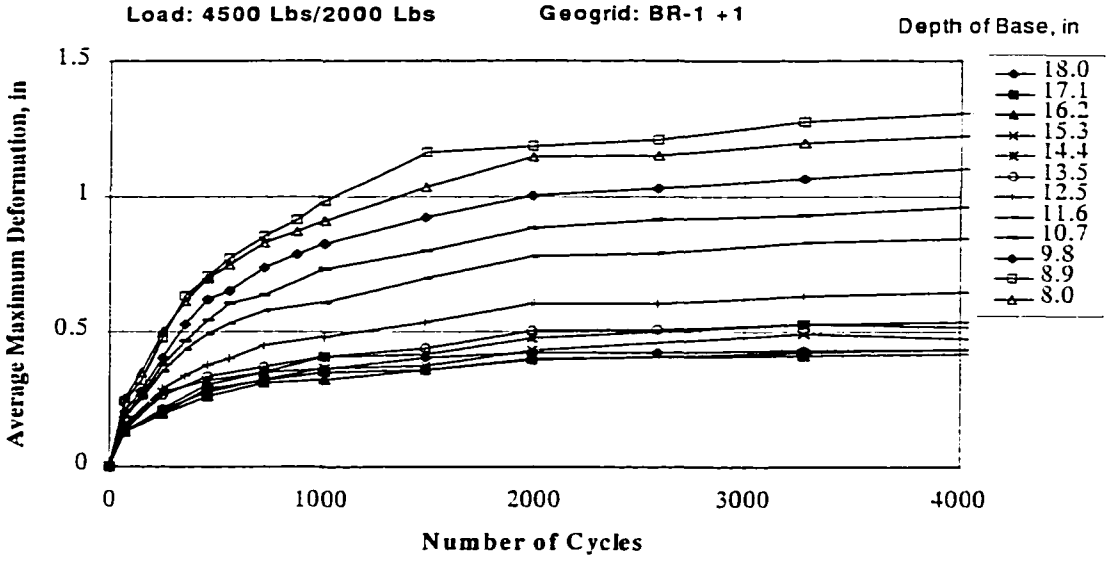

Fig. 4.2.10 Section 4 - N vs. D (0-2,000 cycles)

4.2.4.3 Surface Deformation Measurements - Profile

The shape of the rut at selected lines for varying numbers of cycles is shown in Figures 4.2.11 through 4.2.21. The lines in Sections 1 through 3 have the same base thickness (7.1", 9.3", and 11.5"), however, Section 4 has different base thickness of 9.8" and 11.6". The data in the figures show how the deformation increased as the number of cycles increased.

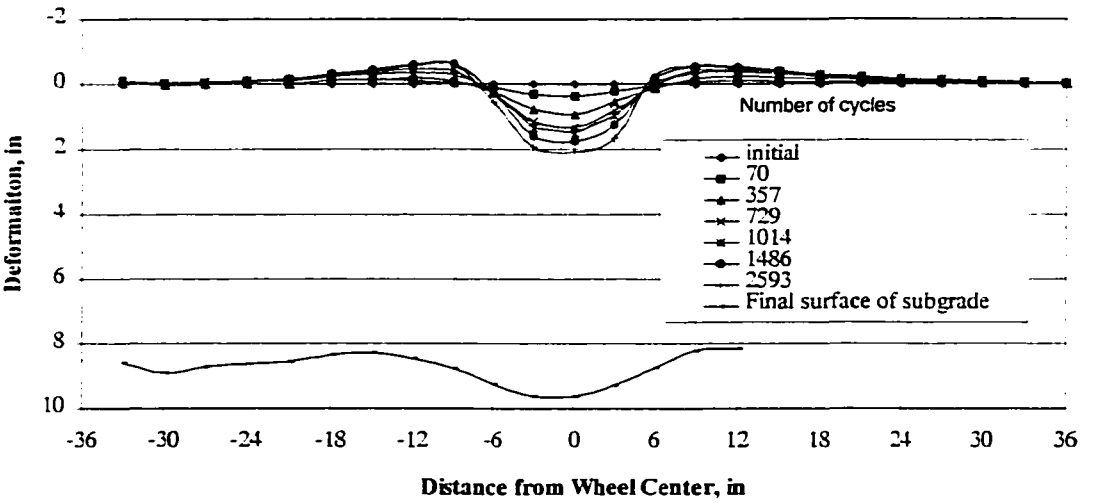

Fig. 4.2.11 Shape of Rut / Section 1 - Line 4 - at 7.1" Base

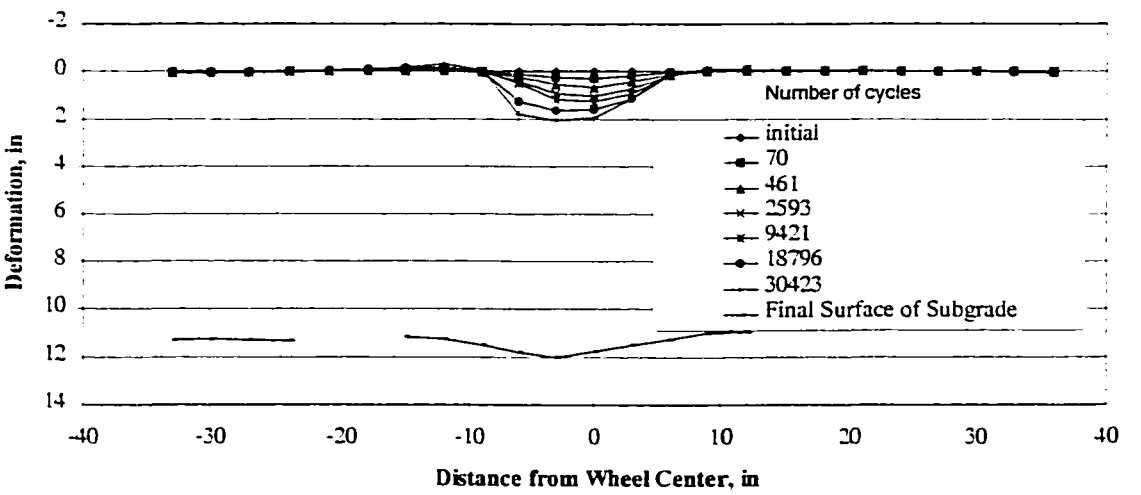

Fig. 4.2.12 Shape of Rut / Section 1 - Line 8 - at 9.3" Base

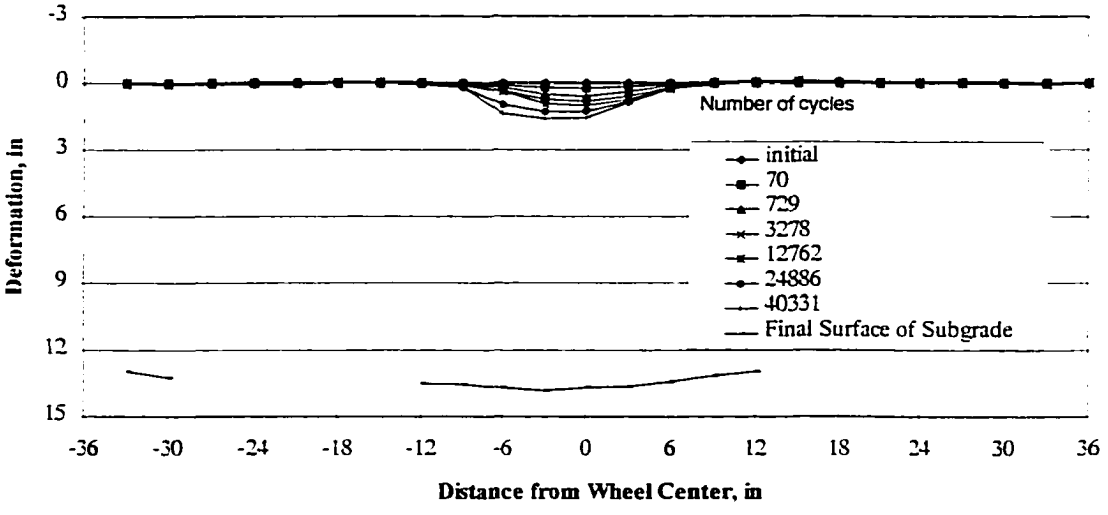

Fig. 4.2.13 Shape of Rut / Section 1 - Line 12 - at 11.5" Base

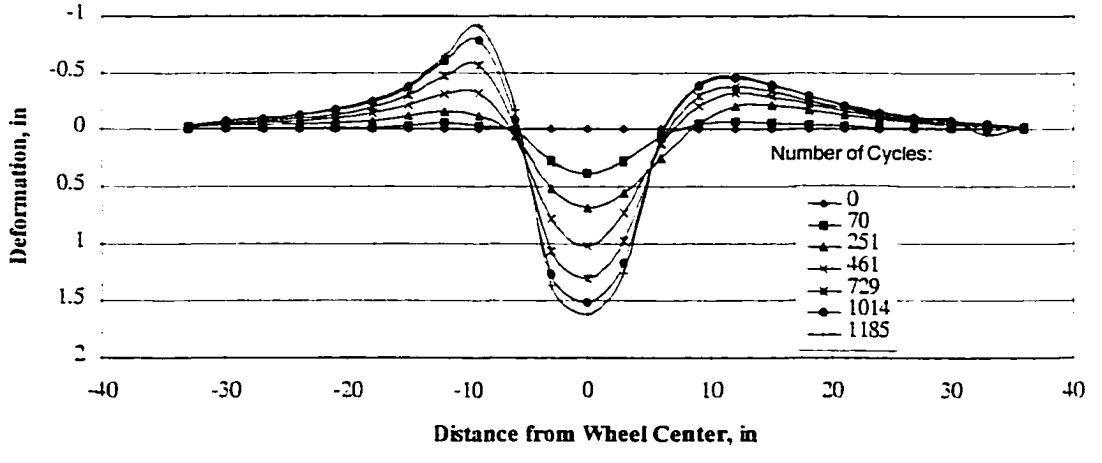

Fig. 4.2.14 Shape of Rut / Section 2 - Line 22 - at 7.1" Base

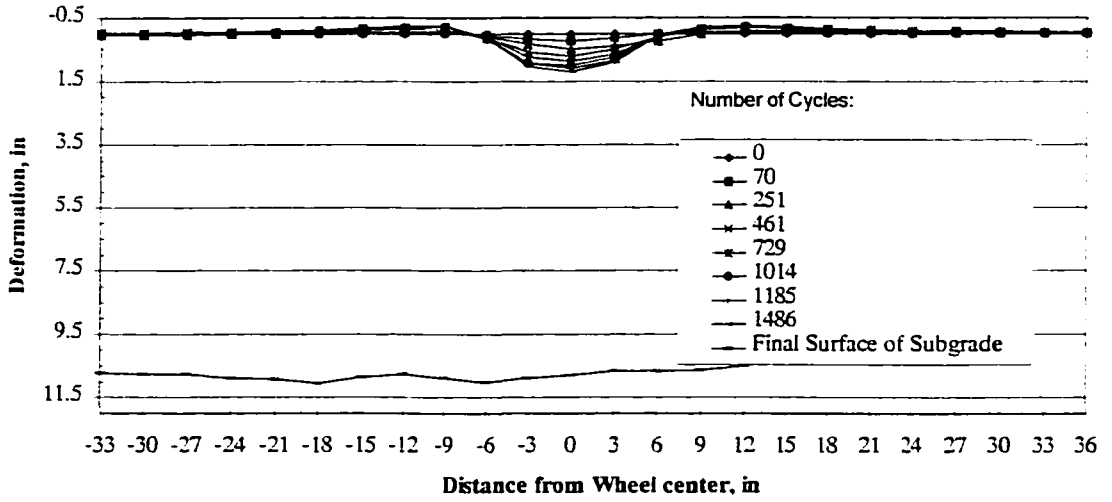

Fig. 4.2.15 Shape of Rut / Section 2 - Line 18 - at 9.3" Base

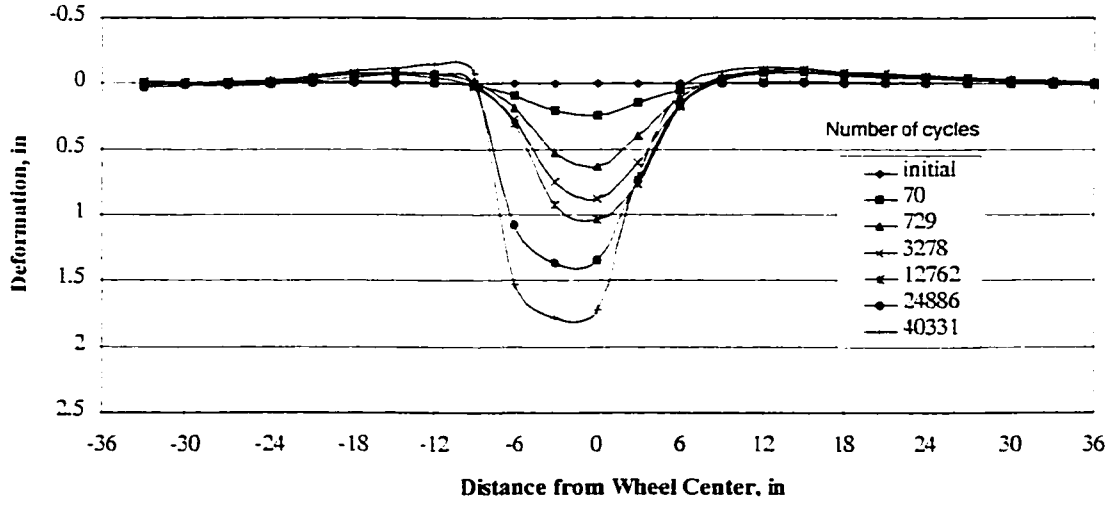

Fig. 4.2.16 Shape of Rut / Section 2 - Line 14 - at 11.5" Base

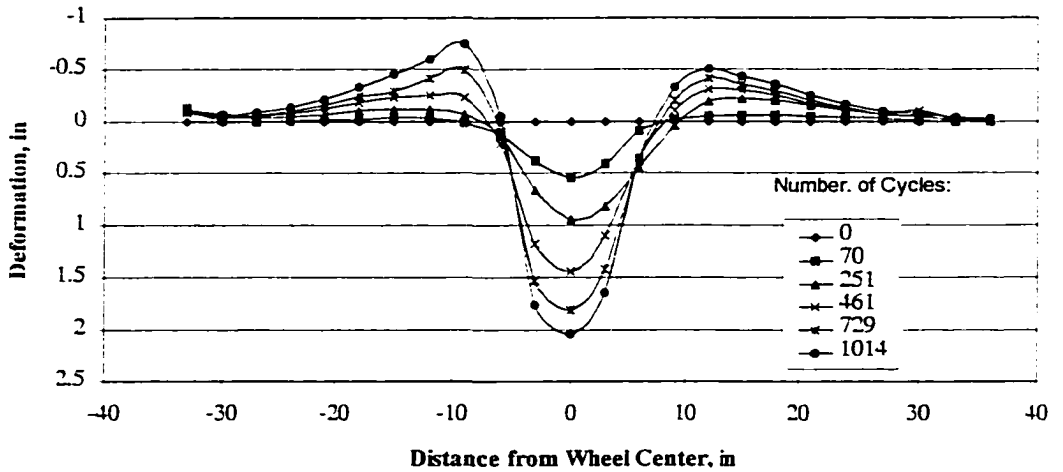

Fig. 4.2.17 Shape of Rut / Section 3 - Line 25 - at 7.1" Base

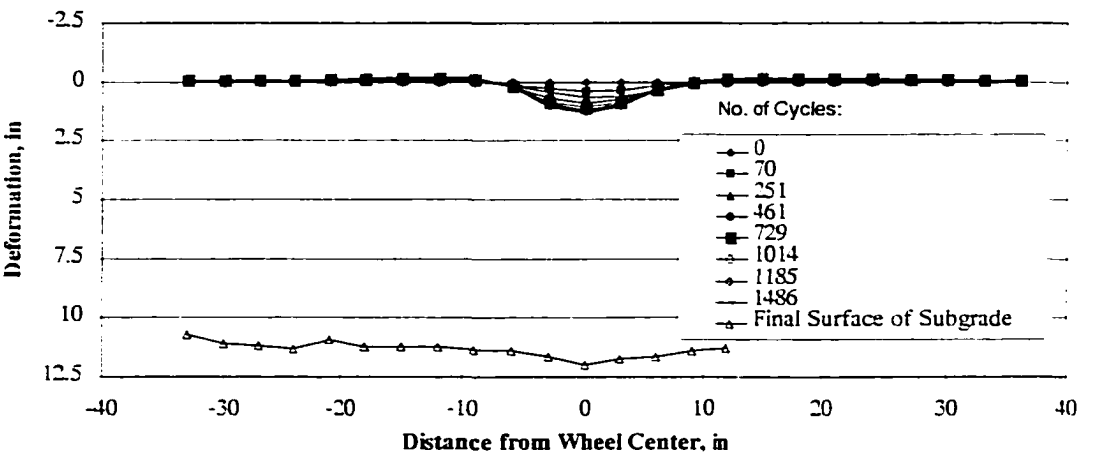

Fig. 4.2.18 Shape of Rut / Section 3 - Line 27 - at 9.3" Base

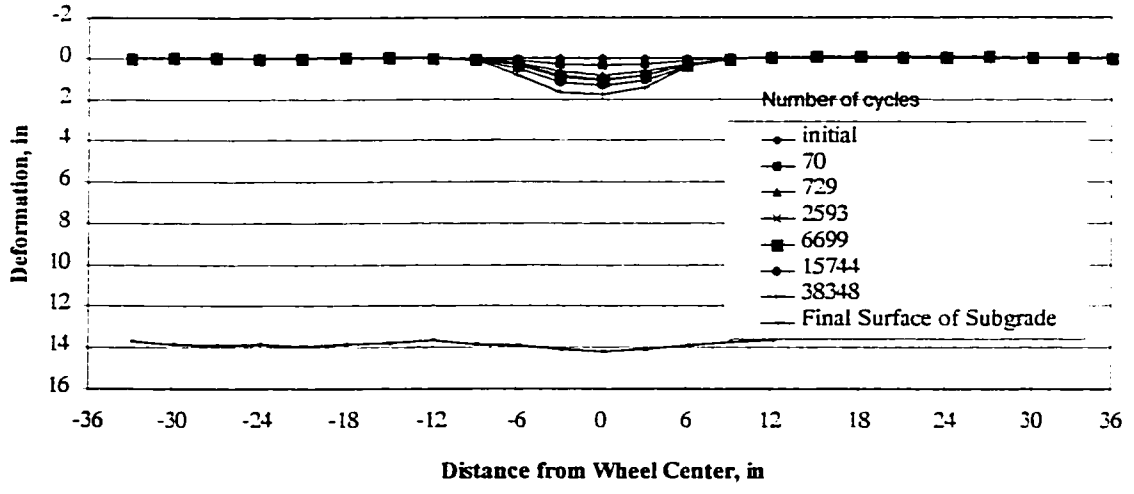

Fig. 4.2.19 Shape of Rut / Section 3 - Line 29 - at 11.5" Base

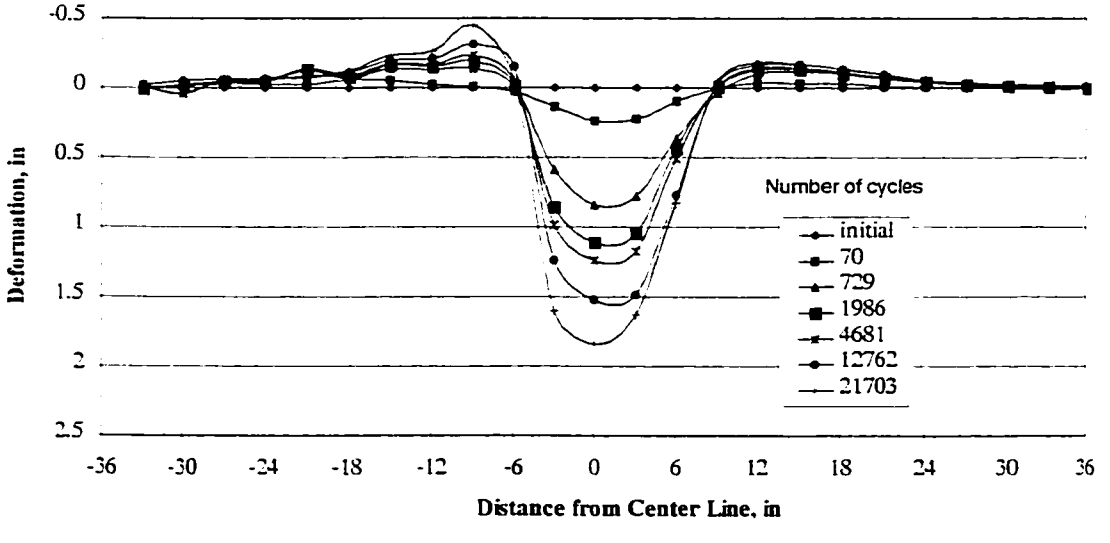

Fig. 4.2.20 Shape of Rut / Section 4 - Line 44 - at 9.3" Base

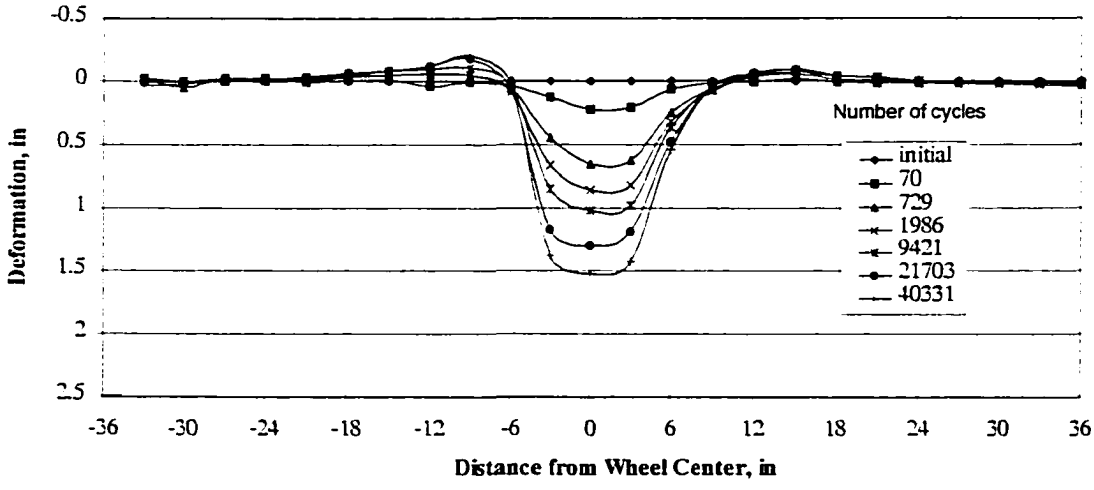

Fig. 4.2.21 Shape of Rut / Section 4 - Line 42 - at 11.5" Base

4.2.5 Comparison of the Test Results

Figures 4.2.22 through 4.2.24 illustrate the comparison of the four sections at the same number of cycles and the same thickness of base (7.1", 9.3" and 11.5"). Note that for the double BR1 reinforced section, the minimum thickness of the base is 8 inches, thus Fig. 4.2.22 does not include data from this section.

It is clear that the BR2 reinforced section has less deformation after a given number of cycles than the other sections.

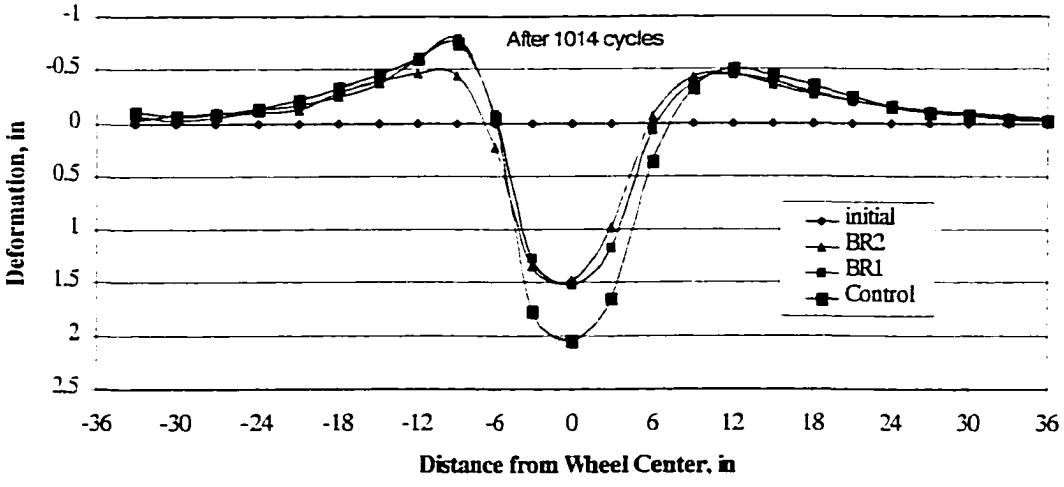

Fig. 4.2.22 Cross section of 7.1" base at 1014 cycles

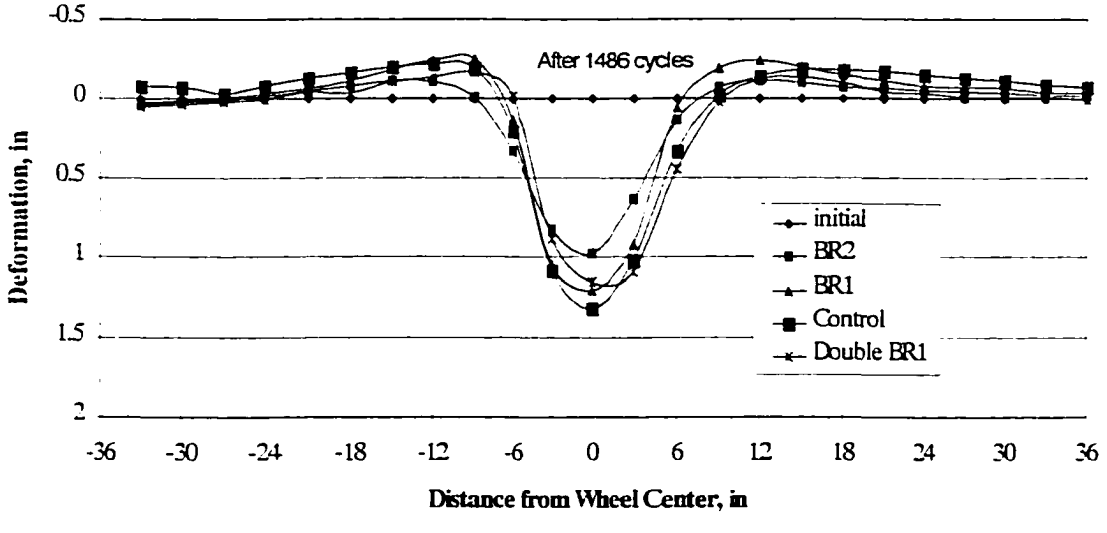

Fig. 4.2.23 Cross section of 9.3" base at 1486 cycles

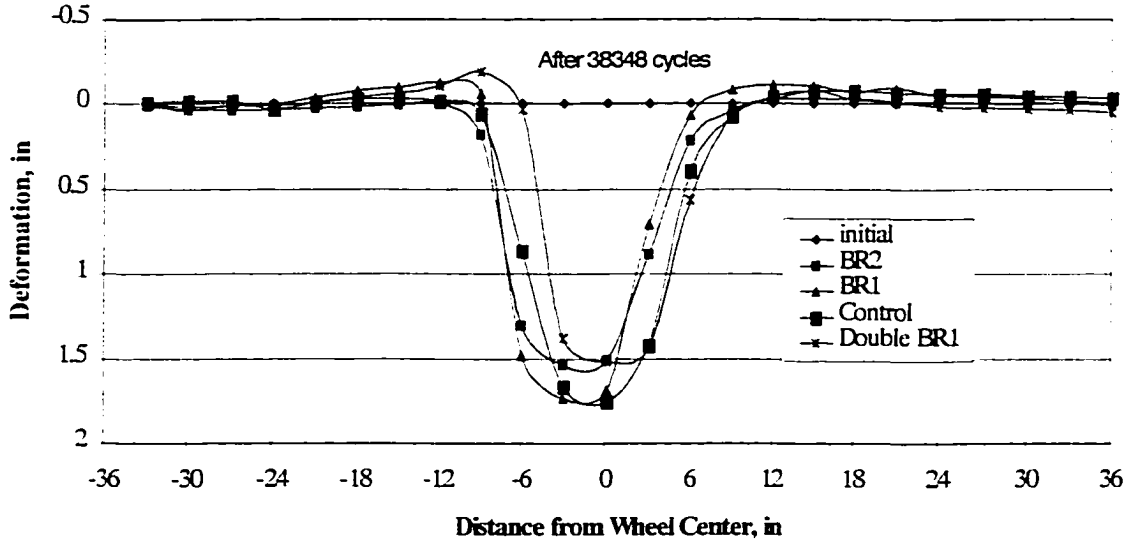

Fig. 4.2.24 Cross section of 11.5" base 38348 cycles

Figures 4.2.25 through 4.2.27 compare the deformation of the four sections to the number of cycles at 7.1", 9.3" and 11.5" of base. For the same deformation, the BR2 reinforced section can carry many more repetitions than the BR1 reinforced section, the BR1 reinforced section is better than the Control section, and the double BR1 reinforced section performed almost the same as the single BR1 reinforced section at 9.3" of base. Fig. 4.2.27 also shows that the double BR1 reinforced section increases pavement life compared to the BR2 reinforced section after 31000 cycles, and compared to the BR1 reinforced section after 26000 cycles.

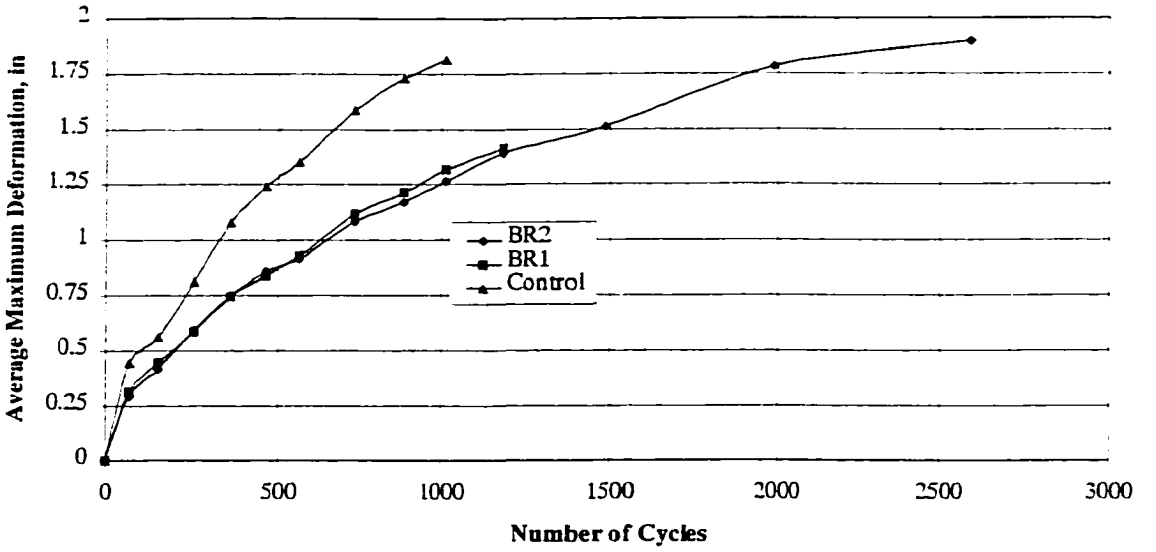

Fig. 4.2.25 Deformation vs. cycles at 7.1" of Base

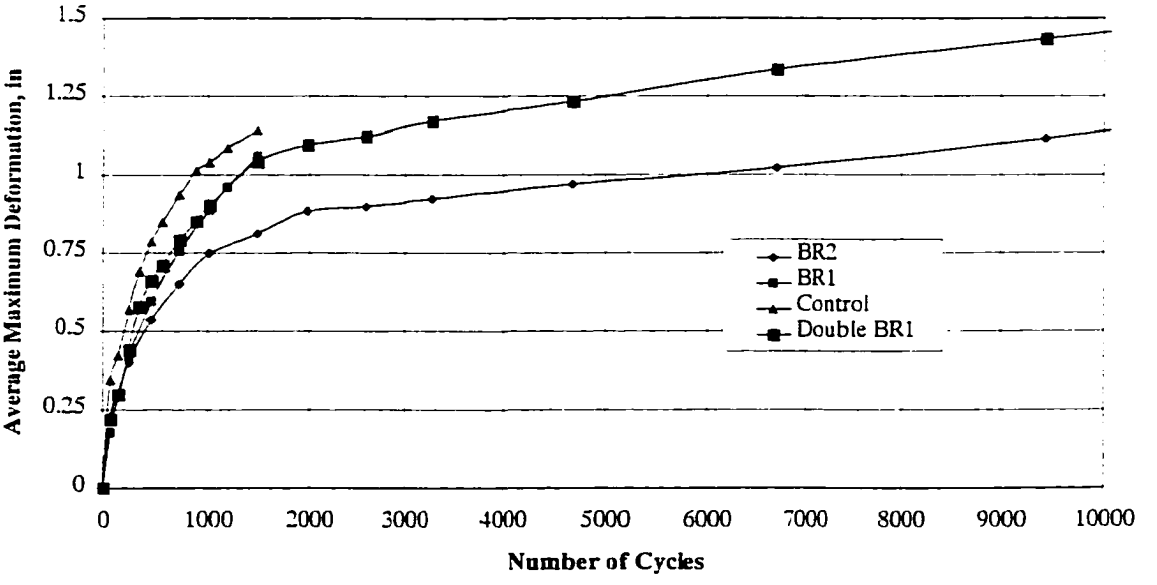

Fig. 4.2.26 Deformation vs. cycles at 9.3" of Base

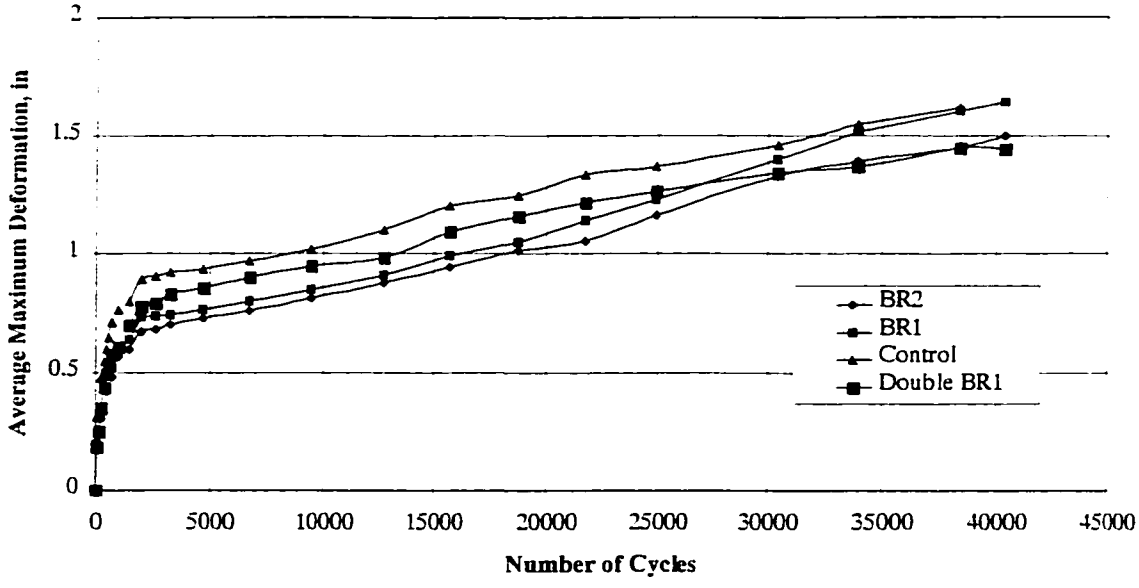

Fig. 4.2.27 Deformation vs. cycles at 11.5" of Base

4.3 Influence of variations in test parameters in the test setups

4.3.1 Boundary conditions

a. Width of Box

The deflection basins were calculated using ELSYM 5 for a range of asphalt moduli and an infinitely wide road as shown in Figure 4.3.1. Figure. 4.3.2 shows the deformation at various distances from the centerline as a percentage of the centerline deformation. The percentage is only 3% at a distance of 24" nearly 0% past 27" from wheel center. The wheel was at least 30 inches from the edge of the box, so the edge of the box had no elastic influence on the test results. Since there is no elastic influence, there should be no plastic influence.

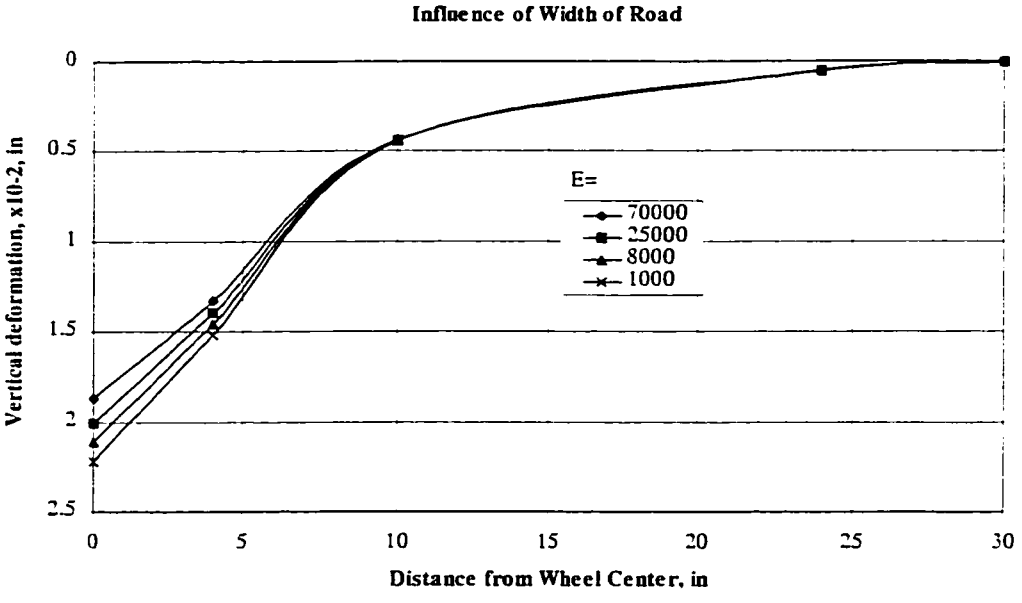

Fig. 4.3.1 Vertical deformation vs. distance form wheel center

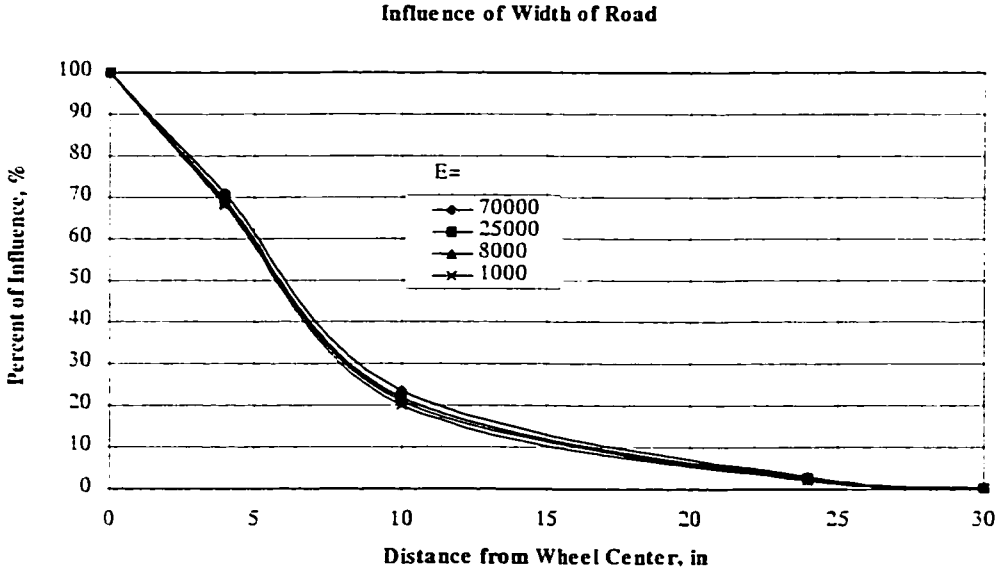

Fig. 4.3.2 Percentage of influence of width of road

b. Depth of the box

Fig. 4.3.3 compares the vertical deflections calculated using ELSYM5 for a 2 foot thick, a 3 foot thick and an infinitely thick subgrade with a 6-in base. The curves show that the thickness of the subgrade had significant elastic influence, on the order of 11% to 15%, when comparing the limited depth sections to the infinite depth section. But, if the reinforced sections and unreinforced sections are compared at the same depths of base, the relative effect is nearly zero, see Fig. 4.3.4. The stresses at the lower depths are small, hence there should be less effect from plastic deformation than elastic deformation.

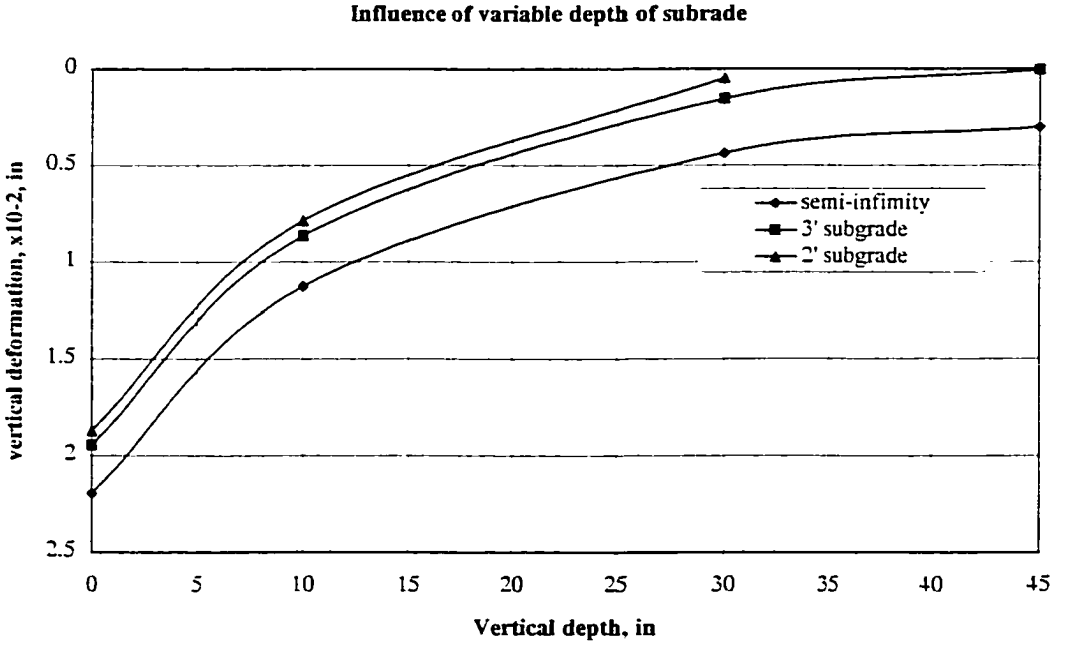

Fig. 4.3.3 Vertical deformation vs. variable thickness of subgrade

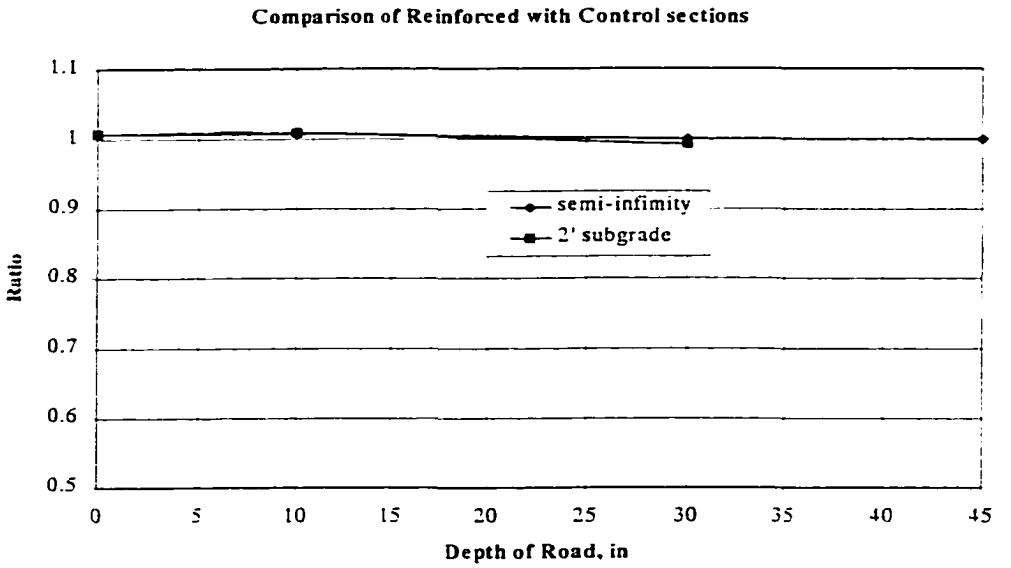

Fig. 4.3.4 Comparison of deformation ratios in reinforced and control sections

c. The conditions at each end of test section

There was a 2 foot runout area at each end of the test road. As discussed before, obstructions over 24 inches from load do not have much influence on the vertical deflection. Similarly, the data within two feet of the intersection between each test section was not used in the test results.

d. Sloping bottom of base

The maximum slope was 12 inches over 11 feet in Test B. Therefore, the maximum slope is 9.1%, or 5.2°. The error in transforming the vertical load to a normal load is infinitesimal, as shown below.

Maximum Normal Load = Vertical Load*cos(5.2°) = 4500x0.996 = 4482 lbs

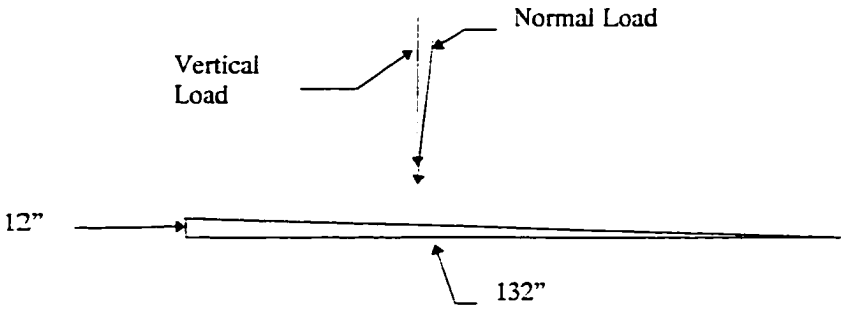

Fig. 4.3.5 Influence of base slope on load

e. Thicker Asphalt

Fig. 4.3.6 shows the difference in elastic deformation for 2.5" A/C and 2.0" A/C.

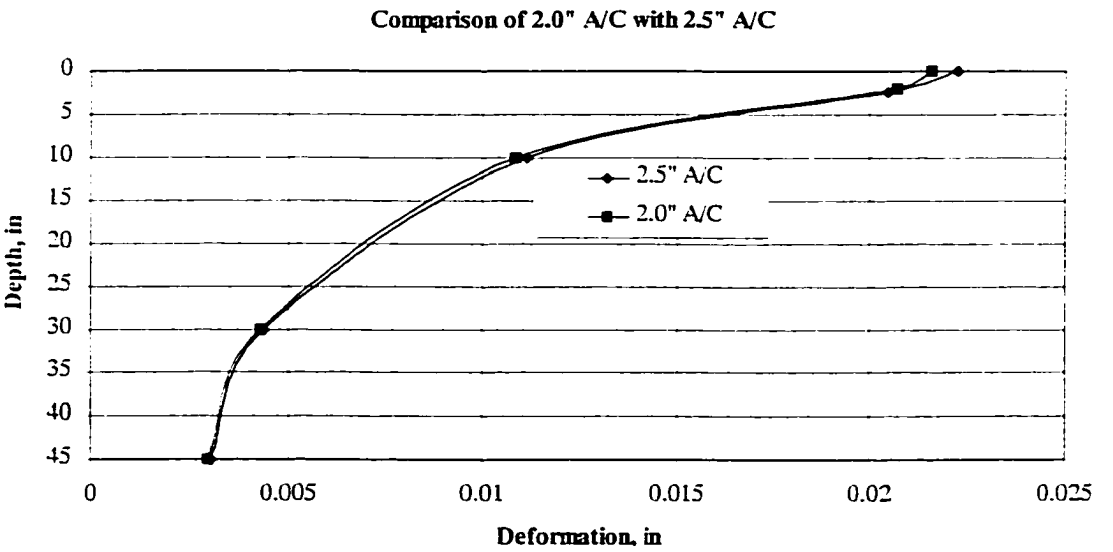

Fig. 4.3.6 Influence of Thicker Asphalt

The two curves are very close together indicating that variations in asphalt thickness in the range encountered in these tests did not effect the test results elastically and should not effect them plastically.

4.3.3 Influence of material properties

Using an elastic analysis (ELSYM5), the stiffer A/C, the less deformation (Fig. 4.3.1), the stiffer base, the less deformation (Fig. 4.3.7), and the stiffer subgrade, the less vertical deformation (Fig. 4.3.8). The variations in elastic response are probably related to plastic response. Since the same construction procedure were used throughout, the properties from section to section should be similar and therefore the actual value should not significantly impact the comparison between sections.

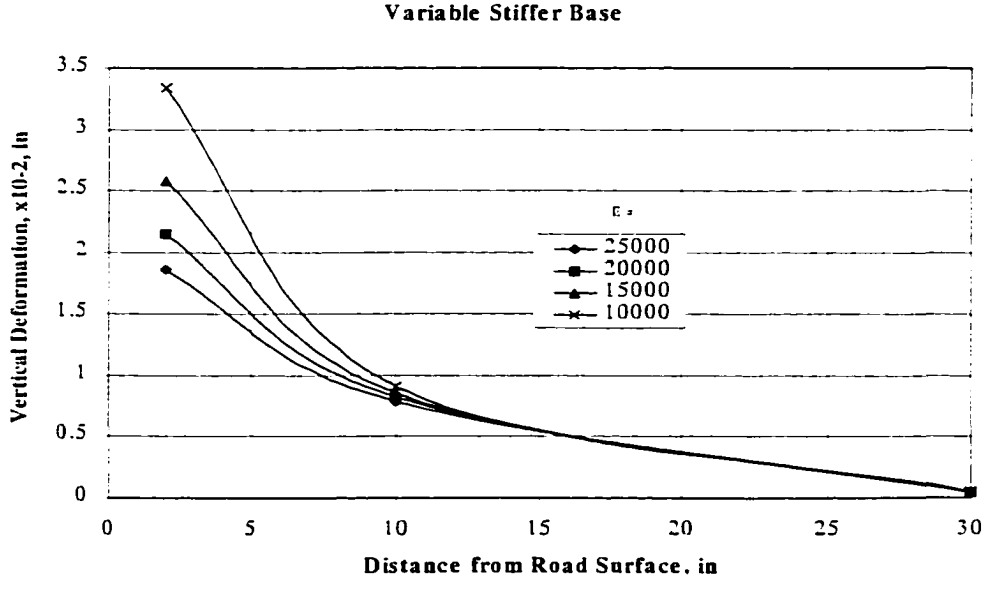

Fig. 4.3.7 Influence of stiffer base on the vertical deformation

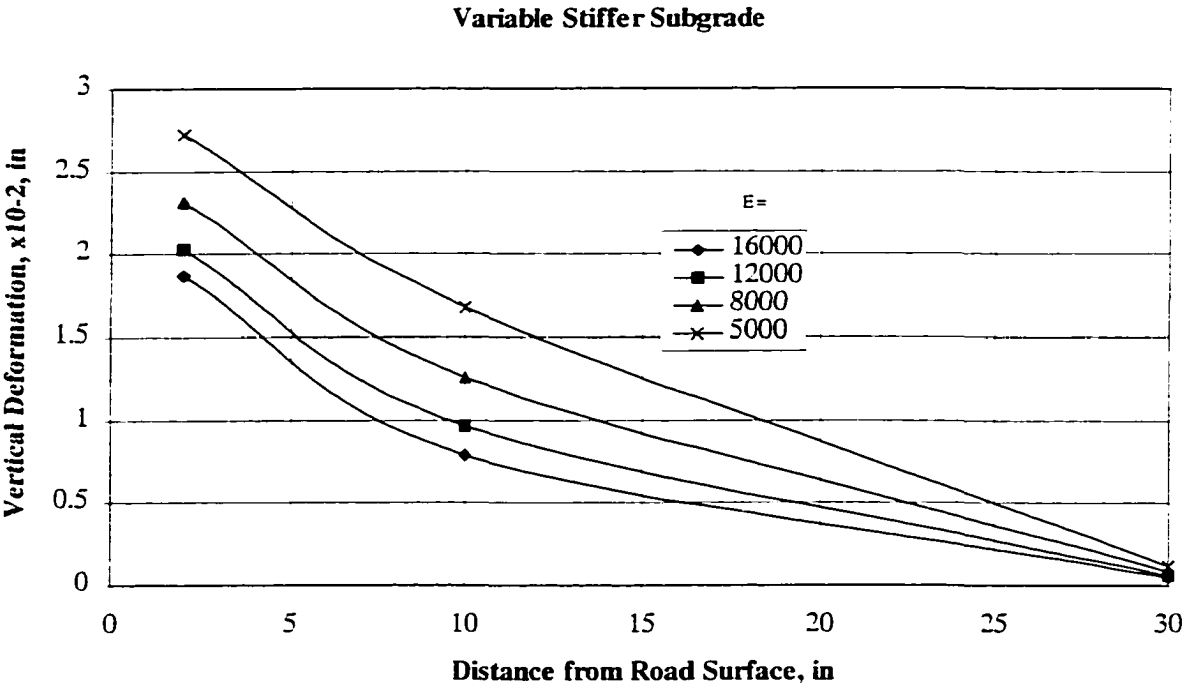

Fig. 4.3.8 Influence of stiffer subgrade on the vertical deformation

Chapter 5. Analysis of the Test Results

This chapter presents an analysis of the test results based on the two full scale traffic tests (Tests A and B). The benefit of using geogrids as base reinforcing materials will be evaluated using three different concepts: traffic benefit ratio, base saving, and pavement cracking. The permanent vertical deformation of the pavement surface is used as the measure of performance because it is the field failure criterion. The goal of this analysis is to develop a design guide that shows how much benefit, in terms of longer pavement life, can be achieved by using a geogrid.

The Traffic Benefit Ratio (TBR) is defined as:

$$TBR_{\delta} = \frac{NRG_d}{NRC_d}$$

where TBR_{δ} = Traffic Benefit Ratio in a certain deformation,

NRG_d = Number of repetitions on geogrid reinforced section,

NRC_d = Number of repetitions on control (nonreinforced) section.

5.1 Test A

5.1.1 Number of Cycles vs. Design Deformation

The first step in the analysis is to plot the number of cycles required to develop a given level of pavement distress for the range of base thicknesses considered. Figures 5.1.1 through 5.1.5 show the number of cycles required to develop a given deformation (0.5", 0.75", 1.00", 1.25", and 1.50") for various base thicknesses ranging

from 3" to 10". These figures will be used later to analyze the Traffic Benefit Ratio and base savings. At the ends of the test sections, the deformation was influenced by the conditions past the end. Hence data for 2 and 10 inches of base were not used.

Several concepts can be developed from Figures 5.1.1 through 5.1.5:

- The number of cycles to a given level of displacement increases with the increase in base thickness for both reinforced and control sections.

- At the same thickness of base, the number of cycles to a given level of displacement in the reinforced section is more than in the control section. The magnitude is dependent on the thickness of the base.

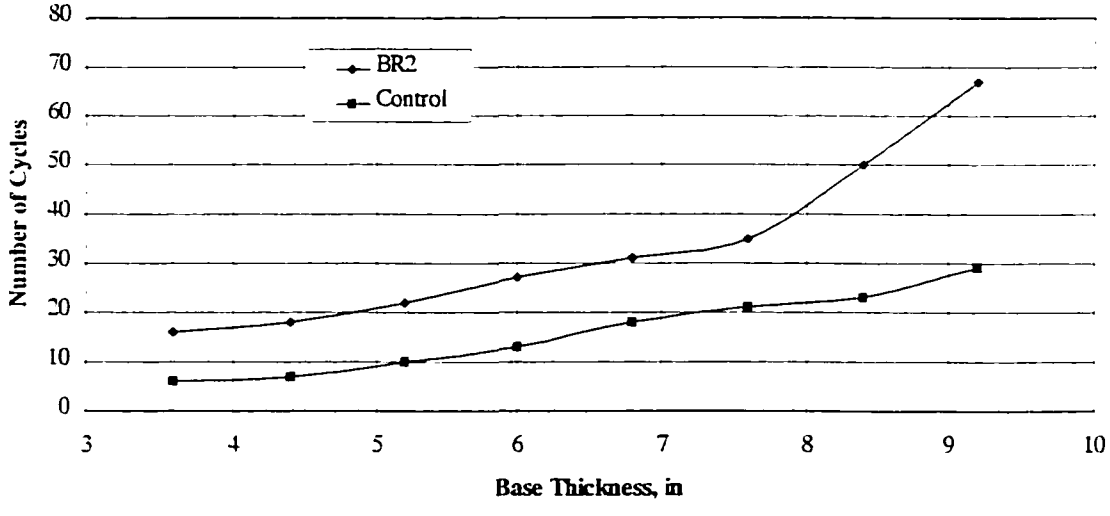

Fig. 5.1.1 Number of cycles vs. base thickness at 0.5" deformation

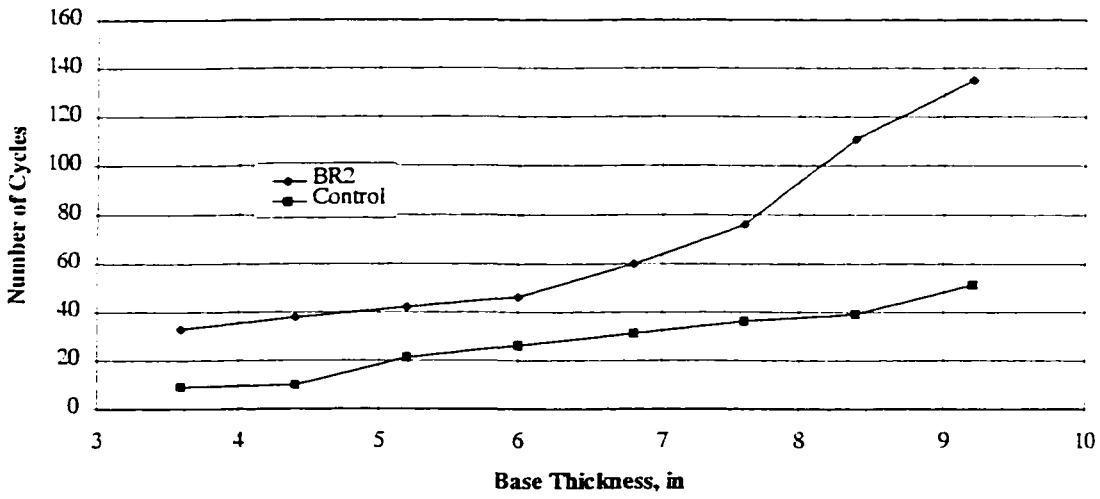

Fig. 5.1.2 Number of cycles vs. base thickness at 0.75" deformation

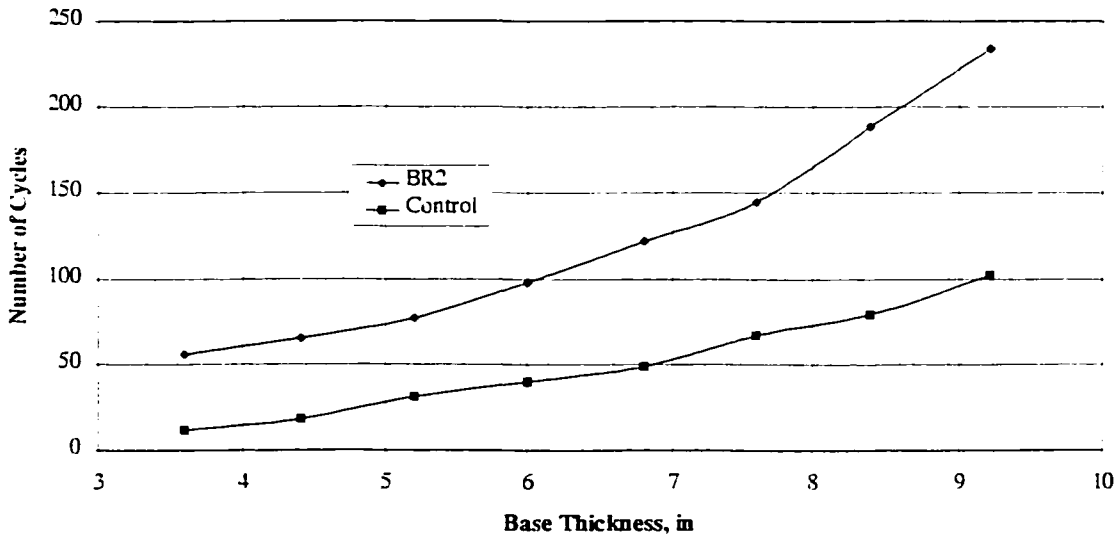

Fig. 5.1.3 Number of cycles vs. base thickness at 1.0" deformation

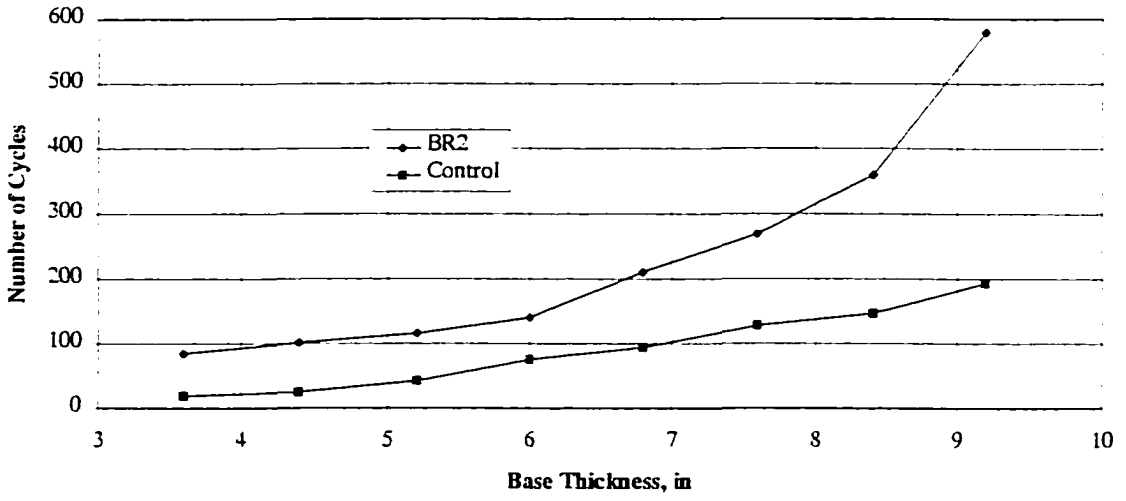

Fig. 5.1.4 Number of cycles vs. base thickness at 1.25" deformation

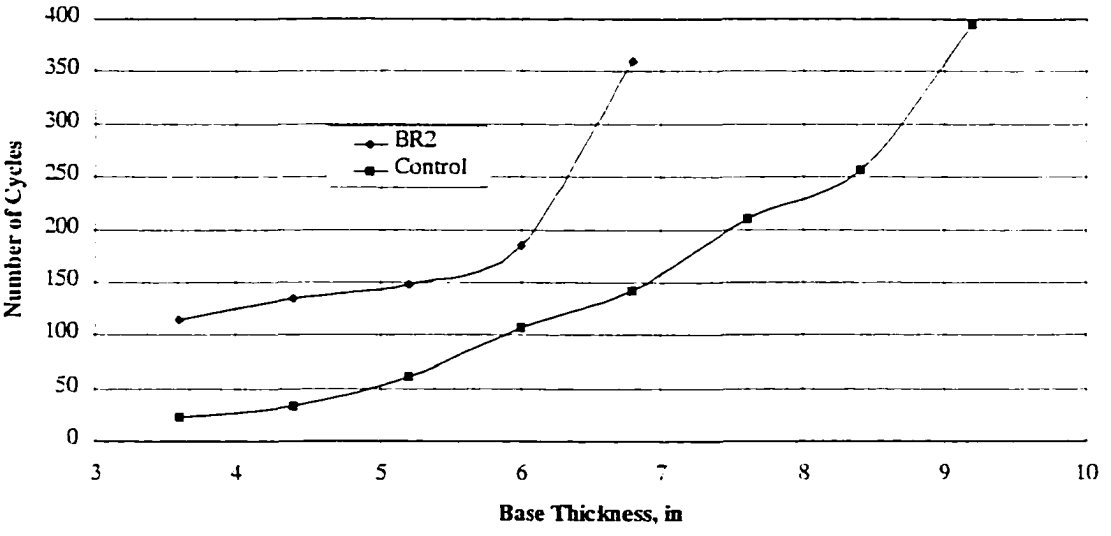

Fig. 5.1.5 Number of cycles vs. base thickness at 1.5" deformation

5.1.2 Traffic Benefit Ratio

The Traffic Benefit Ratio (TBR) was developed from Figures 5.1.1 through 5.1.5. The TBR was calculated by using the number of cycles in the reinforced section divided by the number of cycles in the control section for a constant design deformation and base thickness.

The Traffic Benefit Ratios are shown in Figure. 5.1.6.

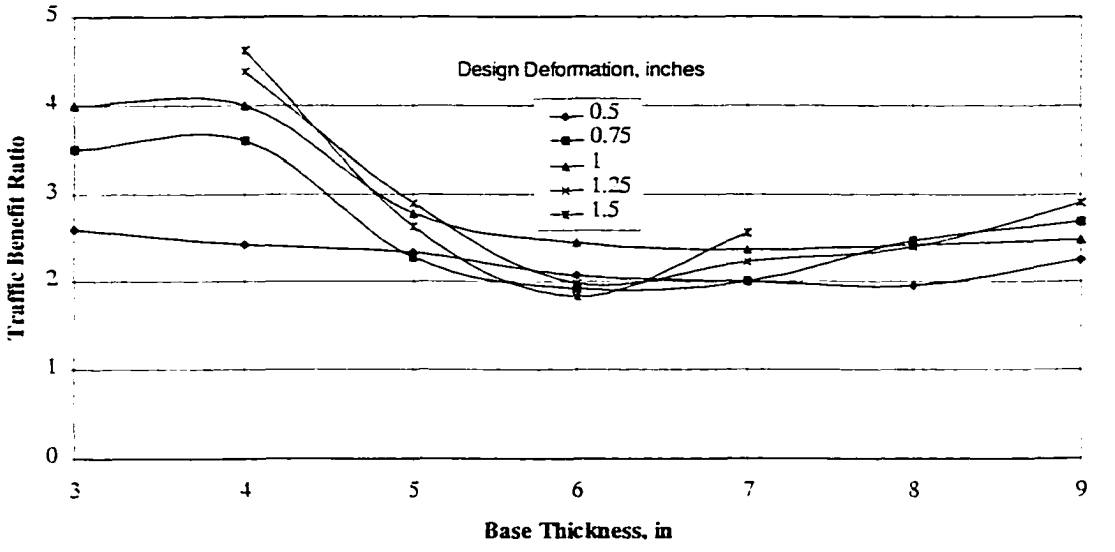

Fig. 5.1.6 TBR for various design deformations at various base depths

The TBRs are maximum at a base thickness of about 4 inches and minimum with more than about 6 inches of base. From 6 inches to 8 inches of base thicknesses,

the TBRs from 0.5" deformation to 1.5" deformation seem to be stable, ranging from 1.8 to 2.6. At greater than about 8 inches of base thickness the TBR tends to increase.

5.1.3 Savings of Base Thickness

Another way to view the benefit of using geogrid as a base reinforcing material is to determine how much base material can be replaced by the geogrid for equal performance. This is called base saving. Looking at Figures 5.1.1 through 5.1.5, at the same number of cycles, the base thickness in the reinforced section is less than in the control section. For instance, from Figure 5.1.2 (0.75" deformation), at 40 cycles, the base thickness in the reinforced section is 4.8", while the base thickness in the control section is 8.4". The geogrid, therefore, takes the place of 3.6 inches of base, or yields a base saving of 3.6 inches.

Figure 5.1.7 presents the relationship between the base thickness in the reinforced section and the base thickness in the control section for equal performance.

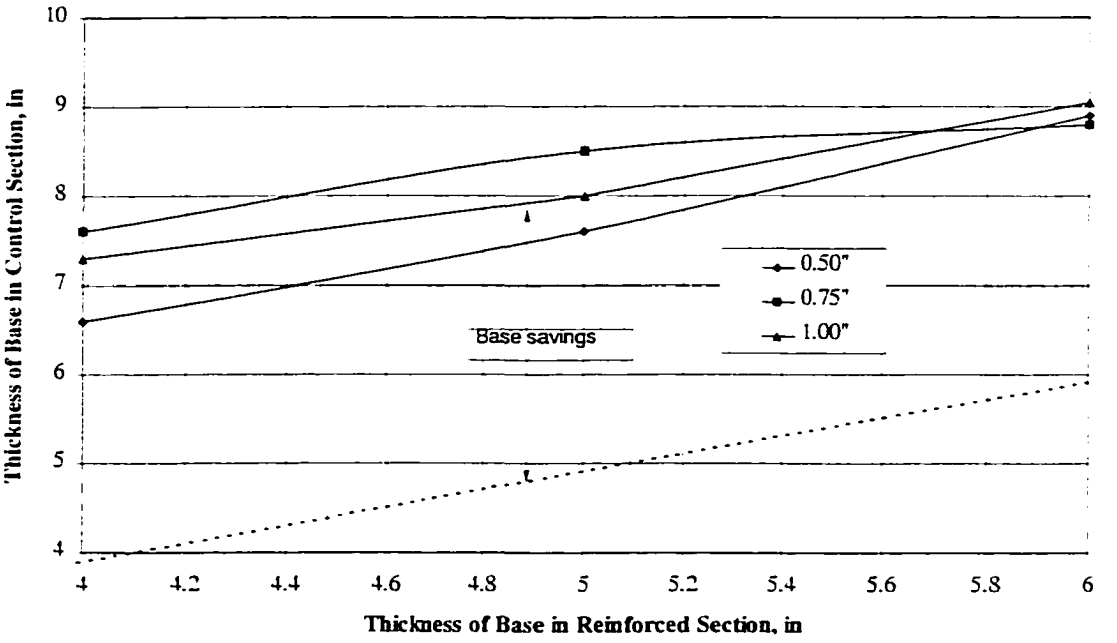

Fig. 5.1.7 Thickness of reinforced section versus control section

The maximum saving occurs at 5 inches of base thickness in the reinforced section, which equals 8.5 inches of base thickness in the control section. The base saving varies from 2.5 to 3.5 inches depending upon the design deformation and the depth of base.

5.2 Test B

Using the same analysis method as Test A, the relationship of base thickness versus number of cycles at design deformations of 0.5, 0.75, 1.0, 1.25, and 1.5 inches is plotted; then the Traffic Benefit Ratio is analyzed.

5.2.1 Design Deformation vs. Number of Cycles

Figures 5.2.1 through 5.2.5 show the relationship of the number of cycles to base thickness required to develop a given level pavement deformation of 0.5, 0.75. 1.0, 1.25, and 1.5 inches, respectively.

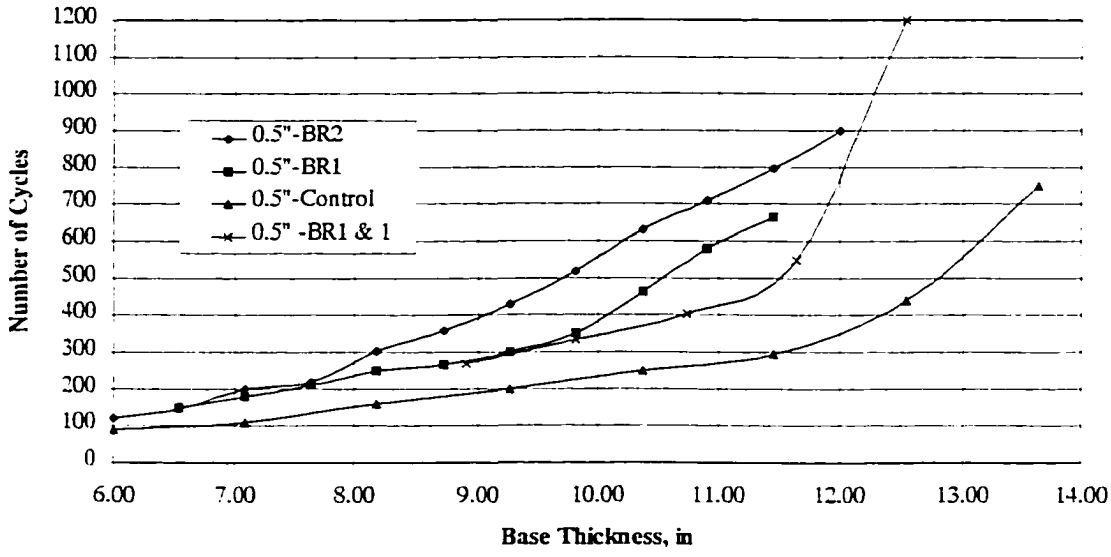

Fig. 5.2.1 Number of cycles to a 0.50" deformation vs. base thickness

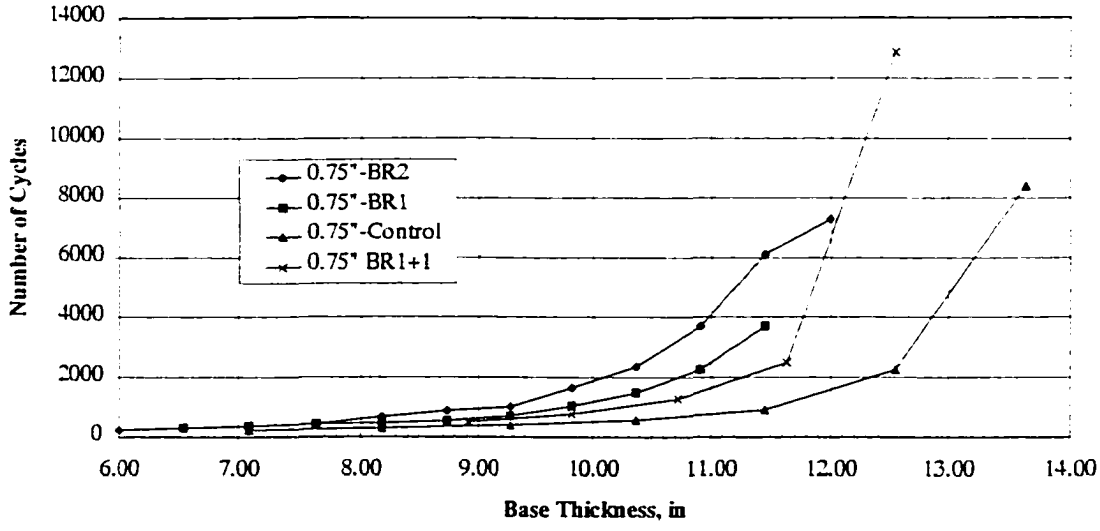

Fig. 5.2.2 Number of cycles to a 0.75" deformation vs. base thickness

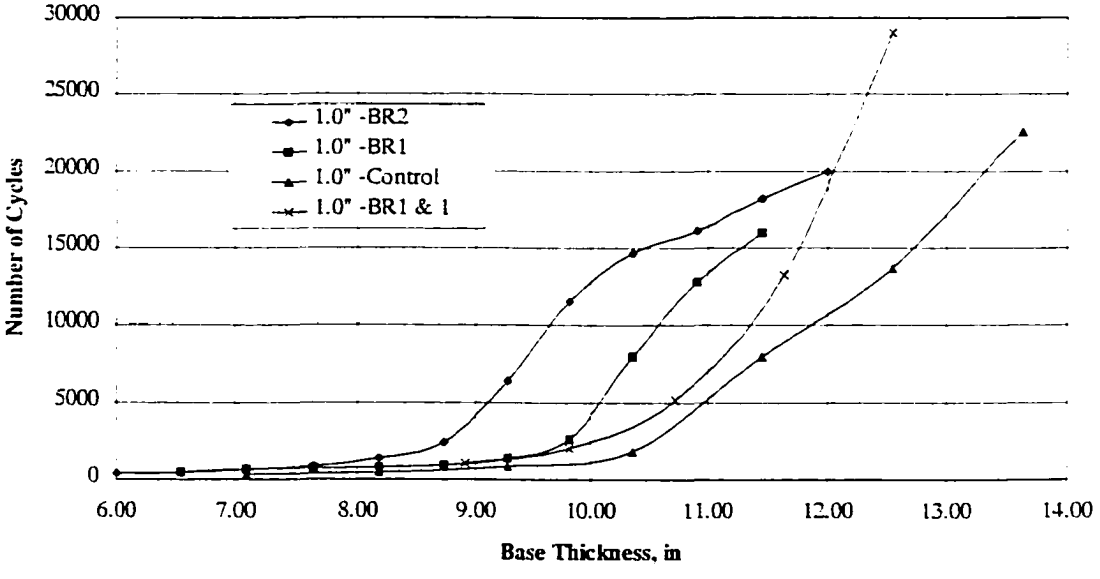

Fig. 5.2.3 Number of cycles to a 1.00" deformation vs. base thickness

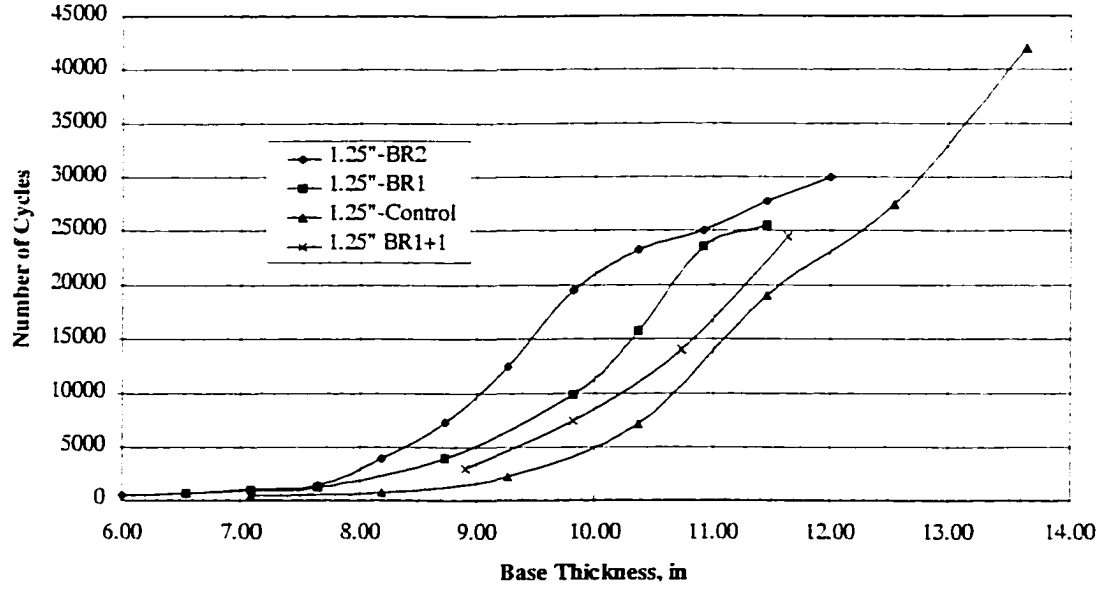

Fig. 5.2.4 Number of cycles to a 1.25" deformation vs. base thickness

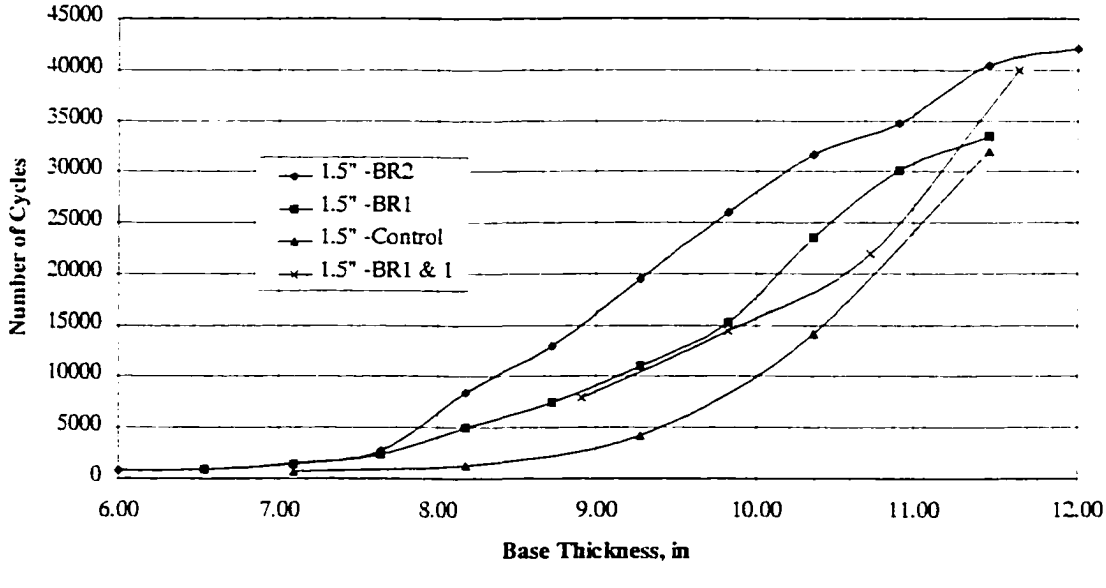

Fig. 5.2.5 Number of cycles to a deformation 1.50" vs. base thickness

As expected, in the unreinforced sections a thicker base always increases the number of cycles required to create a given level of distress. In the unreinforced sections, there seems to be a threshold base thickness at which there is a marked difference in performance. The threshold seems to be at lower thicknesses of base as the limiting deformation is increased beyond 1 inch. Cracking became noticeable at a deformation of about 1 inch, which seems to be about the deformation at which the behavior changes.

Next, the behavior of the reinforced sections will be considered. As expected, it requires more cycles to reach a given deformation in the reinforced sections than in the unreinforced sections, and the stiffer reinforcement seems to accentuate the benefit. BR2 seems to increase the performance more at base thicknesses in excess of 7 or 8 inches than at thinner base thicknesses. This result may be real, or it may be that test conditions are not uniform as the wheel approaches the end of the test section. Where the design base thickness is 6 inches, the subgrade is rounded (between the two sections) and thus the thickness is actually supported by a combination of two test sections. There is probably some combined effect for at least two feet on either side of the end of the test section, at base thicknesses up to 7 or perhaps even 8 inches.

Above some base thickness, the geogrid should give no improvement. According to Fig. 5.2.5, it appears that this thickness is about 12 inches. At lower design deformations, this thickness seems to increase. There is not enough

information to pinpoint this thickness at low deformations, but looking through these figures in reverse order, shows the following trend:

Design Deformation in	No Effect Base Thickness in
1.50	12
1.25	13
1.00	13.5
0.75	14 (?)
0.50	15 (?)

At low deformations the value might be on the order of 16 inches.

5.2.2 Traffic Benefit Ratio

The Traffic Benefit Ratio (TBR) has been defined as the number of cycles required to reach the design deformation in the reinforced section divided by the number of cycles required to reach the design deformation in the control section.

Figures 5.2.1 through 5.2.5 can be used to develop the TBR. For instance, looking at Fig. 5.2.1 we see that at a base thickness of 10 inches, 550 cycles were required to deform the section reinforced with BR2 to 0.5 inches while it only took 230 cycles in the control section. The TBR is, therefore, 2.4 for this particular condition.

The TBR for design deformations ranging from 0.5 to 1.5 inches are shown in Figures 5.2.6 to 5.2.10. Several things are obvious from these curves:

a) There seems to be an optimum base thickness for each condition.

b) As base thickness increases, the TBR starts between 1.5 and 2, rises to a maximum and then decreases to 1 at large thicknesses.

c) The optimum base thickness and the maximum TBR are both dependent upon the design deformation.

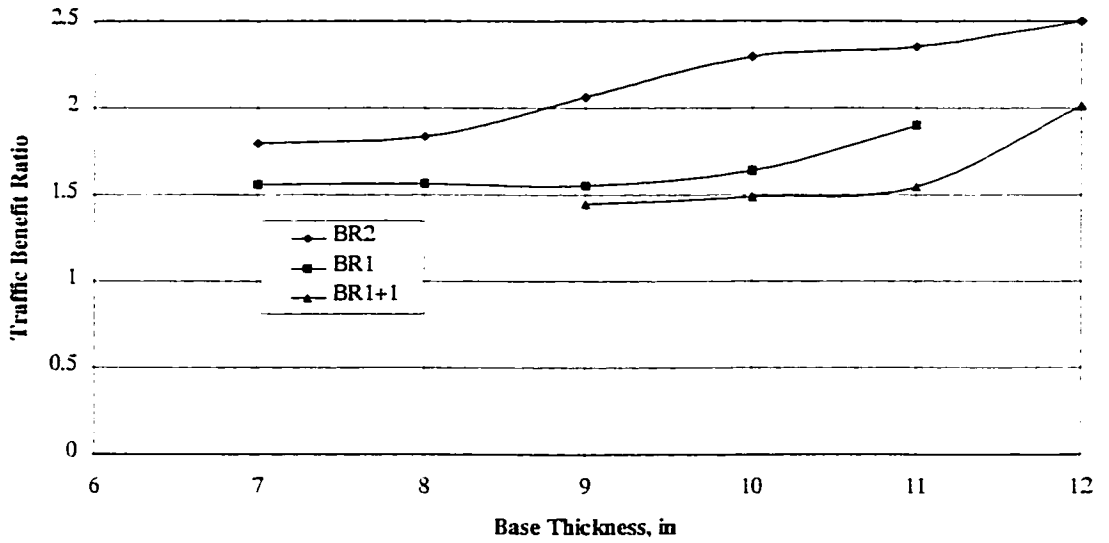

Fig. 5.2.6 TBR for various base thicknesses at a deformation of 0.5"

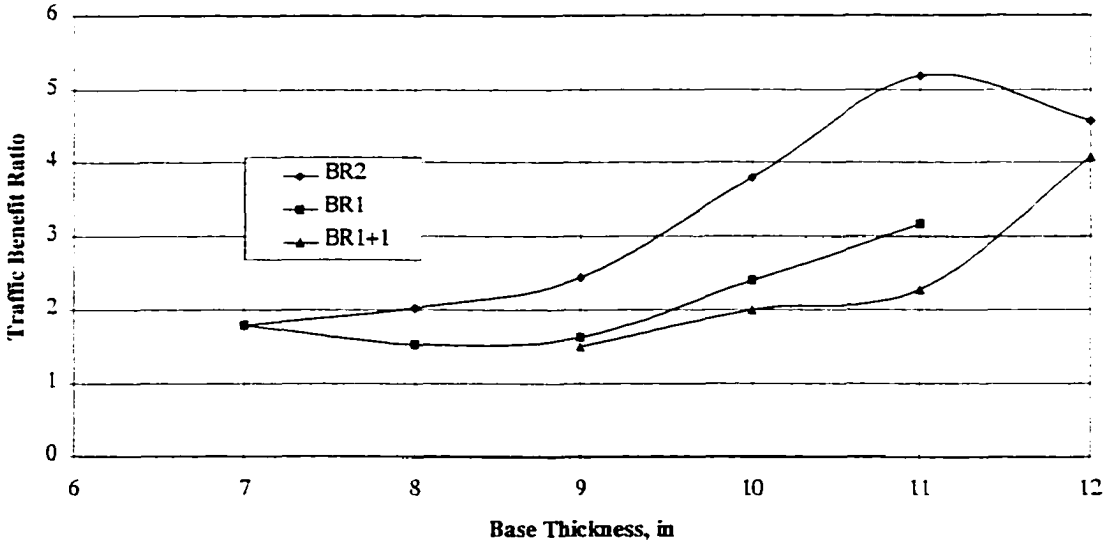

Fig. 5.2.7 TBR for various base thicknesses at a deformation of 0.75"

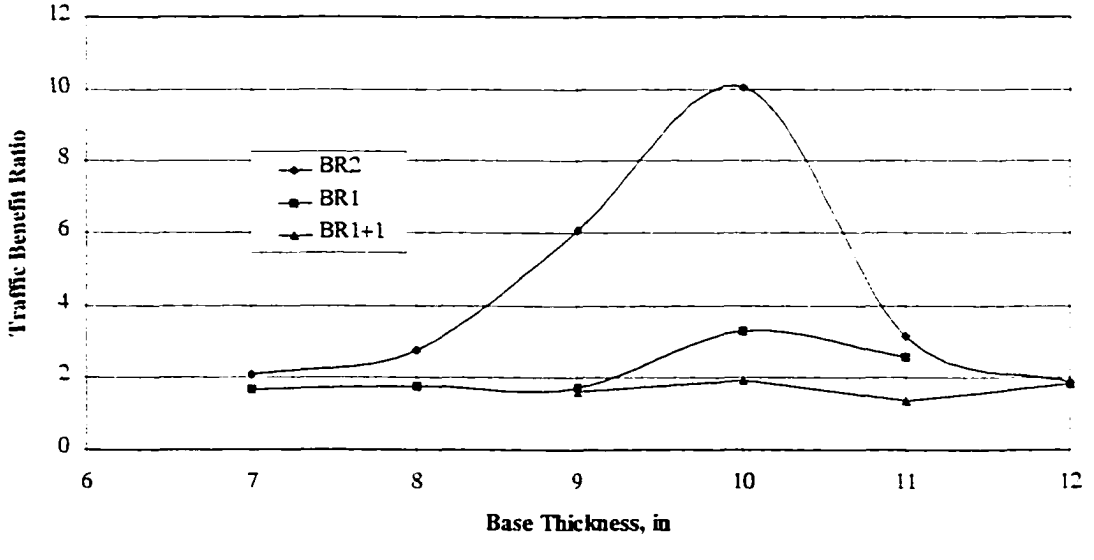

Fig. 5.2.8 TBR for various base thicknesses at a deformation of 1.0"

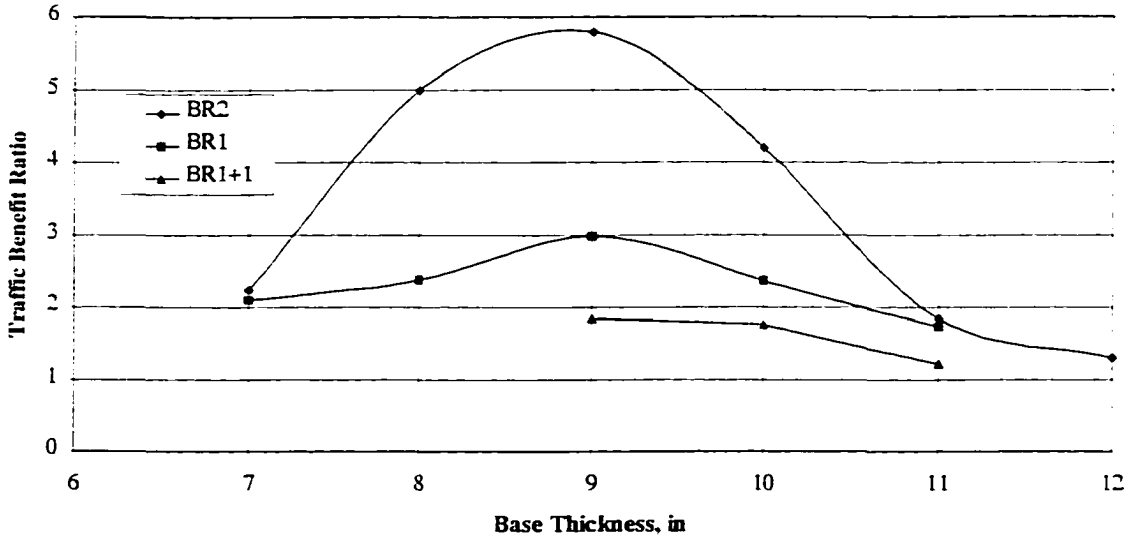

Fig. 5.2.9 TBR for various base thicknesses at a deformation of 1.25"

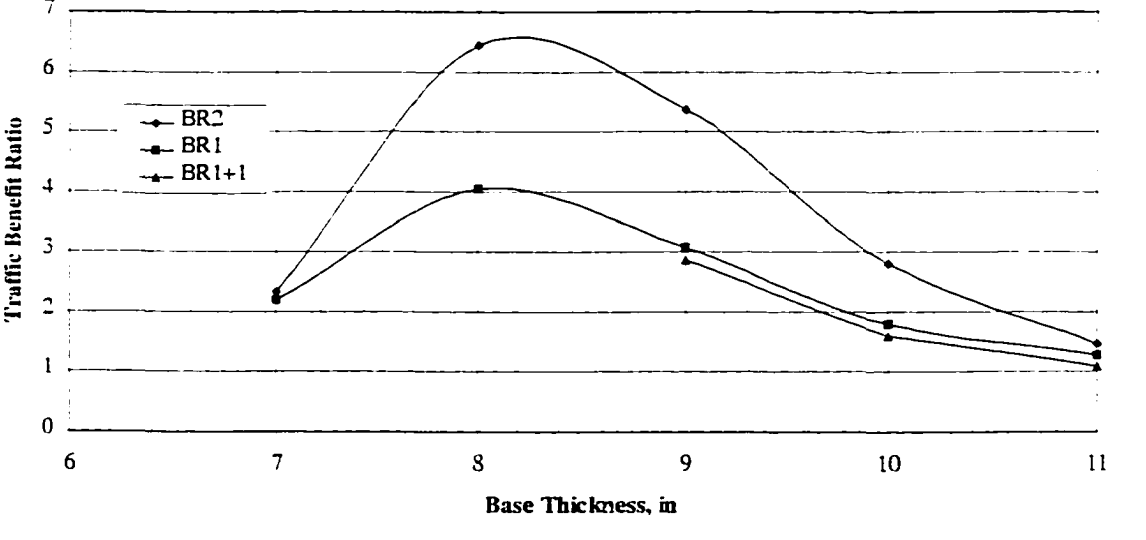

Fig. 5.2.10 TBR for various base thicknesses at a deformation of 1.5"

5.2.3 Base Thickness Savings

The other way of looking at the benefit of using geogrid for base reinforcement is to see how much less base is required when using a geogrid for the same performance as the nonreinforced base. This information can be extracted from Figures 5.2.1 through 5.2.5. Fig. 5.2.1 shows that at 500 cycles the unreinforced section deformed 0.5 inches with 12.75 inches of base, while the section reinforced with BR2 required only 9.75 inches of base. The geogrid successfully replaced 3 inches of base. This information is shown graphically in Fig. 5.2.11, Fig. 5.2.12, and Fig. 5.2.13 for BR2, BR1 and Double BR1 respectively. Note that the savings are greatest when lower design deformations are used. With a design deformation of 0.75 inches, savings are about 1.5 inches with single or double BR1, and about 2.5 inches with BR2 .

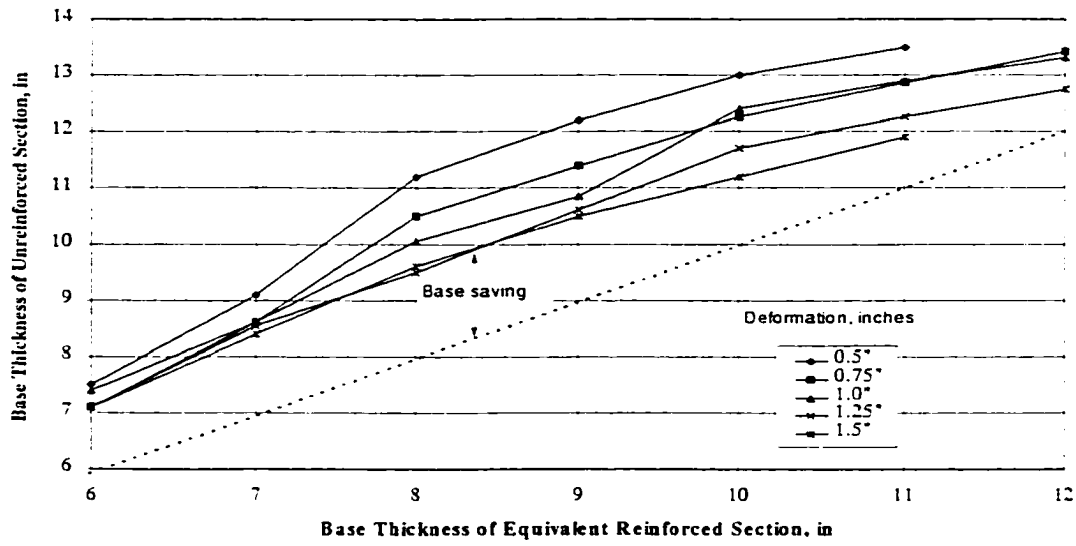

Fig. 5.2.11 Unreinforced thickness vs. equivalent reinforced (BR2) thickness

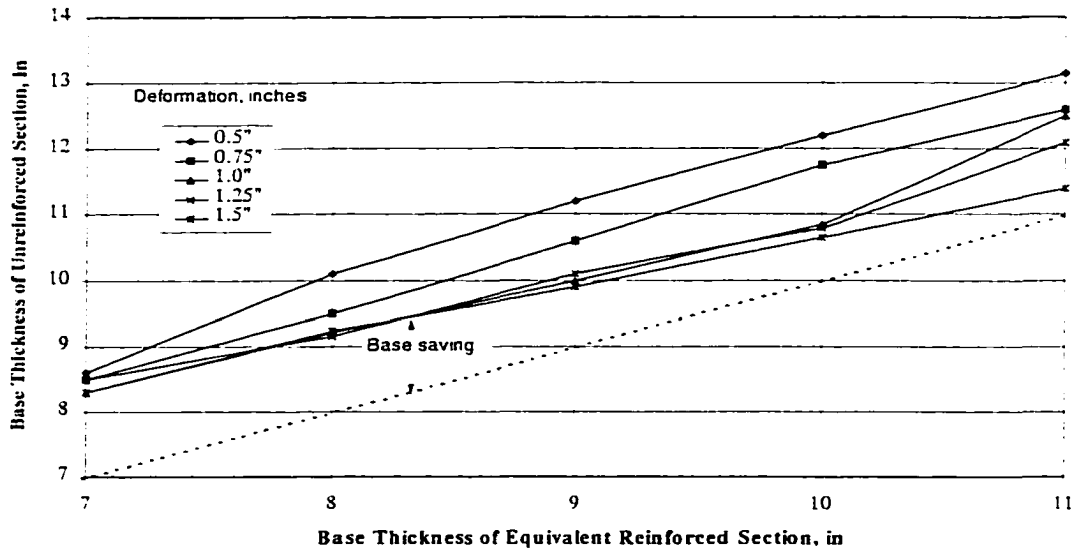

Fig. 5.2.12 Unreinforced thickness vs. equivalent reinforced (BR1) thickness

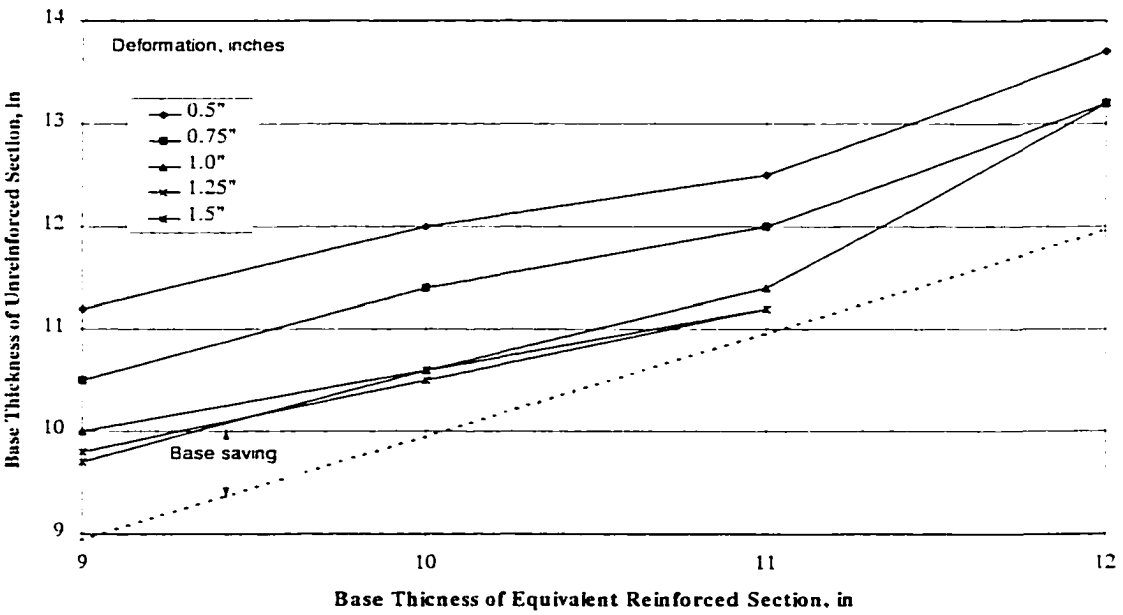

Fig. 5.2.13 Unreinforced thickness vs. equivalent reinforced (Double-BR1) thickness

5.3 Comparisons Based on the Two Individual Tests

This section presents a comparison of BR1 and BR2 geogrids as base reinforcement materials using the results of the two individual single wheel load tests.

5.3.1 Traffic Benefit Ratio

5.3.1.1 BR1 Reinforced Base

Table 5.3.1 includes the Traffic Benefit Ratio (TBR) of BR1 reinforcement for various base thicknesses at different pavement surface deformations. The TBR increases with the increase of base thickness and deformation, as mentioned previously. The average TBR is 2.16.

Table 5.3.1 Comparisons of TBR for BR1 reinforcement

Test	Base Thickness, in	Deformation, in					
		0.50	0.75	1.00	1.25	1.50	Average
B	7	1.6	1.8	1.7	2.1	2.2	1.88
B	8	1.6	1.5	1.8	2.4	4.1	2.28
B	9	1.6	1.6	1.7	3.0	3.1	2.2
B	10	1.6	2.4	3.3	2.4	1.8	2.3
B	11	1.9	3.2	2.6	1.7	1.3	2.14
Average		1.66	2.1	2.22	2.32	2.5	2.16

Fig. 5.3.1 presents the TBR versus base thickness. At 11 inches of base thickness, the TBR goes down. The average traffic benefit ratio for deformation of 0.5 through 1.5 inches is 2.2. Using a third order nonlinear curve, the relationship between TBR versus base thickness is:

$$TBR = 0.0183b^3 - 0.5621b^2 + 5.6552b - 16.434 \qquad (5 \le b \le 11)$$

where b = base thickness, in.

The correlation coefficient, R^2, is 0.85.

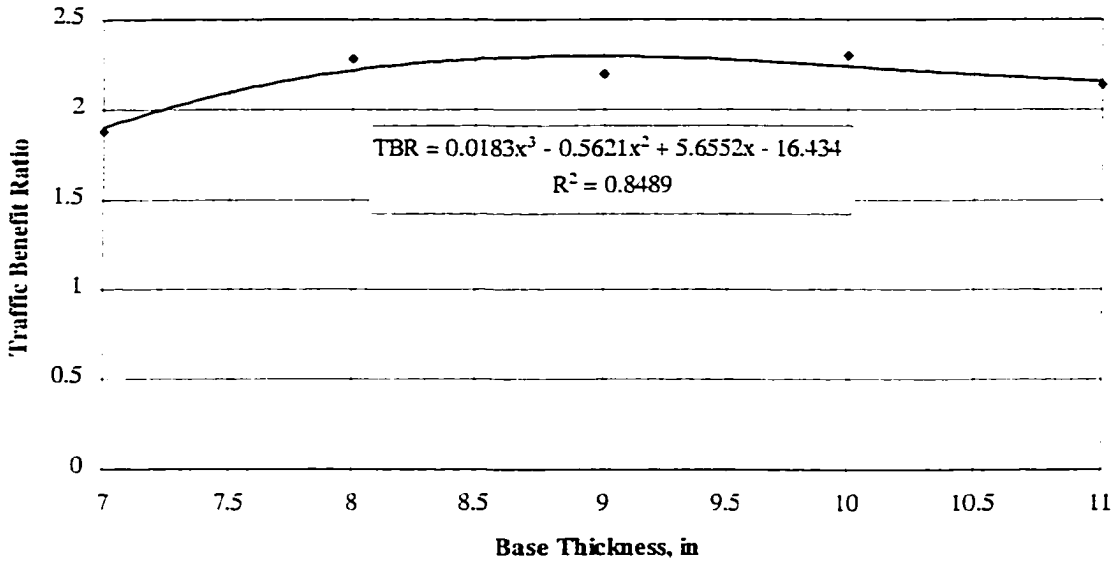

Fig. 5.3.1 TBR vs. base thickness with BR1 reinforcement

Fig. 5.3.2 shows the TBR versus the average deformation. The relationship between TBR and deformation is:

$$TBR = 0.76d + 1.40 \quad (0.5 \le d \le 1.5)$$

Where d = deformation of pavement surface, in.

The correlation coefficient, R^2, is 0.91.

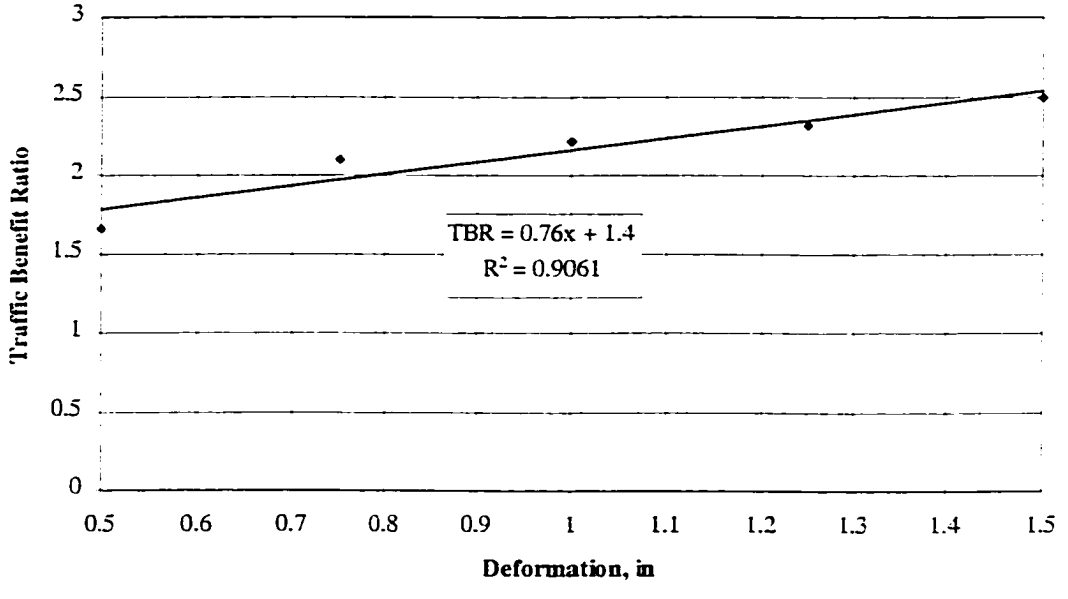

Fig. 5.3.2 TBR vs. average deformation with BR1 reinforcement

5.3.1.2 BR2 Reinforced Base

Table 5.3.2 shows TBR for the BR2 reinforced base. Test A starts at 5 inches of base thickness and Test B starts at 7 inches of base thickness. The averages of the TBRs for the BR2 geogrid are shown in Table 5.3.2.

Table 5.3.2 TBR with base thickness and deformation

Base Thickness, in	Deformation, in					
	0.5	0.75	1.0	1.25	1.5	Average
5	2.3	2.3	2.8	2.9	2.6	2.6
6	2.3	2.3	2.8	2.9	2.6	2.6
7	1.9	2.0	2.4	2.4	2.4	2.8
8	1.9	2.3	2.6	5	6.4	3.6
9	2.2	2.6	6.1	5.8	5.4	4.4
10	2.3	3.8	10	4.2	2.8	4.6
11	2.4	5.2	3.2	1.8		3.2
12	2.5	4.6	1.9			3.0
Average	**2.2**	**3.1**	**4.0**	**3.6**	**3.7**	**3.3**

Based on Table 5.3.2, the relationship of total average TBRs to base thickness and deformation are shown in Fig. 5.3.3 and Fig. 5.3.4 respectively. The peak value of the TBR occurs at about 10 inches of base and is 4.6. After 11 inches of base, the TBR decreases. The average TBR for a deformation of 0.5 through 1.5 is 3.3. Using a third order nonlinear curve, the relationship between TBR and base thickness is:

$$TBR = -0.0487b^3 + 1.1357b^2 - 8.1318b + 20.952 \qquad (5 \le b \le 12)$$

where b = base thickness, in.

The correlation coefficient, R^2, is 0.92.

The relationship between TBR and deformation is:

$$TBR = 2.6667d^3 - 11.314d^2 + 15.462d - 3.08 \qquad (0.5 \le d \le 1.5)$$

Where d = deformation of pavement surface, in.

The correlation coefficient, R^2, is 0.93.

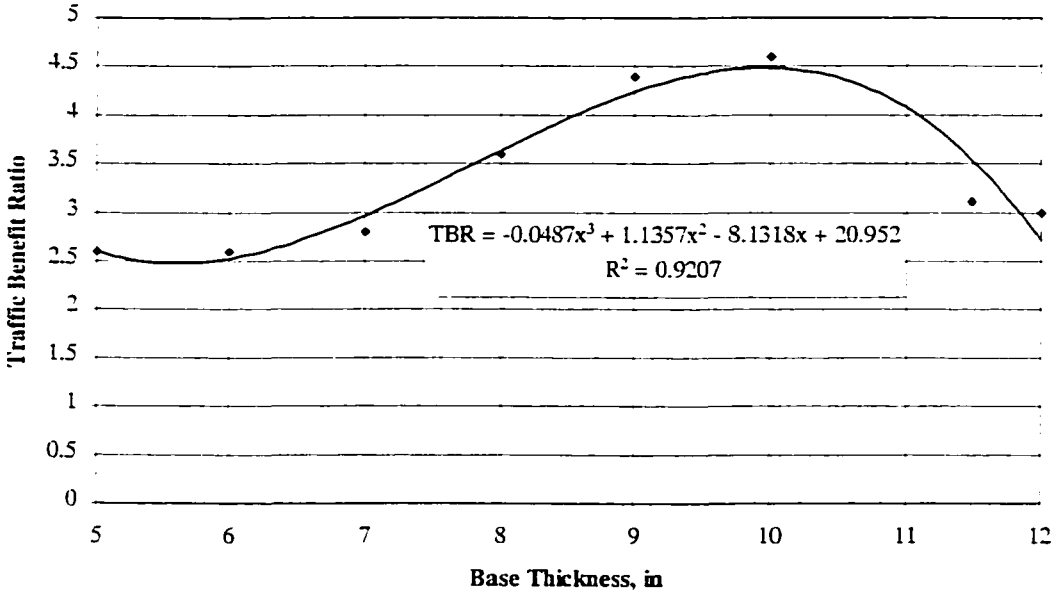

Fig. 5.3.3 TBR versus base thickness with BR2 reinforcement

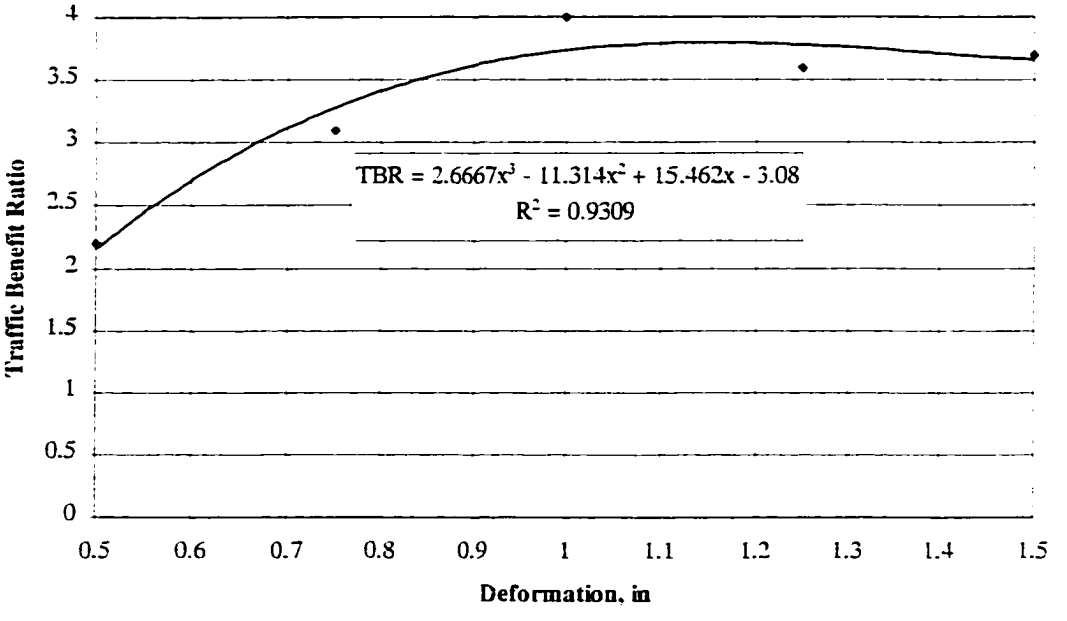

Fig. 5.3.4 TBR versus average deformation with BR2 reinforcement

5.3.1.3 Design Chart Based on the Deformation and Base Thickness

Based on the analysis above, the relationship of maximum TBR to base thickness and deformation is presented in Fig. 5.3.5.

Fig. 5.3.5 shows both the optimum base thickness and the maximum TBR. To use the figure, start on the right axis with the design deformation. Move horizontally until the straight line is reached. Move straight down to read the optimum base thickness from the horizontal axis. From the straight line move vertically to the proper

curve and then horizontally to the left axis to read the maximum traffic benefit ratio. For example, starting with 0.9 inch for the design deformation we find an optimum base thickness of 10.3 inches and a benefit ratio of 9 for the section reinforced with BR2.

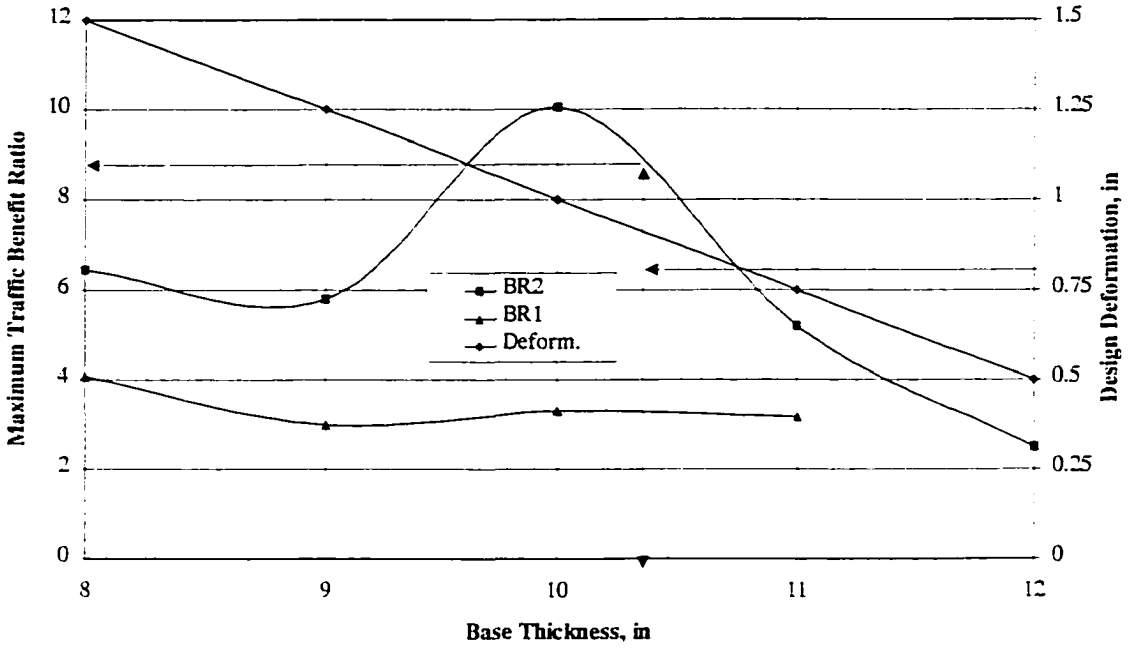

Fig. 5.3.5 Base thickness vs. maximum TBR and deformation

Design should be based on some procedure, such as the AASHTO or the TAI procedure, and then the TBR from this study may be applied to the result. For example, if the AASHTO design procedure shows 100,000 ESAL's in the

unreinforced section and the TBR for that geometry is 2, one would expect the reinforced section to withstand 200,000 ESAL's

5.3.2 Base Savings

Average thickness relationships between the unreinforced and reinforced sections are developed from the base savings analysis of Test A and Test B.

Figure 5.3.6 is a plot of the results from the BR2 reinforcement for the average values of deformation from 0.5 inches to 1.5 inches. The following formula is generated for the relationship between the BR2 reinforced section and the non-reinforced section:

$$T_{NR} = 0.86293 T_{BR2} + 3.33732 \qquad (3 < T_{BR2} < 12)$$

where: T_{BR2} = Thickness of BR2 reinforced base, in.

T_{NR} = Thickness of non-reinforced base, in.

The correlation coefficient, R^2, is 0.9785.

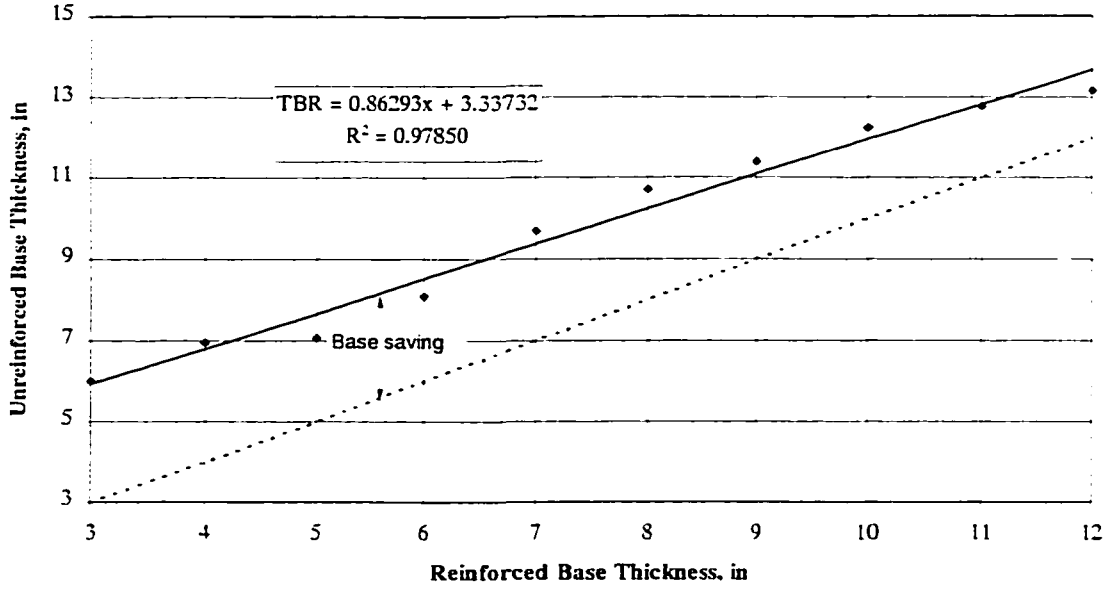

Fig. 5.3.6 Base savings for BR2 reinforced base for Test A and Test B

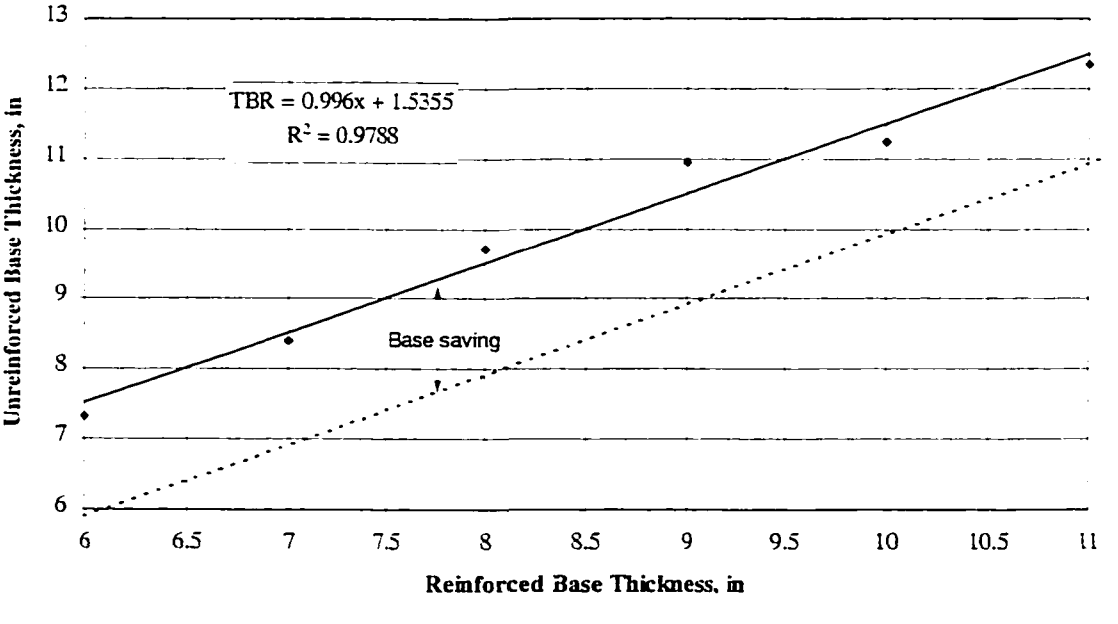

Fig. 5.3.7 Base savings for BR1 reinforced base for Test A and Test B

Fig. 5.3.7 shows the relationship between the BR1 reinforced base and the non-reinforced base for average values of deformation from 0.5 to 1.5 inches. This relationship can be expressed as:

$$T_{NR} = 0.9960T_{BR1} + 1.5355 \qquad (6 < T_{BR1} < 11)$$

where T_{BR1} = thickness of BR1 reinforced base, in.

The correlation coefficient, R^2, is 0.9788.

5.3.3 Longitudinal Crack Spreading

Another approach to evaluate the benefit of geogrids as base reinforcing materials is to monitor the initial longitudinal crack spreading at different base thicknesses. Fig. 5.3.8 shows the initial crack spreading at different base thicknesses and numbers of cycles.

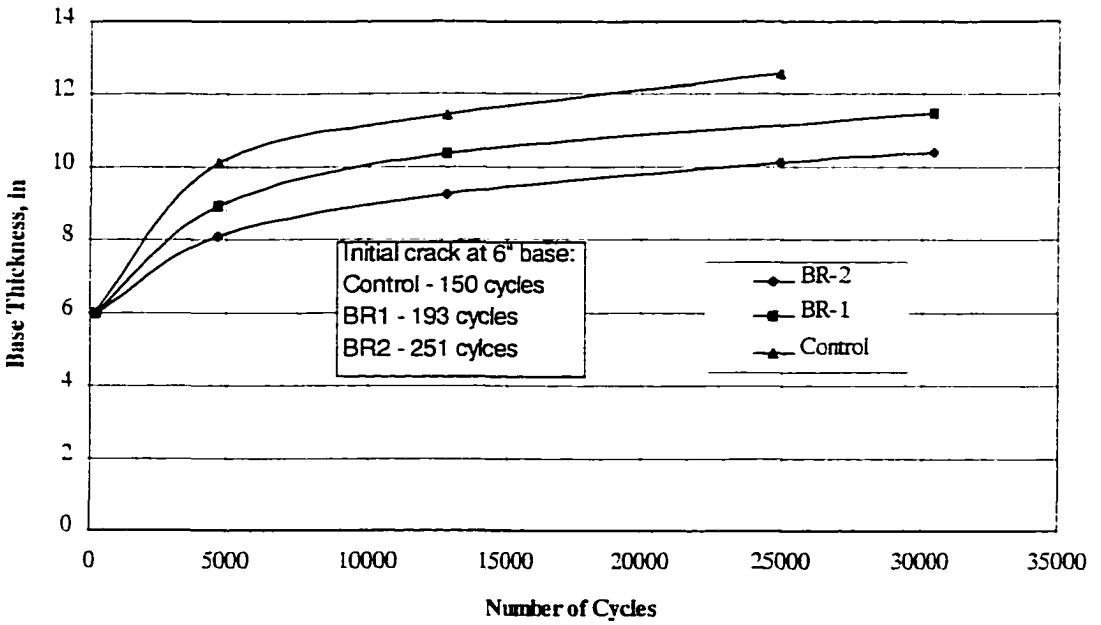

Fig. 5.3.8 Longitudinal pavement crack spreading

At 6 inches of base thickness, the initial longitudinal cracks occurred at either 150 cycles (control section), 193 cycles (BR1 section) or 251 cycles (BR2 section). At the same base thickness (Fig. 5.3.8), the BR2 reinforced base can sustain more cycles than the BR1 reinforced base, and the BR1 reinforced base can sustain more cycles than the unreinforced base. At the same number of cycles (Fig. 5.3.8), a thicker base is needed in the control section than in the BR1 section and the BR2 section.

Re-plotting Fig. 5.3.8 using a logarithmic scale, the relationship of base thickness to number of cycles is nearly a straight line (see Fig. 5.3.9). The correlation

coefficients of the BR1, the BR2 and the control sections are all over 0.98. The quantitative analysis results are presented in Fig. 5.3.10.

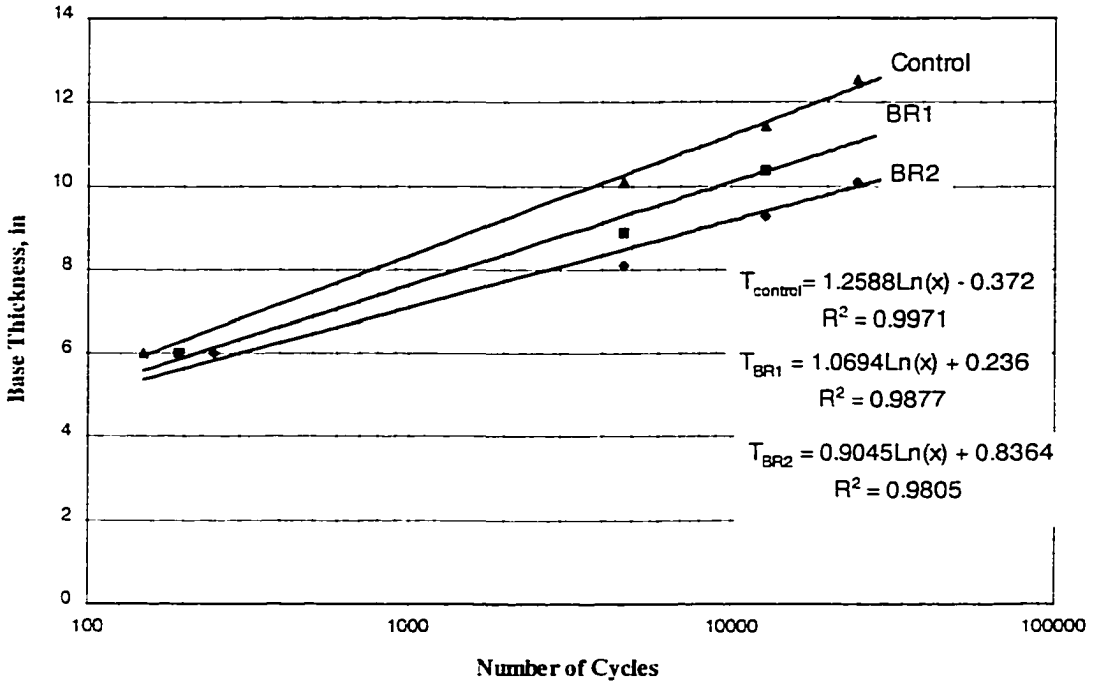

Fig. 5.3.9 Best fit lines for crack spreading in logarithmic scale.

The relationships of base thickness (T) to number of cycles when the initial crack occurred in the BR1, BR2 and control sections are as follows:

Control section:

$T_{BR1} = 1.2588Ln(N) - 0.372$

Correlation coefficient is 0.971.

BR1 reinforced section:

$T_{BR1} = 1.0694Ln(N) + 0.236$

Correlation coefficient is 0.9877.

BR2 reinforced section:

$T_{BR1} = 0.9045Ln(N) + 0.8364$

Correlation coefficient is 0.9905.

The initial crack benefit is defined as the number of cycles required to reach the initial crack for a reinforced section divided by number of cycles for the unreinforced section at the same base thickness. Fig. 5.3.10 shows that: (1) the crack benefit obtained from the BR2 reinforced section is higher than from the BR1 reinforced section, (2) as the base thickness increases from 6 inches to 11 inches, the crack benefit increases, (3) the average crack benefit is about 2 for the BR2 reinforced section and is about 1.3 for the BR1 reinforced section.

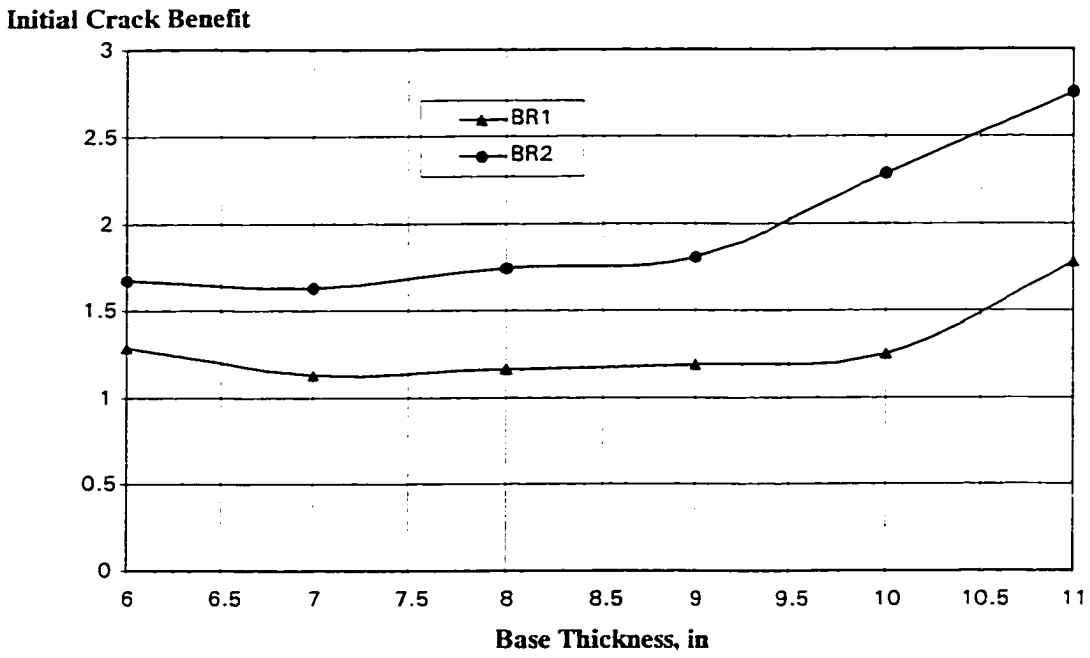

Fig. 5.3.10 Benefit vs. base thickness based on initial crack.

5.4 Discussion of the Theoretical Analysis of Geogrid as Base Reinforcement

As discussed in Chapter 1, the geogrid has three major reinforcement mechanisms: reinforcement, interlock and separation. Several authors have addressed the general ways in which geogrids can reinforce road sections. The concepts include:

1. As the soil profile is deformed during rutting, the geogrid is put into tension on a curve. A curved membrane causes the pressure on the concave side to be higher than on the convex side. This reduces the load on the subgrade directly under the wheel load and increases the pressure on the subgrade outside the wheel rut. Both of these factors tend to reduce rutting in the subgrade. These effects are very small at

low deformations and become more prominent at higher levels of rutting. This effect is at least partially quantifiable (Kinney, 1979).

2. Much of the rutting is caused by a downward and outward movement of the soils. Placing a tension member in this environment should stiffen the system in much the same way as reinforcing steel stiffens a concrete beam. Although this concept has received a lot of discussion, it has not been quantified.

3. The rolling wheel causes a deformation of the surface which can be considered a energy input into the pavement system. The geogrid is stretched and relaxed during this process which absorbs some of the energy which would ordinarily go into the soil.

4. The inclusion of a geosynthetic in the system causes more soil to move and the overall movements to be greater through much of the soil mass (Kinney, 1979). The overall movement as the wheel passes may not be changed much, but the strains in each soil element are significantly decreased leading to less plastic deformation, i.e. rutting.

5. The inclusion of a geosynthetic separates the base and subgrade materials thereby maintaining the integrity of the base material.

6. The inclusion of a geogrid effectively stops a failure plane from crossing that boundary.

7. The confinement has been stressed in the literature since the earliest days of using geogrids for road reinforcement. The argument is that the base course materials in the road move outward during loading and that the inclusion of a geogrid restricts

that motion. Less outward motion (the confining effect) translates to higher lateral stresses in the base material. Higher lateral stresses result in a stiffer stronger granular base material. This effect has been demonstrated very effectively by placing sand in a paper cup and then standing on the cup to show how a weak membrane confining the sand can make it very stiff and strong. The concept is also used in the use of geowebs. Geowebs look somewhat like bottle separators used in cardboard boxes. They are filled with unbound granular materials and have been shown to hold enormous loads over very soft subgrades.

On the surface, it would appear that one should be able to mathematically model the system, by the finite element method, with all of the factors discussed above would be lumped into the overall behavior of the system. The problem is complex, but conceptually doable with the use of a sophisticated finite element program such as ABAQUS on the University of Alaska Fairbanks' Cray supercomputer. The problem must include:

1. A three dimensional analysis. The rolling wheel causes stresses and soil particle movement in all directions.

2. Non-linear materials with plastic deformation.

3. A moving wheel load.

4. Coupling between layers, which includes a nonlinear force deformation relationship with a plastic component.

In order to generate the finite element material models, one must know the material behavior and be able to model it correctly. There is a significant amount of

information lacking to accurately model this system. This lack of knowledge is so severe that, in one test where two grids with what appeared to be nearly identical material properties were used, one made the system dramatically stronger while the other actually made the system weaker (Webster, 1992).

The Waterways Experiment Station (WES) performed a series of full scale load tests (Webster, 1992) in which six different grids were used in a variety of pavement profiles and loading conditions. In this study it was found that the six grids had dramatically different effects on the systems and there was not a strong correlation between the standard properties of the geogrids and their performance in the test sections. These properties include those that would be used in a finite element analysis, such as:

Tensile strength

Dimensions of the ribs

Dimensions of the apertures

Stiffness of the ribs

Junction strength

Grid construction technique

Parent material

One property did seem to have a high correlation with performance. It has been dubbed "the two finger test" in the industry. It consists of inserting the thumb and forefinger into one of the openings and pulling the grid through the fingers. The more it hurt, the better the performance. For obvious reasons, this test has not become

an ASTM standard. Is the sharpness of the edge of the rib the determining factor? If so, one would think this effect would appear in a direct shear test, but it does not seem to (Kinney and Yuan, 1995).

Subsequent to the WES tests, WES retained the University of Alaska to try to determine a way to categorize the grids according to their performance. This study included a series of tests in which the intent was to explore all the physical aspects of the grids in an attempt to find one attribute, or a combination of attributes, that correlated to the grid performance. One was found. It is called the "Geogrid Torsional Rigidity Index Test" and is currently required by the FAA for use on all geogrids used in airfield reinforcement applications. It consists of anchoring a piece of geogrid around the periphery of a 12 inch square hole, grabbing the center node and twisting it in the plane of the geogrid. The ratio of the torque to the angle of rotation correlated very well with the geogrid performance. What is there about this test that did not show up in the other types of tests, several of which apparently measured very similar things?

The largest use of geogrids today is in the area of reinforced retaining walls and steepened embankments. Many analyses have been done using various degrees of sophistication from simple limiting equilibrium analyses to finite element analyses. All of the analyses underestimate the effect of the geogrid by a very large margin, leading to the conclusion that there is some factor that has yet eluded researchers. There is now a contingent within the industry who believes that the presence of the

geogrid changes the strength and deformation properties of the surrounding soil in some manner.

It seems impossible to analyze geogrids as base reinforcement using the currently developed FEM technology, such as ABAQUS. First, it is impossible to generate representations of the geogrid elements which consider the different junction strengths and stiffness of the ribs. Second, the loading conditions should include the vertical force and horizontal shear force between the wheel and road surface. Third, in the road test, a large deformation (at least 1.5 inches) was considered. In the FEM analysis, it is difficult to consider the moving load which acts on the rutted road surface. Fourth, it is also impossible to consider the geogrid interlock mechanism in the FEM analysis. The aggregate of the base material is pushed into the geogrid holes and this prevents movement of aggregate.

Chapter 6. Conclusions

A full scale test track proved to be an effective method of comparing the performance of paved roads, with and without geogrid reinforcement. Two full scale tests were conducted to measure the performance of geogrids as base reinforcing material in paved roads. The load, speed, and direction of the test cart were automatically controlled by computer. Many types of measurements were made. However, the pavement surface deformation proved to be the single most valuable indicator, from these tests, of pavement performance and thus the benefit of using geogrid reinforcement.

1. The full-scale tests proved to be practical and feasible for testing pavement systems.

2. The sloped base subgrade interface proved to be an effective way to get a lot of data from a limited number of tests.

3. The full-scale tests confirmed that the rut depth is a function of loading repetitions and depth of base course. Rut depth increases with increasing repetitions, and decreases with increased base thickness.

4. The tests established that, for the conditions tested, the geogrid increased the life of the pavement by a factor of 1 and 10 depending upon the depth of base and type of geogrid reinforcement. Over a wide range of conditions, the TBR for BR-1 is above 1.5 and for BR-2 is above 2.0. These conclusions are limited to the conditions tested in this study including: soft clay subgrade, crushed rock granular base, 2 inches

of asphalt, a single truck tire loaded to 4500 pounds, and Tensar BR1 and BR2 geogrid reinforcement.

5. Geogrids not only decrease the pavement deformation, but also decrease the heaving of the pavement surface.

6. The impact of reinforced base depends on the design deformation. There is significant benefit under the conditions tested for design rutting in the range of 0.5 to 1.0 inches.

7. There is an optimum depth of base for maximum geogrid benefit. For the conditions tested, it is about 10 inches.

8. Beyond some depth, the geogrid is not effective. For the conditions tested, that depth is about 14 inches.

9. Geogrid reinforcement can also increase the life of the pavement with respect to longitudinal cracking. The cracking benefit is defined as the ratio between the number of repetitions to cracking in a reinforced section to the number of repetitions in a unreinforced section. The crack benefit was found to be about 1.5 for BR-1 and 2.0 for BR-2.

10. The inclusion of the geogrid gives about the same effect as adding 1 to 2 inches of base course material depending upon the conditions and reinforcement.

Chapter 7. Recommendations

The test track work described herein was limited to a single wheel, a soft clay subgrade and 2 inches of asphalt over 8 to 10 inches of granular base. All test sections failed after 10's to 1000's of cycles, far less than would be expected on a real road. There were several reasons for this difference. The test sections were designed based on the results of cyclic plate loading tests on model pavement systems. However, cyclic plate loading tests tend to overestimate pavement performance. The clay was so soft that it was difficult to get good compaction on the base and paving materials, hence the asphalt pavement surface was not very strong and the base, where it was in contact with the geogrid, was not very compact. It is entirely possible that the results would have been dramatically different had a stiffer base been used with more realistic pavement profiles. It is recommended that additional tests be performed.

Widening of the loaded area of a geogrid decreases the radius of curvature and the strain in the geogrid. Therefore, logic would lead to the conclusion that wander on the pavement surface would reduce the effectiveness of the geogrid, but this is far from a foregone conclusion, and tests using wander should be run. Logic would also lead to the conclusion that dual wheels would reduce the effectiveness of the geogrid: again, this is far from a foregone conclusion and tests using dual wheels should be done.

Many studies have been done using cyclic plate loading and static plate loading, indicating that the location of the geogrid in the profile makes a significant difference. All of the tests run herein used the geogrid at the contact between the base and subgrade because this is the least expensive place to put it in the field. If another location would be more beneficial, then it could be cost effective to place it there. Therefore, tests should be run using several layers of geogrid and geogrid at different locations in the profile.

The facilities in this test were fully controlled by a computer and are very useful for the research on pavement systems. More research work could be done by considering the effects of A/C thickness, mechanical properties, loading conditions, wheel speed and/or temperature in the pavement system.

Bibliography

Abd El Halim, A.O. (1983). "Geogrid Reinforcement of Asphalt Pavements," Ph.D. Thesis, University of Waterloo, Ontario, Canada.

Abd El Halim, A. O., Haas, R., and Chang, W. A. (1983). "Geogrid Reinforcement of Asphalt Pavements and Verification of Elastic Layer Theory," Transportation Research Board, Research Board Record No. 949, pp. 55-65.

ABAQUS (1995), Finite Element Computer Program, Version 5.4, Hibbitt, Karlsson and Sorensen, Inc.

American Society for Testing and Materials (1993), Annual Book of ASTM standards, Vol. 04.08, Philadelphia, Pa.

Austin, D.N., and Coleman, D.M. (1993). "A Field Evaluation of Geosynthetic-Reinforced Haul Roads Over Soft Foundation Soils," Geosynthetics '93 Conference Proc., Vol. 1, pp. 65-80.

Capaccio, G., and Ward, I. M. (1974). "Properties of Ultra-high Modulus Linear Polypropylene," *Nature Physical Sciences*, Vol. 243, pp. 130-143.

Carroll, R. G. jr., Walls, J. G., and Haas, R. (1987). "Granular Base Reinforcement of Flexible Pavements Using Geogrids," Proc. Geosynthetics '87, New Orleans, IFAI, pp. 46-57.

Greenwood, J. H. (1991). "The Creep of Geotextiles," Prof. 4th Intl. Conf. Geotextiles, Geomembranes and Related Products. Rotterdam, Blakema, pp.645-650.

Haas, R. (1984). "Structural Behavior of Tensar Reinforced Pavements and Some Field Applications," Proc. Symp. Polymer Grid Reinforcement in Civil Engr., ICE, London, Paper #5.2.

Hicks, R.G. (1980), "Use of layered theory in the design and evaluation of pavement systems," Alaska Department of Transportation and Public Facilities, Report No. FHWA-AK-RD-83-8.

Hsuan, Y. G. Koerner, R. M., and Lord, A. E. Jr. (1993). "A Review of the Degradation of Geosynthetic Reinforcing Materials and Various Polymer Stabilization Methods," ASTM STP 1190, S. C.J. Cheng, ed., ASTM, Philadelphia, pp. 228-244.

Ingold, T.S. (1983). "Laboratory Pull-out Testing of Grid Reinforcement in Sand," Geotechnical Testing Journal, ASTM, Vol. 6, September.

Kinney, T. C. (1993). "Using Geogrids to Limit Longitudinal Cracking of Roads in Interior Alaska," Geosynthetics '93 Conference Proc., Vol. 1, pp. 109-121.

Koerner, Robert M. (1994). *Designing with Geosynthetics*, Prentice Hall, Englewood Cliffs, New Jersey.

Koerner, G. R., and Koerner, R. M. (1991). "The Installation Survivability of Geotextiles and Geomembranes," Proc. 4th Intl. Conf. On Geotextiles, Geomembranes and Related Products, Rotterdam, Balkema, pp.597-602.

Koerner, R. M., Wayne, M. H., and Carroll, R. G., Jr. (1989). "Analytic Behavior of Geogrid Anchorage," Proc. Geosynthetics '89, San Diego, CA: IFAI, pp. 525-536.

McGown, A., Andrews, K. Z. and Kavir, M. H. (1982). "Load-Extension Testing of Geotextiles Confined in Soil." Proc. 2nd Intl. Conf. Geotextiles, Las Vegas, NV, IFAI, Vol. 3, pp.93-96.

Sarsby, R. W. (1985). "The Influence of Aperture Size/Particle Size on the Efficiency of Grid Reinforcement," Proc. 2nd Canadian Symp. on Geotextiles and Geomembranes, Edmonton, Alberta, pp7-12.

Tensar Earth Technologies (1993). "Technical Report for Tensar Base Course Reinforcement Geogrid Properties."

Webster, S. L. (1993). "Geogrid Reinforced Base Course for Flexible Pavements for Light Aircraft: Test Section Construction, Behavior Under Traffic, Laboratory Tests, and Design Criteria", Geotechnical Laboratory, Department of the Army, Waterways Experiment Station, Corps of Engineers, Technical Report GL-93-6.

White, D.W. (1990). "Literature Review of Geotextiles to Improve Pavements for General Aviation Airports", Department of Army, Waterways Experiment Station, Corps of Engineers, Report Number DOT/FAA/RD-90-26.

Wilson-Fahmy, R., and Koerner, R. M. (1993). "Finite Element Modeling of Soil-Geogrid Interaction in Pullout Loading Conditions," Jour. of Geotextiles and Geomembranes, Vol. 12, No. 5, pp479-502.

Yoder, E.J. (1975), "Principles of Pavement Design", 2nd Ed, John Wiley and Sons, Inc, New York.

Yuan, X. (1993). "Relating Index Tests to the Performance of Geogrids in Reinforced Aircraft Runway Pavement Systems,", M. S. thesis, University of Alaska Fairbanks.

Zaghloul, S. and White, T. (1993), "Use of a Three-Dimensional, Dynamic Finite Element Program for Analysis of Flexible Pavement", Transportation Research Record, No. 1388, pp60 - 69.

IMAGE EVALUATION TEST TARGET (QA-3)

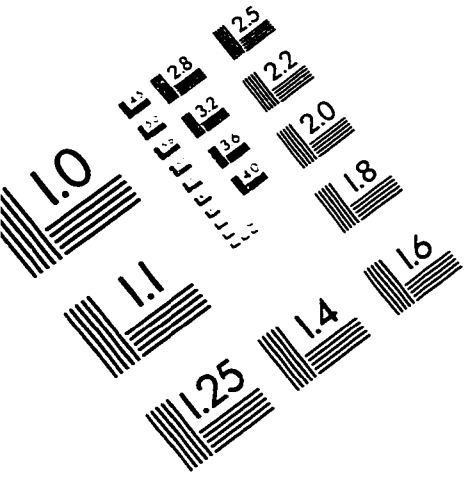

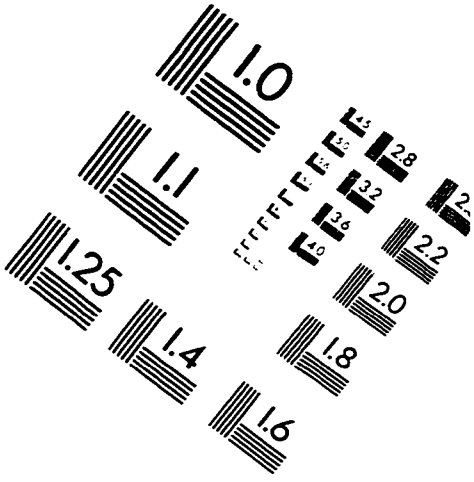

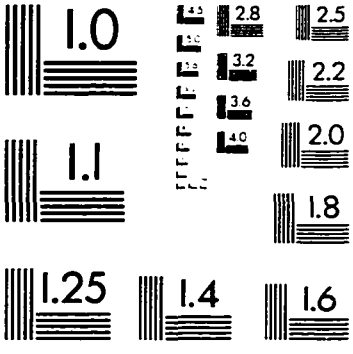

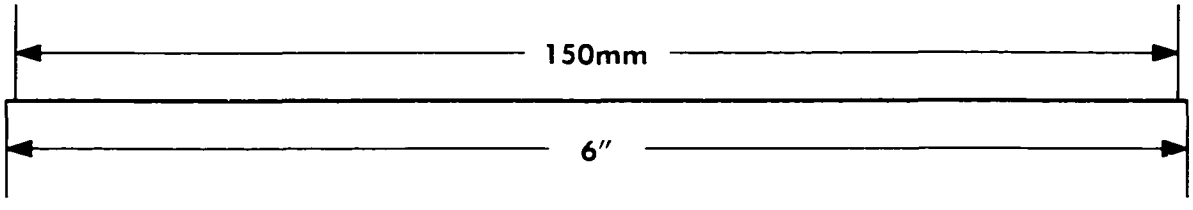

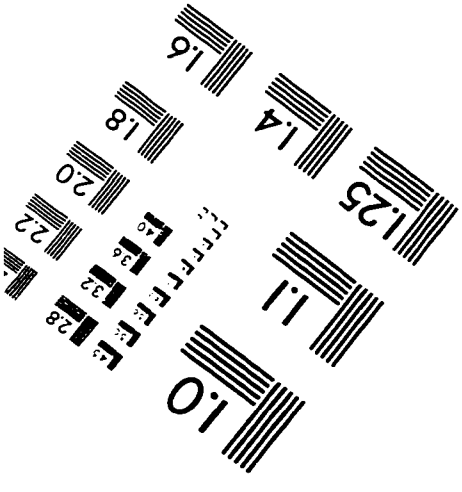

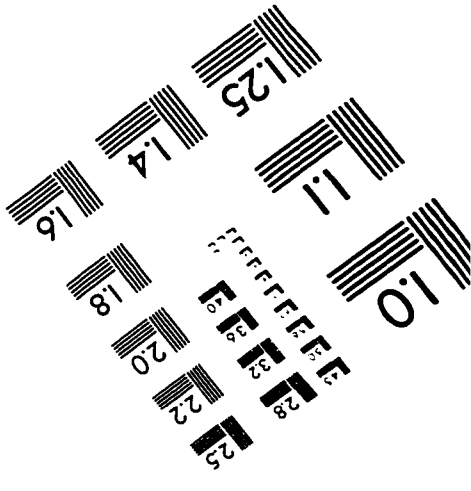

APPLIED IMAGE, Inc
1653 East Main Street
Rochester, NY 14609 USA
Phone: 716/482-0300
Fax: 716/288-5989